NEUROPHYSIOLOGICAL INVESTIGATIONS

OF VISUAL OBJECT COMPLETION PROCESSES

by
Marina Shpaner

A dissertation submitted to the Graduate Faculty in Psychology in partial fulfillment of the requirements for the degree of Doctor of Philosophy, The City University of New York

2011

This manuscript has been read and accepted for the Graduate Faculty in Psychology in satisfaction of the dissertation requirement for the degree of Doctor of Philosophy.

Date	John J. Foxe, Ph.D. Co-Chair of Examining Committee
Date	Sophie Molholm, Ph.D. Co-Chair of Examining Committee
Date	Maureen O'Connor, Ph.D. Executive Officer

Supervisory Committee:

Jonathan B. Levitt, Ph.D.

Matthew J. Hoptman, Ph.D.

Adam Kohn, Ph.D.

THE CITY UNIVERSITY OF NEW YORK

Abstract

NEUROPHYSIOLOGICAL INVESTIGATIONS

OF VISUAL OBJECT COMPLETION PROCESSES

by

Marina Shpaner

Advisers: John J. Foxe, Ph.D. and Sophie Molholm, Ph.D.

Research over the past several decades has provided exciting insights into the cortical underpinnings of vision. Whereas early efforts concentrated on identifying and characterizing the distinctive properties of neuronal populations, more recent investigations focus on how separate channels of information are integrated. Here, we examined the cortical dynamics of object completion within the framework of interacting parallel pathways. The “frame and fill” model advances fast and coarse scene analysis in the dorsal visual stream as the foundation of more detailed object-related processing in the ventral visual stream. Our first study assesses sensitivity to illusory contour (IC) stimuli within the lateral occipital complex (LOC) as compared to salient region (SR) stimuli, a stimulus class that lacks the classic bounding contours of illusory shapes. Using high-density electrical mapping of visual evoked potentials, we show that early LOC activity is substantially stronger to IC than to SR stimuli, while later LOC activity is stronger to SR than to IC stimuli. We further suggest that crude region based segmentation takes place in the dorsal stream regions prior to contour interpolation. The second study more closely examines contour interpolation in the context of complex visual scenes. We use different levels of clutter to obscure the salience of the centrally presented IC, thus taxing the initial scene delineation process. In support of the “frame-and-fill” model, we show that high levels of clutter

significantly affect the early illusory contour sensitivity in the LOC and result in an apparent switch to more effortful mode of contour interpolation. The final study focuses on mechanisms of contour integration in the ventral stream. We arbitrate between two previously advanced mechanisms of contour integration: serial facilitative interactions between collinear cells in the primary visual cortex or pooling of inputs in higher order visual areas. We use retinotopic presentations of Gabor contours embedded in Gabor noise in order to assess the timecourse of earliest cortical activity. We report earliest contour-related cortical responses in the higher-order visual areas and not in the primary visual cortex, indicative of pooling of inputs in extra-striate areas. Overall, the results of our studies support the tenets of the “frame-and-fill” model of cortical processing.

Dedication

This work is dedicated to my beloved husband Sergey and my children Naomi and Benny, who are the joy of my life.

Acknowledgments

I am most grateful to my mentors, John Foxe and Sophie Molholm, for their unconditional support and encouragement throughout my graduate school years. Going forward I hope to bring with me not only the science they have taught me, but also their enthusiasm and dedication. I feel lucky to have been part of a laboratory where exchange of knowledge in multiple research domains is combined with opportunities for independent work. I have learned a lot from my colleagues at NKI, CCNY and AECOM, whose continuing friendship I value very much. Special thanks are owed to Micah Murray for insightful methodological discussions and for introducing me to Cartool and to Emma Forde, Manuel Gomez-Ramirez, Sherlyn Yeap and Daniel Senkowski for help with data collection and experimental design.

I could not have done this without the support of my family. Thank you all for egging me on a lot and for letting me be some of the time. I look forward to a new chapter in our lives and to many more exciting beginnings.

TABLE OF CONTENTS

LIST OF FIGURES AND TABLES

GENERAL INTRODUCTION

The interaction between the human organism and its environment is orchestrated by the nervous system, which endows us with the exceptional versatility of behaviors (Maturana & Varela, 1992, p. 138). The visual system, the subject of the current series of investigations, guides a range of mental and physical faculties from emotional interpersonal communication to hand-eye coordination. While much is already known about the internal workings of the visual system, certain basic mechanisms are yet to be fully understood. One such mystery concerns the basic mechanisms of object recognition. Objects constitute the building blocks of our physical and mental reality and have direct functional significance for human actions. Our interaction with visual objects encompasses their multiple dimensions, such as shape, color, depth and movement. Exactly how the visual system interprets the myriad fragments detected by individual nerve cells, assembling them into amalgamated images, is a matter of intense inquiry. Insights can be gathered from psychophysical, anatomical, and physiological investigations, as well as from computational modeling. This doctoral thesis focuses on how humans form perceptual representations of objects. The goal of this work is to extend our understanding of the way the brain integrates parcellated information from retinal receptors to produce the experiential perception of a whole and distinct object. In introducing the work in this doctoral thesis, I will provide a brief overview of the architecture of the visual system, the possible mechanisms of encoding visual information, the interactions between separate streams of information within the visual system and the dynamic relationship between different levels of the visual hierarchy, the markers of object-related neural activity obtained with human electrophysiology and, finally, the ways in which all of these lines of evidence inform the theories of object recognition.

The Architecture of the Visual System

Much insight into the physiological mechanisms of vision has been gained by studying the anatomy of mammalian visual systems. Such studies are helpful because anatomical considerations constrain hypotheses of neural mechanisms of object recognition. A typical mammalian visual system consists of hierarchically organized and interconnected areas, which comprise multiple reciprocal feedforward, feedback and lateral connections (Felleman & Van Essen, 1991). The first significant hub for neural signals traveling from the retina into the visual areas of the cerebral cortex is the Lateral Geniculate Nucleus (LGN) of the thalamus. Once conceived of as a simple relay nucleus for feedforward activity, the LGN has since emerged as a nucleus more fully engaged in modulating cognitive functioning (Saalmann & Kastner, 2009; Sherman, 2005). Indeed, the number of feedback connections linking the cerebral cortex with the LGN far exceeds the number of feedforward connections (Saalmann & Kastner, 2009; Sherman, 2005; Sincich & Horton, 2005). In addition, the primary visual cortex (V1), the lowest cortical area in the visual hierarchy also known as the striate cortex, receives most of its afferent projections from the LGN. Upstream projections from V1 eventually reach the ventral and lateral occipito-temporal areas—regions of the cortex shown to be especially sensitive to objects and shapes (Hirabayashi & Miyashita, 2005; Hung, Kreiman, Poggio, & DiCarlo, 2005; Sugase, Yamane, Ueno, & Kawano, 1999).

Neural information flows through the visual system along multiple parallel but interconnected streams, a mechanism first described by Livingston and Hubel (1988), see Figure 1 for a rough illustration. The parallel streams of information begin in the retina, where scientists have identified seventeen distinct types of retinal ganglion cells, forming as many as thirteen distinct parallel pathways to the LGN (Nassi & Callaway, 2009). Each of these ganglion cell

types tiles the entire visual scene and transmits specific visual information. The three main parallel pathways between the retina and the cortex are the magnocellular, the parvocellular, and the koniocellular pathways (Kaplan, 2008). The parvocellular pathway projects to layer 4Cβ and layer 6 of V1. It is formed by cells with small receptive fields, low contrast sensitivity and relatively slow axonal conduction. These cells encode red-green opponency and are most sensitive to high spatial and low temporal frequencies (Kaplan, 2008; Nassi & Callaway, 2009). The magnocellular pathway transmits broadband, achromatic signals to layer 4Cα and layer 6 of V1. In contrast to the parvocellular pathway, the magnocellular pathway receives input from cells with large receptive fields, high contrast sensitivity and fast conductance velocities. All of these characteristics make the magnocellular pathway particularly sensitive to high temporal and low spatial frequencies (Kaplan, 2008; Nassi & Callaway, 2009). The koniocellular pathway possesses blue-on/yellow-off color-opponency and projects to layer 1 and to the cytochrome oxydase (CO)[1] blobs of layer 2/3 in V1. The exact projections of the other subsidiary varieties of retinal ganglion cells to V1 remain uncertain (Kaplan, 2008; Nassi & Callaway, 2009). As yet, it is unclear how the sensory characteristics of the ganglion cell pathways translate into perceptual experience (Nassi & Callaway, 2009).

It was once believed that the magnocellular and the parvocellular channels remained separated in V1, resulting in a clear segregation of color, form and motion processing in the cortex (Livingstone & Hubel, 1988). The color-sensitive koniocellular and parvocellular inputs to CO blobs of V1 were believed to project to thin stripes of V2 and to upstream ventral areas. The orientation-sensitive parvocellular inputs were thought to project to the so-called interblobs of V1, then to the pale stripes of V2 and in turn to upstream ventral areas. The diffuse

[1] Cytochrome oxydase staining reflects the cells with high metabolic activity.

magnocellular projections were thought to have terminated in the thick stripes of V2 and then to project onwards to the dorsal motion-sensitive middle temporal area (MT) (Livingstone & Hubel, 1988). In recent studies, a more complex picture is emerging. As the feedforward sweep of neural activity reaches V1, the neural information flowing through the separated parallel pathways is integrated (Sincich & Horton, 2005). Specifically, it has been shown that magnocellular and parvocellular inputs converge inside V1 to form a retinotopically-organized matrix of local circuits, representing the entire visual space (Nassi & Callaway, 2009). The circuits of this matrix are formed by cell-type specific arrangements of axonal and dendritic connections (Nassi & Callaway, 2009).

The inputs, as reorganized in V1, subsequently form afferent parallel projections to higher-tier extrastriate areas. The first such extrastriate visual area, known as V2, also consists of retinotopically-organized repeating functional subunits. Initial studies of V2 reported a clear separation of afferent inputs from the V1 blobs and interblobs relating to a pattern of CO-stained compartments (known in V2 as thin, pale and thick stripes) (Livingstone & Hubel, 1988). As described earlier, magnocellular, koniocellular and parvocellular inputs were originally thought to subserve different streams of information, and have clear anatomical demarcations in V2. However, more recent research indicates that, while the V2 stripes are likely to be divided into submodules with hue-specific maps in thin stripes and disparity-selective clustering in thick stripes, some intermixing of V1 inputs is also present (Nassi & Callaway, 2009). Yet, the original proposal remains mostly intact in that the dorsal stream is dominated by the magnocellular channel while the ventral stream is dominated by the parvocellular channel, with contributions from each channel present in both streams (Nassi & Callaway, 2009; Sincich &

Horton, 2005). Thus, as a general pattern, areas V1 and V2 integrate parallel inputs in order to construct new, separate, yet interacting, outputs for at least two parallel streams of information.

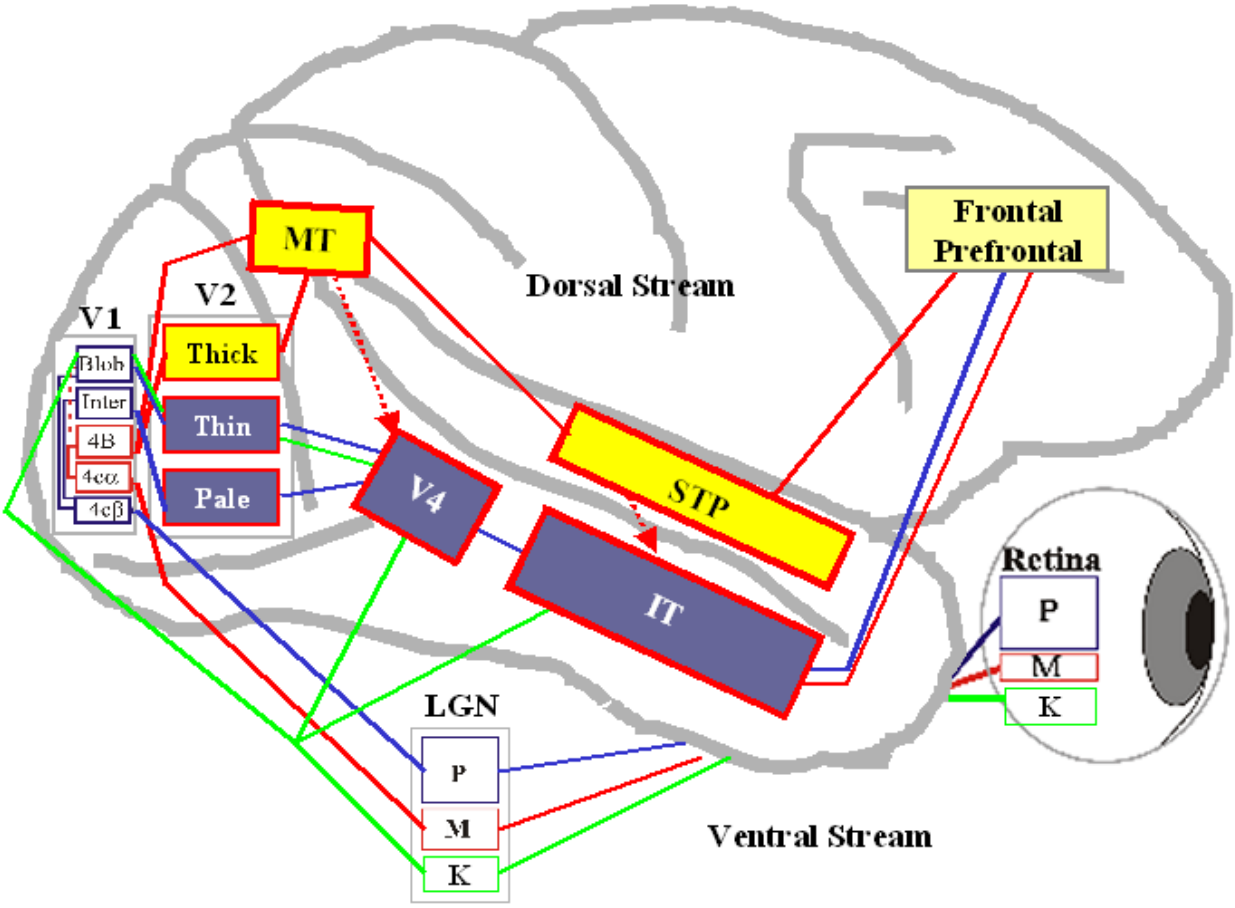

Figure 1. Parallel Visual Streams and the 'Frame and Fill' Model

Parallel channels of the visual system are shown on a simplified diagram of a primate brain. Green lines are the koniocellular connections, red lines are the magnocellular connections, blue lines are the parvocelullar connections. Dorsal stream is in yellow, ventral stream is in purple. Dashed red errors represent the "framing" of the ventral stream by the dorsal stream inputs. (LGN = lateral geniculate nucleus; MT = middle temporal; STP = superior temporal polysensory; IT = inferotemporal.) This diagram is modified with permission, courtesy of Dr. Charles Schroeder.

The ventral stream regions along the cortical hierarchy exhibit increasingly complex response characteristics. Cells in V1 can respond to simple lines, cells in V2 and V4 can respond to more complex shapes and gratings, and cells of the inferotemporal areas (IT) are able to respond to object categories and even object identities (Hirabayashi & Miyashita, 2005; Hung, et

al., 2005; Pasupathy & Connor, 2002; Quiroga, Reddy, Kreiman, Koch, & Fried, 2005; Reddy & Kanwisher, 2006; Sugase, et al., 1999). The functional organization of the higher-order ventral stream areas (beyond retinotopically-organized V1 and V2) has not been resolved (Reddy & Kanwisher, 2006). Some scientists argue that category-specific and feature-specific clustering is the general organizational principle within the temporal lobes with special clusters for faces, places and body parts (Fujita, Tanaka, Ito, & Cheng, 1992; Reddy & Kanwisher, 2006; Tanaka, 1996); while others maintain the importance of distributed representations within a neuronal population in the visual areas along the ventral stream, with meaning emerging from interactions of a large number of broadly tuned neurons (Ewbank, Schluppeck, & Andrews, 2005; Haxby et al., 2001).

The Neural Code of Feature Binding

Since visual information is initially fragmented according to the receptive properties of the retinal ganglion cells and retinotopically across the visual field, effective object recognition requires assembling and reconstructing such information from the responses of individual neurons. Several cellular mechanisms have been advanced as possible candidates for integrating information across the neuronal population. Since the 1960's, when Hubel and Wiesel first published their studies of cell properties in the cat's visual cortex (1962), it has been understood how response properties of simple cells in V1 result from integration of afferent inputs from the LGN and how tuning characteristics of the complex cells can be modeled as a summation of their respective simple cell inputs. In order to integrate afferent inputs, upstream cells can rely on rate coding, i.e., the summation of spiking activity over time. Such a processing scheme would critically depend on the "architecture of cortical connections" (Uhlhaas et al., 2009). As the complexity of tuning increases across the levels of the visual hierarchy, it may be possible to

group simpler visual elements by cardinal cells via “sparse” coding. Sparse coding is a coding scheme by a relatively small number of highly selective neurons. The extreme example of sparse coding is the so-called “grandmother cell”—a hypothetical neuron dedicated to the representation of a specific concept or object, for example, one’s grandmother. The advantages of such “sparse” coding system would include high metabolic efficiency and ease of readout (Reddy & Kanwisher, 2006). However, such a coding system might have difficulty responding to novel visual stimuli and is unlikely to exist at the higher levels of the visual hierarchy. That is, since all the possible feature combinations at any given level of the hierarchy would then require a dedicated detector at the next level, such a schema would be expected to trigger a combinatorial explosion, which could not be accommodated by the finite, albeit enormously complex, architecture of the brain (Gray, 1999; Roelfsema, 2006).

An alternative way in which neural coding could represent visual information would be across a distributed network of neurons. A distributed representation is flexible and responsive to new objects (Roelfsema, 2006). Moreover, it is resilient to cell death and does not depend on the natural variability in the response strength of individual neurons (Reddy & Kanwisher, 2006). However, such a representation requires a way to group together the neural activity related to the same object across a large number of individual neurons, creating a binding problem. One possible solution to this binding problem is the temporal correlation hypothesis (Gray, 1999; Singer & Gray, 1995). According to the temporal correlation hypothesis, the synchronization of activity within self-forming neuronal ensembles can increase the output salience of the neuronal activity for subsequent processing. That is, the combined strength of a neuronal population is more likely to impact the next level of processing if it is synchronized and non-random. Such synchronous activity has been consistently observed in neurons driven by a single stimulus, with

spike rates of cortical neurons oscillating in the 30-70 Hz gamma range (Bressler, Coppola, & Nakamura, 1993; Eckhorn et al., 2004; Engel, Roelfsema, Fries, Brecht, & Singer, 1997; Murthy & Fetz, 1996; Roelfsema, Engel, Konig, & Singer, 1997). The importance of synchronous activity in perceptual grouping has been shown in illusory contour studies where a higher induced gamma activity was observed in response to stimuli comprising an illusory contour as compared to the same stimuli arranged not to form a contour (Tallon-Baudry, Bertrand, Delpuech, & Pernier, 1996). However, a recent debate in the journal Neuron highlights the probable contamination of this activity by artifact from ocular micro-saccades in human EEG (Yuval-Greenberg, Tomer, Keren, Nelken, & Deouell, 2008 and the follow-up communications). At the same time, synchrony in the gamma and beta bands has been implicated not only in feature binding within local neuronal populations but also in forming and maintaining coherent object representations between cortical regions (Sehatpour et al., 2008; Senkowski et al., 2007; Tallon-Baudry, 2009; Tallon-Baudry & Bertrand, 1999; Uhlhaas, et al., 2009). A striking example of object-related synchronous activity is the study by Hirabayashi and Miyashita (Hirabayashi & Miyashita, 2005), which showed synchronous patterns of activity between IT neurons when facial fragments were arranged to form a face. In general, the involvement of synchronous activity in feature binding seems less equivocal in human intracranial recordings and animal models than in human scalp EEG.

In distributed neuronal networks, the modulation in the strength of synchronous activity can signal perceptual differences (Uhlhaas, et al., 2009). That is, activity of similarly tuned neurons in response to a preferred type of a stimulus may drive a more coherent response within a population. An additional way to code visual features within a distributed neuronal population could rely on spike timing (computing the visual image based on the latency of neuronal spiking)

(Hegde, 2008; Uhlhaas, et al., 2009; VanRullen & Thorpe, 2002). Research shows that the more excited cells fire earlier in the gamma cycle, translating amplitude of the excitation into phase of the gamma cycle (Fries, Nikolic, & Singer, 2007). Under this coding scenario, the brighter (or more salient) regions of an image could induce earlier spiking activity than the darker regions, which would be detected by the next level of the network (VanRullen & Thorpe, 2002). Since integration of inputs in such a network critically depends on a temporal reference point, setting such reference point within a dynamically changing visual array presents a challenge. Proponents of such coding schemes speculate that it could be accomplished by keeping track of the onset of fixation during saccades or micro-saccades by corollary discharge (VanRullen & Thorpe, 2002).

In sum, both sparse and population coding likely play a role in feature integration, depending on a specific level of the visual hierarchy, and both types of coding are theoretically viable ways of feature binding. In addition, both types can play a role at different timescales. For example, a distributed response may dominate the early activity followed by gradual fine-tuning of response characteristics (i.e., "response sparsening") through reverberant activations (also see Hegde, 2008).

The Dynamics of the Parallel Processing Streams

Early models of visual processing emphasized functional separation between the ventral and the dorsal streams, with the dorsal pathway more responsive to visual features relevant to identifying the location of objects and the ventral stream more responsive to visual features important for object recognition (Mishkin, Ungerleider, & Macko, 1983). More recent models have recognized that both visual streams may, in fact, transmit similar visual attributes (such as color or disparity), and instead focus on the differences in behavioral goals subserved by the respective visual streams (Milner & Goodale, 2008; Nassi & Callaway, 2009). While the

proponents of these later models have certainly acknowledged the central role of the ventral stream in object recognition established in the earlier models, they also emphasize the dorsal stream's role in the task of action guidance by transmitting motion and depth information (Milner & Goodale, 2008). The most recent theories also point to the influence of the dorsal stream on object perception (see "frame and fill" model below and Figure 1, Bar, 2003, 2009; Bullier, 2001; Chen et al., 2007; Vidyasagar, 1999).

The dorsal and the ventral streams can interact via feedback projections from higher- to lower-order regions of the visual hierarchy and lateral projections between similar levels of the parallel streams (Bullier, 2001; Chen, et al., 2007; Felleman & Van Essen, 1991). Research shows that the magnocellular channel and the dorsal stream areas are activated approximately 10-20 milliseconds before hierarchically parallel ventral stream areas, allowing enough time for lateral and feedback influences on ventral activity (Bullier, 2001; Chen, et al., 2007). By examining laminar profile maps in primates, Chen and colleagues (2007) also found that feedback local field potential (LFP) activity preceded feedforward LFP activity in every tested extrastriate visual area along the ventral stream. Moreover, response onset latencies in the dorsal stream MT were very similar to the response latencies in the V1 (see also Bullier, 2001). Earlier processing along the dorsal stream is possible through the relatively fast speed of magnocellular connections, facilitating rapid transmission of the earliest magnocellular inputs from the V1 further on to MT, as well as through direct inputs to MT from the LGN and other subcortical areas, bypassing the primary visual cortex (Bullier, 2001; Chen, et al., 2007).

Feedback projections have been shown to modulate the ongoing activity within lower-tier target brain regions. To illustrate, MT inactivation has profound and immediate effects on V1 spiking activity, resulting in significant response attenuation (Hupe et al., 2001). This

observation demonstrates that feedback projections can shape the feedforward flow of information and are essential to normal brain activity in the earliest timeframe. Relatively few studies have investigated the systematic organization of feedback projections, particularly in relation to V1 cytoarchitectonics (Sincich & Horton, 2005). While the details remain unresolved, there is mounting evidence of the influences of feedback connections on perception.

Re-entrant activity to the primary visual cortex is one of the better-studied feedback phenomena. It has been investigated extensively using transcranial magnetic stimulation (TMS)[2] in humans and single-cell recordings in animal models (Koivisto, Railo, & Salminen-Vaparanta, 2010; Lamme, 2003, 2004; Lamme & Roelfsema, 2000; Lamme, Super, Landman, Roelfsema, & Spekreijse, 2000; Pascual-Leone & Walsh, 2001; Silvanto, Lavie, & Walsh, 2005; Super, Spekreijse, & Lamme, 2001). Silvanto and colleagues (2005) identified two V1 (40-60 ms and 80-100 ms post stimulus offset) and a single MT critical period (60-80 ms) in motion perception by showing that TMS disrupted awareness in a hierarchically-specific fashion during those timeframes. Most recently, Koivisto and colleagues (2010) extended these findings to the detection of motion without conscious awareness of motion by showing that the TMS impaired the performance of a forced-choice motion-detection task **regardless** of the conscious report of motion.[3]The studies found that interfering with the V1 activity both in the earliest feedforward sweep as well as in the later re-entrant sweep impairs the perceptual report of motion. In a complementary set of experiments, Lamme and colleagues studied figure-ground detection in

[2] TMS causes neuronal depolarization and can be used either to disrupt processing in the target brain area (cause a reversible lesion) or to invoke certain perceptual phenomena (e.g., flashes of light called “phosphenes” or moving phosphenes) (Pascual-Leone, Walsh, & Rothwell, 2000).

[3] In this study, participants reported the direction of motion with an above chance accuracy, even when they believed they had observed no motion. TMS disrupted performance in this experimental condition.

monkeys. For example, in one of their studies, they trained animals to saccade to a target at a certain V1 location (Super, et al., 2001). They found a differential modulation in the neural response starting at about 90 ms after stimulus onset for "seen" vs. "not seen" stimuli. This modulation was context-dependent and saliency-dependent. The relatively late timing of the modulation highlighted the involvement of feedback and horizontal connections in visual awareness. This line of inquiry underscores the significance of recurrent processing in conscious perception.

Electrophysiological Markers of Object Recognition and Their Correlates in Neuroimaging

Electrophysiological and neuroimaging approaches have been used extensively to examine object recognition mechanisms in human participants. Electrophysiological data is appropriate for making inferences about the temporal evolution of neural events through the derivation of an event-related potential (ERP)—the technique utilized in this series of experiments. Complementary neuroimaging investigations can verify the locus of the neuronal activations within the brain due to their precise spatial resolution. An ERP is an average stimulus-locked response to a large number of stimulus presentations. The early visual ERP waveform has a stereotyped sequence of peaks and valleys (called "components"), starting from the C1 (with a peak at 65-90 ms post stimulus onset), followed by the P1 (positivity around 100 ms) and followed by the N1 (negativity around 150 ms) (Di Russo, Martinez, Sereno, Pitzalis, & Hillyard, 2002). The earliest part of the C1 component is believed to be a marker of neuronal activity stemming from the striate cortex due to its highly retinotopic distribution, early timing and repeated source localization to the V1 (Di Russo, et al., 2002; Foxe & Simpson, 2002; Gomez Gonzalez, Clark, Fan, Luck, & Hillyard, 1994; Jeffreys & Axford, 1972a). The P1

component reflects activity in the striate and extrastriate areas (Clark, 1994; Di Russo, et al., 2002). The N1 component has lateral occipito-temporal distribution and reflects activity of multiple occipito-temporal cortical areas, including the LOC and the temporo-parieto-occipital region (TPO) (Clark, 1994; Di Russo, et al., 2002; Sehatpour, Molholm, Javitt, & Foxe, 2006). According to a traditional view, the ERP signals a time-locked and phase-locked response, evoked by synchronized post-synaptic activation. The amplitude differences in this response can be construed as modulations in the neural activity of the underlying cortical generators, while the latency of the response reflects differences in temporal processing (see Luck, 2005).

The C1, the P1 and the N1 components are sensitive to low-level visual characteristics, such as luminance, contrast and spatial frequency (see Regan, 1989 for review). While C1 and P1 modulations in object perception are equivocal (Rossion & Jacques, 2008), N1 is sensitive to object categories (e.g., Bentin, Allison, Puce, Perez, & McCarthy, 1996; Itier, Latinus, & Taylor, 2006; Thorpe, Fize, & Marlot, 1996), with particularly large amplitude responses to the category of faces, even when controlling for low-level visual characteristics of the stimuli (Rousselet, Husk, Bennett, & Sekuler, 2005, 2007). The N1 also becomes more negative in response to illusory contours as compared to real contours or control stimuli not forming a contour (Foxe, Murray, & Javitt, 2005; Halgren, Mendola, Chong, & Dale, 2003; Kruggel, Herrmann, Wiggins, & von Cramon, 2001; Mendola, Dale, Fischl, Liu, & Tootell, 1999; Murray, Foxe, Javitt, & Foxe, 2004; Murray, Imber, Javitt, & Foxe, 2006; Murray et al., 2002; Ritzl et al., 2003b; Shpaner, Murray, & Foxe, 2009) and is enhanced in studies of object-based attention (Martinez, Teder-Salejarvi, & Hillyard, 2007; Martinez et al., 2006). Studies of object recognition and perceptual closure in our laboratory have identified a later correlate of object identification, a modulation with lateral-occipital and lateral-frontal distribution, which we term the Ncl (closure

negativity) (Doniger, Foxe, Murray, Higgins, & Javitt, 2002; Doniger et al., 2000; Doniger et al., 2001; Sehatpour et al., 2010; Sehatpour, et al., 2006; Sehatpour, et al., 2008). Using intracranial recordings in humans, Sehatpour and colleagues (2008) also showed that the Ncl modulation in the LOC follows a similar hippocampal modulation separated by a period of beta-range synchronization between the two brain regions. The authors speculated that this oscillation could signal template matching between incomplete sensory representation in the LOC and the stored object representation in the hippocampus. The Ncl modulation has likely parallels in neuroimaging research, where object-selective activations within the ventral and lateral occipito-temporal regions are consistently reported (for reviews see Grill-Spector, 2003; Grill-Spector & Malach, 2004). Since N1 and Ncl modulations stem from similar cortical generators within the LOC, LOC activations detected with neuroimaging techniques signal a temporally integrated response, due to their relatively poor temporal resolution (e.g., Shpaner, et al., 2009). Inferences regarding the temporal evolution of events cannot be based on neuroimaging, and inferences regarding the localization of neural activity as detected by electrophysiology have to be made with caution.

The timecourse of neural events as assessed with ERPs has to be considered in light of the current understanding of processing speeds within the visual hierarchy. Animal literature reveals the fast course of activation of the entire brain, with the highest levels of the anatomical hierarchy activated within the first 60 ms post-stimulus onset (Chen, et al., 2007; Schmolesky et al., 1998; Schroeder, Mehta, & Givre, 1998). Similarly, using scalp current density analyses in humans, Foxe and Simpson (2002) reported activations within dorsolateral frontal cortex in the timeframe of C1, at just 80 ms post-stimulus onset.[4] Consequently, any effects observed in the

[4] Scalp current density is the second spatial derivative of the ERPs across the electrode array. It is reference independent and is used to aide in visualization of intracranial generators.

P1 and N1 timeframes, and even over late C1, are likely to represent feedforward as well as feedback driven modulations (Foxe & Simpson, 2002; Michel, Seeck, & Murray, 2004). Such view is consistent with the literature on rapid categorization of objects and faces in the N1 timeframe (e.g., Michel et al., 2004). Since many areas of the brain are activated within a short timeframe, analyses of ERP components should include source localization in order to draw conclusions about the likely locus of neural events.

Theories of Object Recognition

Theories of object recognition can be roughly divided into (a) "bottom-up" theories emphasizing the initial contributions from the feedforward flow of neural information for the creation of an internal object representation (e.g., Hung, et al., 2005; Serre et al., 2007; Serre, Oliva, & Poggio, 2007; VanRullen & Thorpe, 2002) and (b) "top-down" theories emphasizing the critical importance of feedback and lateral influences (Ahissar, Nahum, Nelken, & Hochstein, 2009; Bar, 2003; Bullier, 2001; Chen, et al., 2007; Vidyasagar, 1999). The bottom-up framework motivated computational models, which posit that rapid computation of an object representation can occur in a feedforward fashion through a cascade of ventral stream events: for example, through spike time coding (VanRullen, Guyonneau, & Thorpe, 2005; VanRullen & Thorpe, 2002). These models hold that the rapid feedforward sweep of activity along the ventral stream precedes other processing (Serre et al., 2007). By contrast, computational models within the top-down framework focus on the initial coarse analysis in forming object representations (Hamker, 2005; Walther & Koch, 2006). This framework underscores the critical role of feedback in the initial stages of object perception, with either the parietal or pre-frontal areas of the dorsal stream directing the processing in the temporal areas of the ventral stream (Bar, 2003; Bullier, 2001; Chen, et al., 2007; Vidyasagar, 1999).

Bottom-up theories of visual processing have been developed with the goal of reproducing the fast course of object recognition and contour integration in humans and animal models and are based on the notion that recurrent processing would take a longer timecourse (e.g., Riesenhuber & Poggio, 1999; Serre, Oliva, et al., 2007; Thorpe, et al., 1996; VanRullen & Thorpe, 2002). There are many ways to implement these models. Some are based on the "simple-to-complex" cell hierarchy of the ventral stream areas (e.g., Riesenhuber & Poggio, 1999; Serre, Oliva, et al., 2007). Experimental evidence in support of such theoretical models includes a recent study where a regularization classifier was trained to categorize and identify objects based on very short duration of spiking activity (12.5 ms) in a population of IT neurons in monkeys (Hung, et al., 2005). The classifier can be construed as the target neuron receiving information from IT, for example in the prefrontal region. At its peak efficiency at 125 ms post-stimulus onset, the classifier could categorize objects from 8 categories at 70 percent accuracy and could also identify objects above chance. Other models take advantage of the asynchronous firing of the V1 cells, which can integrate information locally by exerting influence on the firing pattern of neighboring cells through local horizontal interactions (an issue, which we examine more closely in Chapter 3 of this thesis) (VanRullen, Delorme, & Thorpe, 2001). In general terms, this class of models relies on the specific tuning of neurons to increasingly complex feature conjunctions for the initial fast analysis of the visual image (Roelfsema, 2006).

Top-down theories of visual processing strive to account for the coarse-to-fine manner of visual analysis, where the global elements of the scene are processed prior to the fine details (for review see Hegde, 2008). Most direct support for this global-to-fine processing scheme comes from numerous behavioral observations, where the global elements of the stimulus are perceived prior to local elements (for review see Hegde, 2008). One such theory is the Reverse Hierarchy

Theory (Ahissar, et al., 2009; Hochstein & Ahissar, 2002). Here, implicit "vision at a glance" is accomplished through the rapid feedforward sweep of activity and the consequent explicit "vision with scrutiny" takes place in the feedback direction, refining the image and generating a detailed and relevant percept. This theory is based on psychophysical research, but does not make specific predictions regarding the flow of the neural activity, other than to say that higher levels of the visual hierarchy are accessed first. Alternative, physiologically-grounded theories endow the dorsal stream with the power to generate a coarse low spatial resolution representation of an image in higher-order visual areas, which then can feedback to the inferotemporal cortex to be integrated with bottom-up flow of information in the ventral stream, see Figure 1 (Bar, 2003). In this thesis, these models are referred to as "frame-and-fill" models (Chen, et al., 2007). Here, the dorsal stream "frames" the scene for further refinement "filling in" of the missing detailed information by the ventral stream. These theories garner support from the relative temporal dynamics of the two parallel streams as well as from converging evidence regarding the importance of feedback projections in visual perception and awareness (see previous sections).

One of the most important limitations of computational models based on bottom-up theories is their inefficiency in processing images under realistic viewing conditions. The bottom-up models admittedly fail to accurately describe object processing under conditions of clutter and occlusion (Serre, Oliva, et al., 2007). Without initial scene analysis on a global level, such models may not be able to disambiguate how to group local elements of the scene. To compensate for this apparent flaw, proponents of bottom-up models reserve the role for top-down attention in potentiating certain neurons over others (e.g., Serre, Oliva, et al., 2007; VanRullen & Thorpe, 2002). This, however, begs the question of what drives the attentional mechanism in the first place, as it is assumed that potentiation happens prior to the onset of the

feedforward activity. Preliminary rough scene analysis and creation of a salience map have been advanced as the possible mechanism of potentiation of the neural responses prior to the refinement of the visual representation in the feedforward sweep of activity (Hamker, 2005; Walther & Koch, 2006). Furthermore, "frame-and-fill" models propose a mechanism whereby initial fast and coarse spatial delineation of the scene guides local image analysis in accordance with the known temporal dynamics of object recognition.

The Present Endeavor

The set of research studies presented here is inspired by ERP literature on illusory contours and perceptual closure. When designing these studies, we sought to examine the following series of events in object processing: initial dorsal stream coarse analysis of the visual space, followed by categorization of objects in the lateral occipital and temporal regions, and final conscious identification of objects via recurrent connections between multiple areas of the brain. Throughout this venture we attempt to frame our hypotheses in terms of the temporal cortical dynamics as instantiated through ERPs.

As mentioned earlier, ERP research on illusory contour processing reveals initial response modulation in the N1 timeframe, localized to the LOC. This modulation is very similar to the effects observed in object categorization studies, and presumably reflects initial automatic and implicit processing of objects. The initial modulation is followed by a protracted Ncl effect 50-100 ms later. This effect is correlated with the identification of objects in perceptual closure studies and has intracranial sources in the LOC, the hippocampus and the pre-frontal areas.

The first study in this thesis deals with a recent challenge to the involvement of the dorsal stream in the coarse spatial segmentation (Stanley & Rubin, 2003). Using functional Magnetic Resonance Imaging (fMRI), Stanley and Rubin reported that spatial segmentation takes place in

the LOC, due to equivalent response to illusory contour and so-called “salient region” stimuli. By examining the temporal evolution of events in response to the two classes of stimuli, we argue that the initial LOC modulation is specific to illusory contour processing mechanisms and not to the general process of spatial segmentation.

The second study further investigates the role of spatial segmentation in illusory contour processing by embedding illusory contours within different levels of clutter. We show that initial automatic sweep of activity within the LOC depends on the level of clutter in the scene. Taken together with the established specificity of this initial automatic IC response to IC stimulus class (as compared to real contours or “salient regions”), we argue that efficient spatial segmentation is a prerequisite for the rapid establishment of illusory contour boundaries.

The final study examines the role of the primary visual cortex in contour integration by arbitrating between two alternative ways of binding collinear elements in cluttered displays (pathfinder displays): the first involves local horizontal connections in the V1, while the second involves pooling of inputs in the LOC. We make a case for input pooling.

CHAPTER 1

Early Processing in Human LOC is Highly Responsive to Illusory Contours but not to Salient Regions

Introduction

The neural basis of visual segmentation and object surface completion has been extensively studied using illusory contour (IC) stimuli. Although earlier intracranial studies in animal models and human neuroimaging studies localized IC processing to the hierarchically lowest visual cortical regions of V1/V2 (Bakin, Nakayama, & Gilbert, 2000; Ffytche & Zeki, 1996; Larsson et al., 1999; 2001; Peterhans & von der Heydt, 1989; Ramsden, Hung, & Roe, 2001; Seghier et al., 2000; von der Heydt & Peterhans, 1989), more recent functional Magnetic Resonance Imaging (fMRI) and magneto/electroencephalographic studies emphasize contributions from higher-order regions of the lateral occipital complex (LOC) (Foxe, et al., 2005; Halgren, et al., 2003; Kruggel, et al., 2001; Mendola, et al., 1999; Murray, Foxe, et al., 2004; Murray, et al., 2006; Murray, et al., 2002; Ritzl, et al., 2003b). These latter studies support a model whereby IC sensitivity occurs first in the LOC with subsequent feedback and recurrent processes involving lower-tier areas V1 and V2.

A reasonable challenge to this body of research is that the LOC is not itself sensitive to illusory contours or completion processes, but rather is a general site for more crude region-based segmentation (Stanley & Rubin, 2003). Since LOC neurons pool information from large portions of the visual field, there is a possibility that the IC response observed within the LOC might instead represent a response to the whole figure rather than to the bounding contour per se. Borrowing a computationally cost-effective model for surface detection from the computer vision literature (Sharon, 2000; Shi, 2000), Stanley and Rubin proposed that the LOC detects

crude surfaces and that lower-tier cortices process bounding edges. To test this notion, they introduced modified Kanizsa-type IC stimuli, termed "salient region" (SR) stimuli, which lacked bounding illusory contours but still retained a “first impression of global surface.” Using fMRI, they revealed similar LOC activations for both standard IC stimuli and these modified SR stimuli, and on this basis they concluded that the LOC participates in the rapid detection of SR but is not involved in IC-specific processing. Rather, they proposed that IC processing takes place via feedback to lower-tier visual cortical areas (areas V1 and V2), although it should be noted that they did not explicitly assess activity in these regions for IC processing. This thesis is clearly a temporal one, positing a specific sequence of events that is simply beyond the temporal resolution of fMRI to resolve.

Over the past years, we have developed an electrophysiological metric of IC sensitivity and have shown that IC sensitivity occurs during the latency range of the N1 component of the visual evoked potential (VEP) (Foxe, et al., 2005; Murray, Foxe, et al., 2004; Murray, et al., 2006; Murray, et al., 2002). This robust effect manifests as a more negative VEP deflection to stimuli when the inducers are oriented to form an IC than when no IC is induced, and is localized to bilateral LOC and posterior occipital areas. Hereafter, we will refer to this measure as the IC-effect, in keeping with the previous literature. We applied this metric to obtain the brain’s response to IC and SR stimuli. If Stanley and Rubin’s hypothesis regarding SR processing in LOC is correct, a clear set of predictions follows: initial activity in LOC should be identical for both conditions with a subsequent topographic or amplitude divergence (as the sharp “edges” are filled-in). If, on the other hand, LOC is in fact sensitive to ICs, initial LOC activity should be greater or even exclusive to the IC condition than to the SR condition.

Materials and Methods

Subjects

Thirteen (seven female) neurologically normal paid volunteers, aged 20-42 years (mean = 28.5±7.7 yrs.) participated. All subjects had normal or corrected-to-normal vision and were right-handed as assessed with the Edinburgh Handedness Inventory (Oldfield, 1971). Some of the participants who served had prior experience with ERP recordings while others were novice participants. None could be considered expert psychophysical observers. All subjects provided written informed consent, and the Institutional Review Board of the Nathan Kline Institute for Psychiatric Research approved all procedures. The study conforms to the principles outlined in the Declaration of Helsinki. Subjects received a modest monetary compensation ($10 per hour) for their participation.

Stimuli and Task

Stimuli were presented to subjects on a computer monitor located 92 cm away. Images appeared light gray on dark gray background. The “pacmen” inducers subtended 2.8°, along the 45° diagonals from the center at 3.6° eccentricity, producing illusory square shapes of 7° maximal height and width. This resulted in two types of experimental stimuli: 1) Kanizsa-type IC’s (Figure 2 A&C) and 2) SR’s – modified IC stimuli where inducers’ shape and alignment were altered to eliminate bounding contours but retained a global impression of an enclosed region (as described in Stanley & Rubin, 2003). Inducers were oriented to either form or not form an illusory contour (“IC-in” and “IC-out,” respectively). Likewise, SR stimuli were oriented either facing inward or outward (“SR-in and “SR-out,” respectively), see Figure 2. The support ratio (actual physical length over the entire contour length) for stimuli facing inward was 0.40 (Ringach & Shapley, 1996).

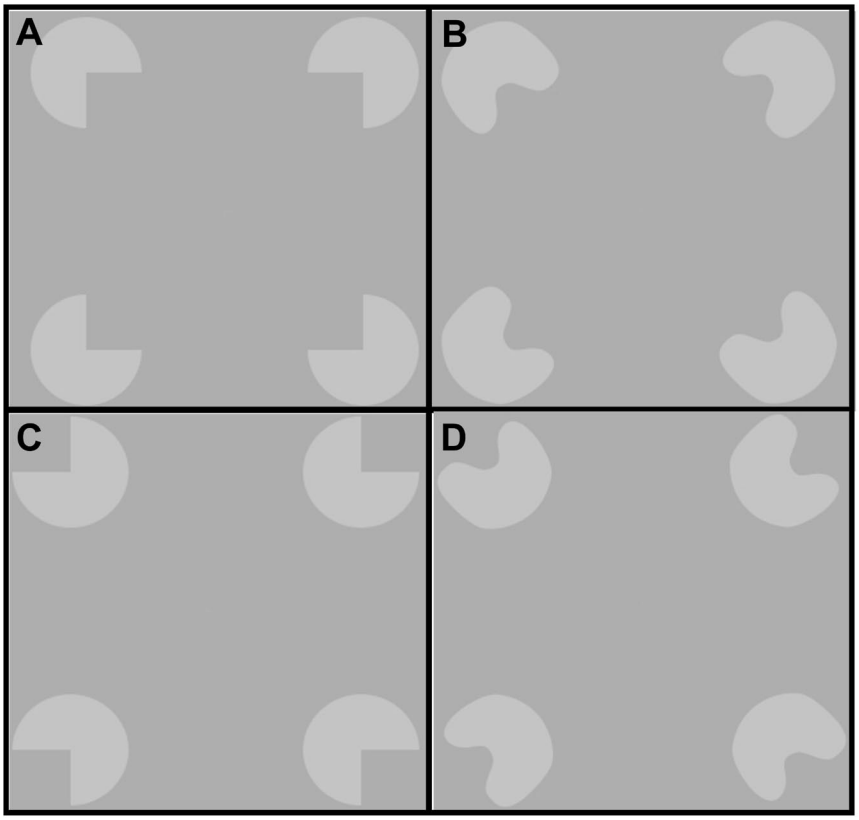

Figure 2. Illustration of the IC and SR Stimuli.

(a) IC-forming stimulus; to be viewed at 30 cm distance to simulate experimental conditions (i.e., 7° illusory contour), IN configuration. *(b)* SR-forming stimulus; to be viewed at 30 cm distance, IN configuration. *(c)* Control stimulus for the IC condition, OUT configuration. *(d)* Control stimulus for the SR condition, OUT configuration.

Stimuli were presented for 200 ms with an inter-stimulus interval incrementally varying from 1 to 2.5 seconds (in 250 ms steps). On each trial, subjects responded with a simple button push to indicate the presence or absence of a "shape" (i.e., contour). Subjects reliably indicated the presence of shapes for the IC condition (94$\pm$7% accuracy), whereas, on average, only 34$\pm$37% of SR stimuli were perceived as containing a shape.[5] The wide range for the perception

[5]While Stanley and Rubin (2004) did not have their participants perform a task during their fMRI recordings, a very basic task was introduced in the present study to ensure active viewing during the lengthy ERP recording. Murray *et al*., (2002) previously showed that the IC-effect is elicited during passive viewing and Murray *et al*., (2006) showed that drastically manipulating task-load did not impact the IC-effect. Thus, we were confident that any effects found would be independent of task parameters.

of a shape in SR condition stemmed from the fact that five subjects reported perception of a shape on may SR trials, while the rest of the subjects did not perceived a shape. Given the low error rates with IC stimuli, behavioral data will not be discussed in any further detail here. Each block contained 40 stimuli with all stimulus conditions randomized and equally probable. All subjects completed at least 30 blocks of the experiment, with 4 subjects completing 35 blocks. Note that VEP analyses included all trials, irrespective of whether an illusory shape was perceived. The study by Stanley and Rubin (2003) does not provide psychophysical data concerning if or how often their participants observed illusory contours with their SR stimuli during the fMRI task. Rather, the authors included all trials in their analyses.

Electrophysiological Data Acquisition

Continuous EEG was acquired through a Biosemi ActiveTwo system from 168 scalp electrodes, digitized at 512 Hz, and referenced to the CMS-DRL ground (which functions as a feedback loop driving the average potential of the subject, i.e. the Common Mode voltage, as close as possible to the AC reference voltage of the AD box, i.e. the amplifier zero). Epochs of continuous EEG (-200 ms before stimulus onset to 500 ms after stimulus onset) were separately averaged from each subject in response to each condition and stimulus type. An artifact rejection criterion of ±100 μV was used at all scalp sites to reject trials with excessive EMG, horizontal or vertical eye movements, and other noise transients. The average number of accepted sweeps per VEP was 216±46. Data from artifact electrodes from each subject and VEP were interpolated (Perrin, Pernier, Bertrand, Giard, & Echallier, 1987) according to their individually digitized electrode positions (Polhemus Fastrak, 3DspaceDX software, Neuroscan, Inc.) and then affined to the average electrode locations across our group of subjects. The mean electrode positions were in turn used during the calculation of the lead field matrix for the source estimations below.

Prior to group-averaging, VEP data were baseline corrected using the 100ms pre-stimulus period and also recalculated to the common average reference. Statistical and topographic mapping for all experiments in this study were performed on broadband data.

Analysis Strategy

A first level of analysis was performed separately for each stimulus type (IC and SR), using point-wise paired *t*-tests between VEP responses from "in" and "out" configurations. Data were referenced to the fronto-polar site for this analysis simply to facilitate comparison with our prior work detailing the timecourse of illusory contour sensitivity (Murray, et al., 2002). For each electrode, the first time point where the *t*-test exceeded the 0.01 α criterion for at least 11 consecutive data points (21.5 ms at a 512 Hz digitization rate) was labeled as onset of the effects (see Guthrie & Buchwald, 1991). The results of this analysis are displayed as a "statistical cluster plot" (see Figure 3b). The x-, y-, and z- axes respectively represent time (post-stimulus onset), electrode location, and the p-value of the *t*-test (indicated by a color value) at each data point.

Our remaining analyses were based on the comparison of differential responses to "in" and "out" configurations between stimulus types, using a set of analyses based on local and global measures of the electric field at the scalp. These analyses and their advantages over canonical VEP waveform analyses have been discussed in detail elsewhere (Michel et al., 2004; e.g., Michel et al., 2001). These analyses provide a statistically-based differentiation of effects that follow from modulation in the strength of responses of statistically indistinguishable brain generators from those that are the consequence of alterations in the configuration of these generators (viz. the topography of the electric field at the scalp).

The global response strength of the electric field was analyzed using the instantaneous Global Field Power (GFP) for each subject and stimulus type. GFP is equivalent to the spatial

standard deviation of the scalp electric field (Lehmann & Skrandies, 1980), and is calculated as the square root of the mean of the squared value recorded at each electrode (versus the average reference). GFP measures are used to minimize observer bias and provide a more concise view of the data. While different sources of electrical activity do not preclude identical GFP waveforms, identical topographic modulations with different GFP amplitudes can be parsimoniously interpreted as a modulation in the response strength within statistically indistinguishable configurations of underlying generators, as has been repeatedly demonstrated in prior investigations of illusory contour processes related to the difference between in and out configurations (Foxe, et al., 2005; Murray, et al., 2006; Murray et al., 2004; Pegna, Khateb, Murray, Landis, & Michel, 2002). Like the analysis of individual VEP waveforms represented in the statistical cluster plots, GFP waveforms were analyzed using a millisecond-by-millisecond paired t-test with an α criterion of 0.01 and a temporal constraint of a significant difference being observed for at least 11 contiguous data points.

Differences in response topography were statistically assessed using Global Dissimilarity (Lehmann & Skrandies, 1980), which is quantified as the square root of the mean of the squared difference between the potentials measured at each electrode (vs. the average reference), each of which is first scaled to unitary strength by dividing by the instantaneous GFP. Global Dissimilarity is therefore an index of configuration differences between two electric fields, independent of their strength. It can range from 0 to 2, where 0 indicates topographic homogeneity and 2 indicates topographic inversion between responses to different stimulus types. A Monte Carlo non-parametric bootstrapping procedure (Manly, 1997), termed topography analysis of variance or TANOVA, was used to identify statistical differences between each pair of stimulus types and was furthermore conducted as a function of time

(Murray, Brunet, & Michel, 2008). Because electric field changes are indicative of changes in the underlying generator configuration (e.g., Fender, 1987; Lehmann, 1987); this test provides a statistical means of determining if and when the brain network activated by IC and SR stimulus types differ. As above, we applied an α criterion of 0.01 and an 11-point temporal criterion.

Finally, intracranial sources of the "in" versus "out" difference were estimated for each stimulus type and subject using the local auto-regressive average (LAURA) distributed linear inverse solution (Grave de Peralta, Gonzalez, Lantz, Michel, & Landis, 2001; Grave de Peralta, Murray, Michel, Martuzzi, & Gonzalez Andino, 2004), which selects the best source configuration based on the biophysical behavior of electric vector fields according to electromagnetic laws (i.e. activity at one point depends on the activity at neighboring points according to electromagnetic laws detailed in Maxwell's equations). The version of LAURA used here employs a realistic head model with 3005 nodes arranged within the gray matter of the Montreal Neurological Institute's average brain. This implementation of LAURA was generated with the Spherical Model with Anatomical Constraints (SMAC; Spinelli, Andino, Lantz, Seeck, & Michel, 2000). Time periods for source estimations were chosen based on the above topographic analyses. As will be detailed below, two time periods were identified (154-203ms and 404-469ms). Mean differences in source estimations for each of these periods were calculated and then used to identify clusters of nodes for statistical analyses. A minimal spatial extent of 5 contiguous nodes was used and each included node had a mean scalar value of at least 50% of the maximal difference. A paired t-test on the un-subtracted values was performed on the mean scalar values across nodes within identified clusters.

Results

Previous research from our group has established an electrophysiological metric of illusory contour sensitivity – the IC effect – that is calculated as the VEP difference between inducer configurations that produce an illusory contour and those that do not. We applied this metric in the present study and calculated VEP differences for each stimulus class (i.e. IC and SR) by subtracting "out" (pacmen facing outward, not forming a contour) from the "in" (pacmen facing inward, forming a contour) conditions. Unsubtracted VEP waveforms from a set of exemplar posterior scalp locations situated at the maxima of the N1 topography are displayed in Figure 3a. Consistent with our prior studies, visual inspection of these group-averaged VEPs revealed a clear difference between "in" and "out" conditions that peaked during the N1 component at ~170ms post-stimulus onset. This modulation was prominent for IC, but not for SR stimuli. A first level of analysis was performed in order to facilitate comparison with our prior study that identified the spatio-temporal dynamics of Kanizsa-type illusory contour processing (Murray, et al., 2002). These analyses entailed a series of timepoint-by-timepoint paired t-tests between "in" and "out" conditions in response to each stimulus type (see Figure 3b and Materials and Methods for details). These statistical cluster plots indicate that IC stimuli resulted in a robust IC effect beginning at ~140-150ms, whereas SR stimuli did not produce the same effect. The general latency and morphology of the IC-effect is highly consistent with previous findings (Foxe, et al., 2005; Murray, Foxe, et al., 2004; Murray, et al., 2006; Murray, et al., 2002).

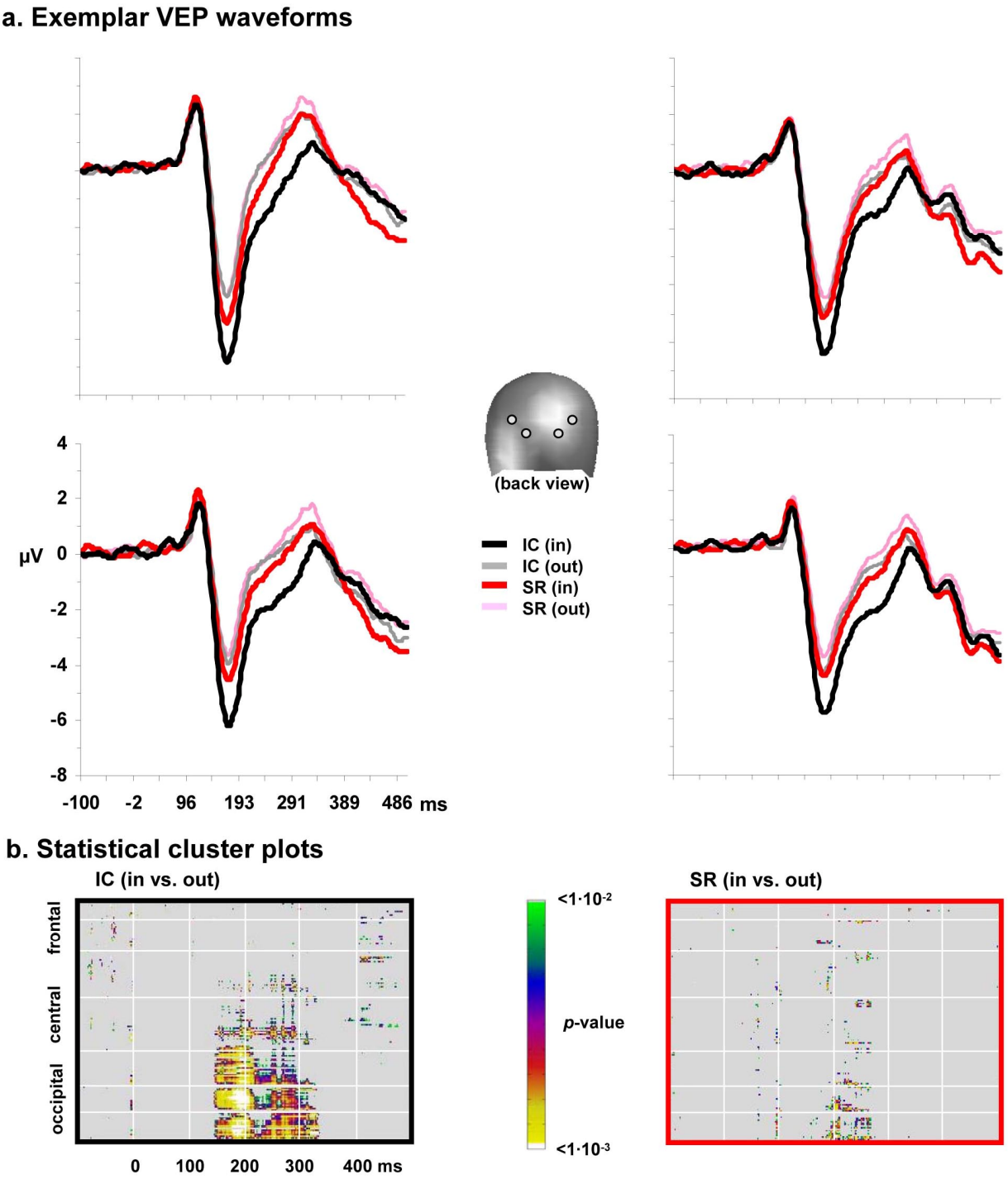

Figure 3. Electrophysiological Response to IC and SR Stimuli over the Entire Epoch.

(a) Group-averaged VEPs for each stimulus type over four posterior scalp sites (see inset for locations and color scheme). *(b)* Point-wise paired *t*-tests ("statistical cluster plots") comparing IN (pacmen facing in) vs. OUT (pacmen facing out) configurations of the three inducer types (p=0.01 threshold, over -100 to 500 ms time period). Color represents the result of the *t*-test. Electrodes are arranged left to right for seven scalp regions, demarcated by solid white lines: occipital, parieto-occipital, parietal, central, fronto-central, frontal, and fronto-polar.

To quantitatively assess commonalities and differences between stimulus types, we calculated VEP difference waveforms and conducted electrical imaging analyses on these differences. Difference waveforms at identical scalp locations to those depicted in Figure 3a are shown in Figure 4a. These locations are situated at the maxima of the "in" versus "out" difference across stimulus types, the topography of which is shown in Figure 5b. Visual inspection of these difference waveforms as well as the statistical cluster plots across the electrode montage (Figure 4b) revealed 2 general time periods of differential responses; one over the approximately 150-300ms time period and the other over the approximately 400-500ms time period. Specifically, there was a larger "in" vs. "out" differential response to IC stimuli over the earlier time period and a larger "in" vs. "out" differential response to SR stimuli over the later time period. Difference wave area measures over the 154-203 ms post-stimulus interval were submitted to a 2x2x2 repeated measures MANOVA, using stimulus type, hemiscalp, and electrode position as within subjects factors. Time periods for these statistical tests were defined based on the topographic analyses described above. There was a significant main effect of stimulus type ($F_{(1,11)}$=13.898; p=0.003), with higher differential effect of the IC than the SR condition. No other main effect and no interaction reached the 0.05 significance criterion. Identical analyses were conducted for the later time period, 404-469ms post-stimulus. There was a significant main effect of stimulus type ($F_{(1,11)}$=28.046; p<0.001), with higher differential effect of the SR than the IC condition. The three-way interaction between stimulus type, hemisphere and electrode also reached significance ($F_{(1,11)}$=6.533; p=0.027), suggestive of the different topographies for the two conditions over this time period that we detail below. No other main effect and no interaction reached the 0.05 significance criterion.

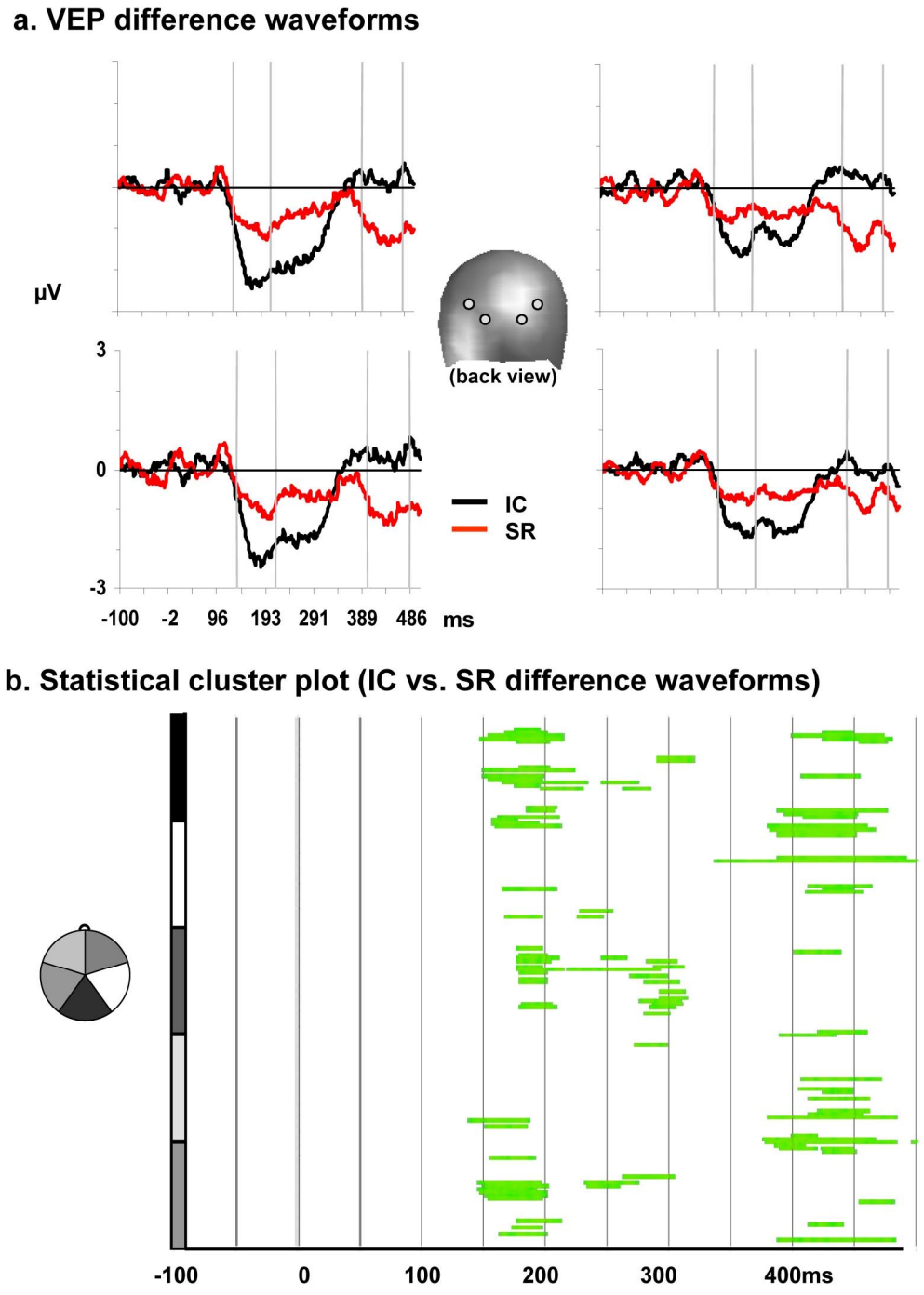

Figure 4. ERP Difference Waveforms (IN-OUT) to IC and SR Stimuli over the Entire Epoch.

(a) Group-averaged ERP difference waveforms over four posterior electrodes (see inset for locations and color scheme). Vertical lines indicate time periods of interest (154-203ms and 404-469ms). *(b)* Point-wise paired *t*-tests ("statistical cluster plots") comparing IC difference vs. SR difference responses (p=0.01 threshold, over -100 to 500 ms time period). Electrodes are arranged into five scalp regions along the vertical axis; regions are displayed to the left of the plot.

To better identify the neural generators underlying VEP differences between stimulus types, we first analyzed the Global Field Power (GFP) to assess modulations in response strength (see Figure 5a). A millisecond-by-millisecond t-test compared these waveforms, and temporally sustained differences were obtained over the 180-258ms and 275-328ms post-stimulus intervals (green trace in Figure 5a). More specifically, GFP was stronger over these intervals in response to IC than SR stimuli.

The difference topography (i.e., “in” vs. “out”) of the electric field at the scalp in response to each stimulus type was also statistically compared using non-parametric analyses of Global Dissimilarity. Temporally sustained topographic differences between IC and SR stimulus types were obtained over two intervals (blue trace in Figure 5a). The first occurred over the 154-203ms post-stimulus period, and the second over the 404-469ms post-stimulus period. These topographic effects are apparent upon inspection of sequential maps of the voltage topography at the scalp for each condition (Figure 5b). Over the earlier time period, IC stimuli exhibited a more focal and left-lateralized negative distribution over the posterior scalp. Over the later time period SR stimuli exhibited a more focal and bilateral negative distribution over the posterior scalp

Analyses to this point indicate that IC stimuli produce different effects than do SR stimuli, with the initial “in” vs. “out” difference being considerably stronger in magnitude and different topographically. This pattern runs contrary to what would be predicted if the previously reported *IC effect* simply indexed sensitivity to salient regions of visual space. Finally, group-averaged source estimations were calculated over the 154-203ms and 404-469ms post-stimulus intervals for each stimulus type (i.e., IC and SR “in-out” difference) and are shown in Figure 6a and b, respectively.

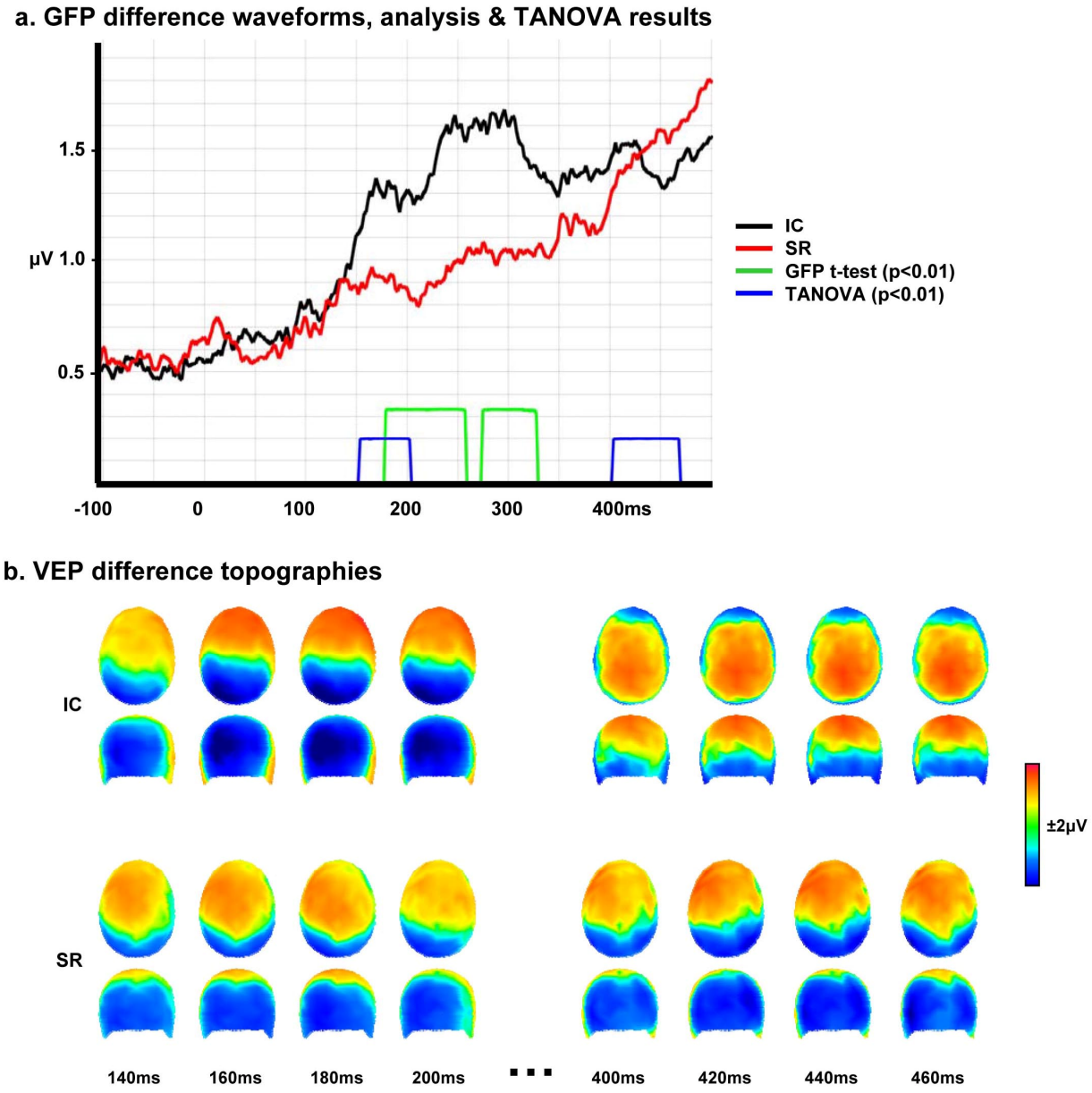

Figure 5. Electrical Imaging Results for IC and SR Subtractions.

(*a*) Group-average global field power (GFP ─ i.e., the spatial standard deviation of the ERP response, see page 26 for details) waveforms (see inset for the color scheme). Time-periods of significant GFP *t*-test and TANOVA analyses are demarcated on the x-axis. The TANOVA analysis compared response topography between difference waveforms (IN-OUT) for the two stimulus types as a function of time. Time intervals of significant (p<0.01) topographic difference using a non-parametric Monte Carlo bootstrapping procedure are displayed. *(b)*VEP difference waveform topographies for the two conditions.

Over the 154-203ms period, IC resulted in robust source estimations within the medial occipital cortex, the lateral occipital cortex, and inferior temporal cortex. By contrast, source estimations for SR stimuli were limited to the medial occipital cortex, with no evidence of strong sources within either lateral occipital or inferior temporal cortices. For both stimulus types, source estimations were stronger within the left hemisphere, consistent with the topography of the VEP (see Figure 5b). The mean difference between source estimations over the 154-203ms period is shown in the right panel of Figure 6a and illustrates that IC, but not SR stimuli, led to robust responses within the LOC (particularly within the left hemisphere; see clusters number 1 and 2). The Talairach and Tournoux (1988) coordinates of the maximal difference (SR-IC) in the left and right hemisphere were -52, -52, -8 mm and 51,-54,-3mm, respectively. These clusters extend across Brodmann's areas (BAs) 37 and 19. Statistical analysis of the mean scalar values from nodes identified within these clusters (see Methods for details) revealed that this cortical activation was stronger in the IC conditions for the left hemisphere cluster ($t_{(12)}$=3.65; $p<0.0035$) and with a non-significant trend for the right hemisphere cluster ($t_{(12)}$=1.78; $p=0.10$), reflecting stronger contributions from sources in the LOC (Figure 6c).

Over the 404-469ms period, both IC and SR resulted in strong sources within medial occipital cortices, lateral occipital cortices, and inferior temporal cortices. Additional weaker sources were evident within the inferior parietal cortex (Figure 6b). The mean difference between source estimations over this period is shown in the right panel of Figure 6b and illustrates that IC lead to stronger sources in left LOC, whereas SR lead to stronger sources in right LOC (clusters 3 and 4, respectively). The Talairach and Tournoux (1988) coordinates of the maximal difference (SR-IC) in the left and right hemisphere were -43, -68, -3 mm and 57,-53,-3mm, respectively. These clusters extend across Brodmann's areas (BAs) 37 and 19. Statistical

analysis of the mean scalar values from nodes identified within these clusters revealed no reliable difference within the left hemisphere cluster ($t_{(12)}$=1.06; p>0.30) and stronger responses in the SR condition within the right hemisphere cluster ($t_{(12)}$=2.40; p<0.035; see Figure 6c).

Figure 6. Source Estimations for IC and SR Subtractions.

Group-averaged LAURA distributed linear source estimations were calculated for the ERP difference waveforms over the 154-203ms time period (panel a) and the 404-469ms time period (panel b). The mean differences between these source estimations are shown in the right column. Significantly stronger contributions from LOC sources were found in the early time period for the IC condition (left Brodmann's area 19/37, cluster 1) and in the later time period for the SR condition (right Brodmann's area 37, cluster 4). *(c)* Mean scalar values of activations within clusters and *t*-test results between conditions.

a. Group-averaged source estimations (154-203ms)

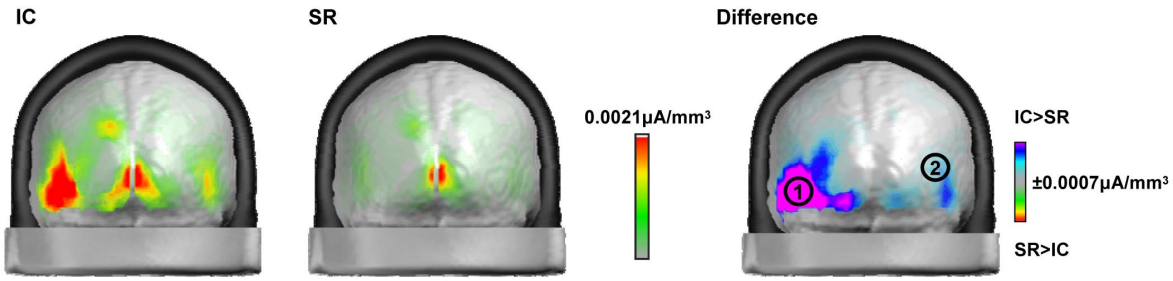

b. Group-averaged source estimations (404-469ms)

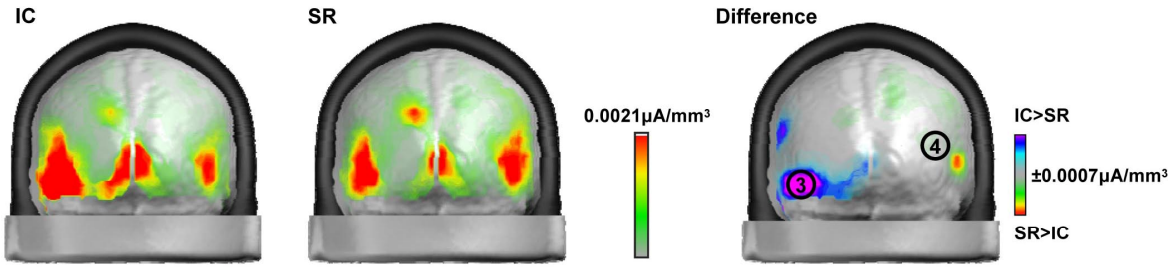

c. Mean scalar values within clusters

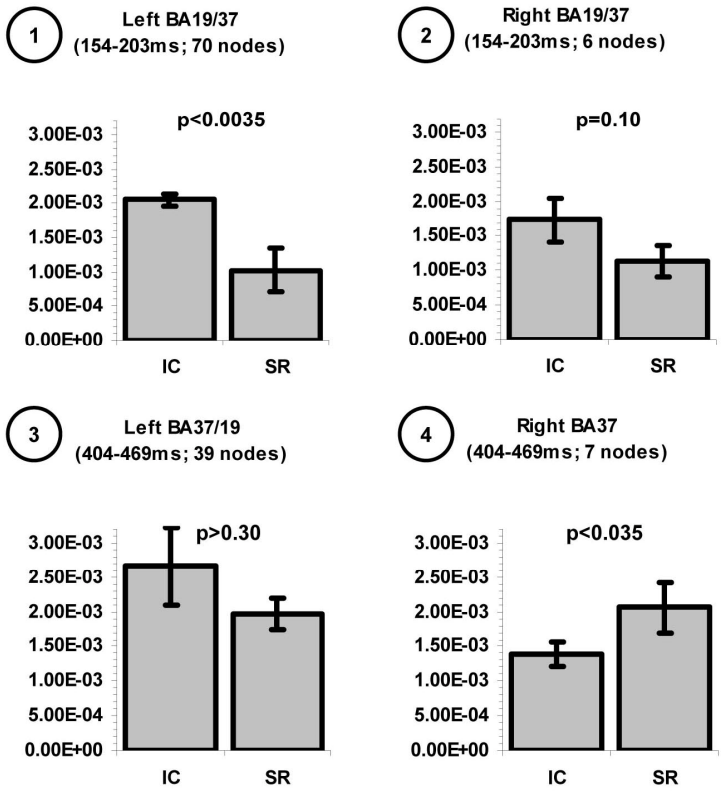

Discussion

The results of this study confirm those of previous studies showing initial IC sensitivity in the human LOC during the latency range of the N1 component (e.g., Foxe, et al., 2005; Halgren, et al., 2003; Kruggel, et al., 2001; Murray, Foxe, et al., 2004; Murray, et al., 2006; Murray, et al., 2002) and clearly argue against the proposition that crude region-based segmentation is the initial common stage for IC and SR processing in the LOC (Stanley & Rubin, 2003). Topographies during the N1 period were statistically different between IC and SR conditions starting around 150 ms and indicative of differences in the configuration of intracranial generators. Source estimations of the active generators during this period of visual completion were localized to higher-tier visual areas bilaterally within the ventral stream LOC, with stronger LOC sources in the IC condition (see Murray, et al., 2002; Sehatpour, et al., 2006). Over a later time period, LOC sources were stronger in the SR condition.

Predictions of the Salient Region Hypothesis

In the present study, we assessed the extent to which there were common mechanisms for IC and SR processing. Applying the Stanley and Rubin (2003) hypothesis to the VEP methodology, the clear prediction is that initial IC and SR effects should be identical in timing, locus and mechanism (reflecting the initial common sensitivity to salient regions within the LOC). Further, their model predicts that differences between IC and SR stimulus processing will emerge later in the lower-level cortical areas (V1/V2). In contrast, if the LOC is selectively responsive to illusory contours themselves, as we have previously proposed (Foxe, et al., 2005; Murray, et al., 2006), we should observe a stronger initial response to IC stimuli within the LOC. Under such circumstances, the topography of IC and SR responses could be identical (or different). The latter prediction is precisely the pattern of responses we observed. The initial

period of specific sensitivity to ICs within the LOC (as evidenced by a substantially stronger differential response between “in” and “out” conditions to ICs than to SRs) was also marked by a significant topographic difference between IC and SR responses, with the IC response relying more heavily on ventral stream sources than the SR response. We also conducted analyses of a later time period between 400 and 480 ms to provide an alternative explanation for the fMRI results observed by Stanley and Rubin (2003). Responses were of greater amplitude over occipital electrodes to SR stimuli during this later processing stage, possibly accounting for the equivalent fMRI activations between the conditions. That is, because the BOLD response measured using fMRI pools activity within a region over time, effects over the early and late timeframes are summed to produce equal IC and SR responses.

When VEP waveforms are considered in isolation, one could argue that the results of the present study indicate a quantitative rather than a qualitative difference between the two conditions. However, topographical analyses and source estimations clearly show that areas of the brain, specifically the LOC, are engaged differentially for the IC and the SR stimuli in the timeframe of N1.

Additional evidence against the salient region hypothesis can be gleaned from an earlier fMRI investigation that included stimulus conditions wherein illusory contours were induced by displaced line gratings, which unlike Kanizsa-type stimuli lack salient regions (c.f. Figure 1 of Mendola, et al., 1999). In this study, Mendola and colleagues observed the strongest differential responses to displaced versus control stimuli within the LOC. These results suggest that the illusory contour perception modulates LOC activity rather than information conveyed by line ends or salient regions. The present results provide further support for the LOC model of illusory contour processing and argue against the LOC model of rapid detection of salient regions.

Implications for the "Identity Hypothesis"

The results of the present study are also germane to a recent and often heated debate in the literature over the mechanisms of so-called modal and amodal[6] contour completion (see e.g. Anderson, 2007; Kellman, Garrigan, Shipley, & Keane, 2007). Kellman and colleagues (2005) have argued that the two classes of stimuli share a common initial mechanism for generating contour connections across space - the so-called "identity hypothesis." In response, Anderson (2007) has argued on the basis of single-cell recording studies (Bakin, et al., 2000; Ffytche & Zeki, 1996; Larsson, et al., 1999; Lee & Nguyen, 2001; Peterhans & von der Heydt, 1989; Ramsden, et al., 2001; Seghier, et al., 2000; von der Heydt & Peterhans, 1989) that modal and amodal stimuli do not share common mechanisms, in that these studies show differential responses in hierarchically early cortical regions. However, our series of studies has demonstrated that these differences in early cortical regions (i.e. V1 and V2) likely stem from feedback from higher order visual areas (Foxe, et al., 2005; Murray, Foxe, et al., 2004; Murray, et al., 2006; Murray, et al., 2002), thus reflecting a later perceptual mechanism (see also Lamme & Spekreijse, 2000). Further, Murray and colleagues (2004) demonstrated identical initial electrophysiological responses to modal and amodal stimuli in human observers. That is, we found identical *IC-effects* for both stimulus classes, and that these effects originated in the LOC bilaterally. Anderson dismissed these findings, stating that it was **"highly unlikely that the identical responses observed by Murray et al. (2004) have anything to do with contour interpolation processes"**, basing this assertion on the findings of Stanley and Rubin (2003). That is, he asserted that the LOC could not be involved in contour interpolation given the

[6] Illusory contour stimuli used in the present study are modal contours (see Figure 1). Amodal contours are contours occluded by a foreground object (see Murray et al., 2004 for examples).

equivalent fMRI activations in LOC for IC and SR stimuli. Clearly, this latter argument is not supported by the results of the current study.

Previous Event-related Potential Results

A previous study by Yoshino and colleagues (2006) compared VEP's to IC and SR stimuli in much the same fashion as was done here; but in complete opposition to the present findings, they concluded that LOC was responsible for crude region-based segmentation with subsequent IC boundary completion. In light of the present findings, a re-consideration of their data is warranted and we contend that their conclusions are thoroughly inconsistent with their reported pattern of results. First, Yoshino and colleagues report an interaction between inducer type, inducer orientation and electrode-site during the N1 latency; a result that they interpret as showing that the N1 potential was larger for IC than the other three conditions at certain electrode sites. But this is not the correct interpretation. Rather, this interaction points to the fact that certain electrode sites had a larger difference between IC-in vs. IC-out conditions than between SR-in vs. SR-out conditions, i.e. the N1 was more sensitive to IC processing. In fact, Yoshino and colleagues rightfully conclude that IC modulation can be "extracted from [the] N1 component". Looking at their figures 2 and 3, it is clear that the effect for ICs during N1 is substantially larger than for SRs, much like is seen here (note that the four electrodes illustrated in the present paper roughly correspond to the PO3 and PO4 electrodes analyzed by Yoshino and colleagues (2006), the electrodes which showed differential effects between IC and SR conditions).

Second, the progression of events observed by Yoshino and colleagues is very similar to the timecourse of activations observed in our study. The "IC effect" ("in" vs. "out") is reported to start at 70 ms post stimulus onset. The authors further report bilateral LOC sources of

activation over 110-180 ms time range. The earliest topographic difference between ICs and SRs begins at 170 ms in their dataset. It follows that the earliest activity in LOC (110-170 ms) was an amplitude modulation (see interaction described above), most sensitive to IC stimuli, and stemming from identical intracranial generators. Consequently, the study of Yoshino and colleagues is fully consistent with the results of our study. As we have discussed previously, the salient-region hypothesis has to be rejected when initial LOC activation is more sensitive to IC stimuli with or without a concurrent topographic difference between IC and SR. The former is the result observed by Yoshino and colleagues; the latter is the result observed in this study.

Stipulating the Contour Detection Mechanism

The results of this study are consistent with a model of IC processing in humans whereby initial IC sensitivity takes place in the lateral occipital cortex (LOC), a complex of higher order visual areas (Foxe, et al., 2005; Halgren, et al., 2003; Kruggel, et al., 2001; Murray, Foxe, et al., 2004; Murray, et al., 2006; Murray, et al., 2002; Ritzl et al., 2003a). This initial activity in the LOC is followed by feedback to V1/V2 and likely thereafter involves recurrent rounds of feedback and feedforward information flow between higher-tier regions with their large receptive fields and lower-tier small receptive field regions. A similar sequence of events has been very convincingly demonstrated by Lamme and colleagues using intracranial recordings in non-human primates for a related class of stimuli, so called figure-ground textures (Lamme & Spekreijse, 2000). Interestingly, an fMRI study of IC processing reported higher V1 activity and a simultaneous decrease in LOC activity as a result of perceptual learning (Maertens & Pollmann, 2005). The authors proposed that initially IC processing relied heavily on LOC, whereas, with learning, local connections in V1 were strengthened. The later sweep of activity in the LOC (here around 400-500ms) represents more effortful perceptual closure mechanisms,

previously implicated in object-recognition for difficult-to-recognize fragmented objects and also in illusory contour studies (Doniger, et al., 2002; Doniger, et al., 2000; Murray, et al., 2002; Sehatpour, et al., 2006; Sehatpour, et al., 2008).

While we agree with Stanley and Rubin (2003) that contour integration processes must be preceded by a more general spatial segmentation process, we show that this general segmentation process does not rely on the LOC. Rather, our results are more consistent with the "frame-and-fill" theory of visual processing, see Figure 1 (Chen, et al., 2007). This theory maintains that an initial "framing" of the scene is processed by structures of the dorsal visual stream, which in turn feeds into ventral stream structures, where the slower parvocellular system "fills in" the details (Bar, 2003; for similar models see Vidyasagar, 1999). Crude region-based segmentation can be viewed as a form of spatial processing, more consistent with the functions of the dorsal stream (e.g., Mishkin, Lewis, & Ungerleider, 1982). Due to the rapid nature of the magnocellular dorsal pathways, crude region-based segmentation is expected to happen relatively early after stimulus onset and earlier than the N1 timeframe (Chen, et al., 2007), likely during the earlier P1 latency (65-100ms). Dorsal stream generators have been shown to contribute substantially to the P1 component (Di Russo, et al., 2002; Foxe, Doniger, & Javitt, 2001; Foxe, et al., 2005), and the P1 is well-known to be responsive to spatial attentional manipulations (e.g., Hillyard & Mangun, 1987; Martinez et al., 1999). Consistent with this notion, Murray et al. (2002) described P1 sensitivity to the spatial distribution of their IC inducers (the pacmen). P1 amplitude systematically increased as the eccentricity of the inducers increased. Importantly, this effect was independent of the presence vs. absence of illusory contours; identical effects were obtained for outwardly and inwardly turned inducers. In the present study, no differences in brain activation were observed prior to the N1 timeframe, as all stimulus types (both inward and outward facing

pacmen) could be considered as equally effective in delineating the spatial extent of the scene. VEP studies directly manipulating spatial aspects of the scene will clearly be necessary to further test this interpretation.

In conclusion, our data show that LOC is considerably more sensitive to illusory contour stimuli than salient region stimuli during early sensory-perceptual processing as measured with temporally precise electrophysiological methods in humans. These results suggest that prior fMRI evidence of equivalent IC and SR responses within the LOC likely reflects temporally-integrated responses. We reject the hypothesis that the common process of spatial segmentation takes place in LOC and, instead, propose that it is more likely to happen in the dorsal stream prior to the earliest processing in LOC.

CHAPTER 2

Interrogating the "Frame and Fill" Model of Visual Object Completion: Electrophysiological Mapping of Illusory Contour Processing Under Cluttered Viewing Conditions

Introduction

As we parse our visual environment, we are necessarily confronted with overlapping objects and surfaces. Observers can readily perceive objects, even when they are partly blocked by other objects or partly invisible due to low ambient lighting. Moreover, humans, other mammals and even birds, have demonstrated capacity to infer illusory boundaries across gaps (Nieder, 2002). Illusory contours (IC) can be induced by defining boundaries with several non-overlapping "pacmen" to create the so-called Kanizsa figure (Kanizsa, 1976; see Figure 1, top left box). The visual system completes the gaps between the "pacmen," resulting in the perception of a shape floating in the foreground.

Over the past decade, advances in the understanding of the anatomical and functional connectivity between regions of the brain and the temporal dynamics thereof gave rise to a new school of thought on visual perception, sometimes referred to as "frame and fill" models (see Figure 1). According to such models, coarse low spatial resolution information is first transmitted through the dorsal visual stream ("frame") to guide the refinement of visual information over the slower ventral stream ("fill") (Bar, 2003; Bullier, 2001; Chen, et al., 2007; Vidyasagar, 1999). The dorsal stream frames a general template to be filled in by recurrent processing within the ventral stream. While such a cortical mechanism could successfully explain a lot of existing experimental observations (see for examples Bar 2003), there is a paucity of physiological data directly testing the predictions of this model in humans.

We wished to investigate whether placing higher processing demands on the "framing" step of the model would interfere with the "filling in" step. We used the highly replicable effects from the illusory contour and object recognition literature (described below) as our metrics of ventral stream processing. Neurophysiological studies of illusory contour processing have implicated lateral occipital regions in the initial contour-related activity, stronger for the illusory contour arrays as compared to the same arrays arranged so as not to form a contour (Fiebelkorn, Foxe, Schwartz, & Molholm, 2010; Foxe, et al., 2005; Halgren, et al., 2003; Kruggel, et al., 2001; Mendola, et al., 1999; Murray, Foxe, et al., 2004; Murray, et al., 2006; Murray, et al., 2002; Pegna, et al., 2002; Ritzl, et al., 2003a; Shpaner, et al., 2009). This initial activity manifests itself as an amplitude modulation of the N1 component of the event-related potential (ERP), termed the N1 IC effect (e.g., Murray et al., 2002). Neuroimaging studies in humans (Kruggel, et al., 2001; Mendola, et al., 1999; Murray, et al., 2002; Ritzl, et al., 2003a) and electrophysiological recordings in animal models (Ahissar & Hochstein, 2000; Sary et al., 2007; Sary et al., 2008) have confirmed the involvement of the lateral occipital regions in illusory contour processing. A complementary line of inquiry in our laboratory has focused on the neural correlates of object completion. In that set of studies, we have defined a later modulation of cortical generators within the lateral occipital regions related to conscious identification of objects, which we have termed the Ncl effect (for "closure" negativity) (Doniger, et al., 2002; Doniger, et al., 2000; Doniger, et al., 2001; Sehatpour, et al., 2010; Sehatpour, et al., 2006; Sehatpour, et al., 2008). We have consistently observed a very similar modulation in the illusory contour studies, suggestive of a similar object-related identification process (see also, Murray, et al., 2006 for the role in shape discrimination). While the *N1 IC* effect appears to be automatic, in that it is unaffected by attention or task demands (Murray et al., 2002, 2006) the Ncl effect

appears to represent a second phase of more effortful "conceptual" processing within the same general regions of the LOC (see Doniger, et al., 2001; Foxe, et al., 2005; Senkowski, Rottger, Grimm, Foxe, & Herrmann, 2005; Tulving & Schacter, 1990).

Most of the illusory contour studies cited above used very simple arrays of elements, whereby all the displayed "pacmen" served to create the perception of a single (or continuous) illusory object. As such, it could be argued that since all displayed elements were constituents of the ultimate object, the "framing" step of the process was not taxed to any great degree. To investigate the influence of spatial "framing" on contour interpolation, we systematically varied the number of "pacmen" displayed on the screen. The extra "pacmen" randomly surrounded the contour-inducing elements in order to clutter the visual array (Figure 7). Using the N1 IC and the Ncl effects as our dependent measures, we compared ERP responses to three clutter levels: no-distracter (ND), low-distracter (LD) and high-distracter (HD). We hypothesized that if "framing" of the scene is the necessary prerequisite for successful object and contour perception, increased levels of clutter should influence and delay the automatic neural process (i.e., the N1 IC effect), but may have little effect on the later object identification-related response (i.e., the Ncl). A systematic decrease in amplitude or a temporal delay in the N1 IC effect from ND to HD, potentially disappearing altogether at a certain level of clutter, would support our prediction.

Materials and Methods

Subjects

Sixteen neurologically normal paid volunteers participated. One participant was dropped from the study due to excess low frequency artifact. One participant was dropped due to excessive baseline alpha-band activity. The remaining fourteen participants (4 female) were between 19 and 50 years of age (mean age = 26±9). All participants had normal or corrected-to-

normal vision, were right-handed as assessed with the Edinburgh Handedness Inventory (Oldfield, 1971). All participants provided written informed consent. All procedures conformed to the principles of the Helsinki declaration and were approved by the Institutional Review Boards of both The City College of New York and The Nathan Kline Institute. Participants received a modest monetary compensation ($12 per hour).

Design and Task

We used pacmen to create six types of experimental displays. Pacmen either formed an illusory shape, an illusory contour of a triangle (henceforth, IC), or were rotated not to form a contour (henceforth, NC) (see Figure 7). Three levels of clutter were created: 1) no distractor (henceforth, ND); 2) low distractor (henceforth, LD), with the central triangle surrounded by six randomly oriented pacmen; 3) high distractor (henceforth, HD), with the central triangle surrounded by twelve randomly oriented pacmen. Stimulus arrays appeared black on a gray background. Three different displays were created for each level of clutter by changing the orientation and/or the position of the pacmen (with the natural exception of the ND IC condition, which could only be created one way). Pacmen were presented centrally on the screen. The cluttered arrays (LD and HD) subtended a maximum of 5.84° of visual angle vertically and horizontally. The ND arrays were smaller, and only subtended 2.28° of visual angle. The illusory contour formed by the pacmen subtended 1.28° vertically and horizontally, with a 0.36 support ratio (ratio of the gap to the length of the illusory shape edge). Stimuli subtending over different regions of space would necessarily result in different neuronal activity and different distribution of responses over scalp. However, our analyses were limited to direct comparisons between spatially equivalent stimulus arrays, that is, we analyzed contour-related effects (IC vs. NC) across clutter levels. Stimuli were presented randomly for 400 ms with an average inter-stimulus-

interval (ISI) between the trials of 900 ms (ranging randomly from 600-1200ms). A total of 250 trials for each condition were presented across twenty blocks. Participants were instructed to maintain fixation on a central fixation dot and monitor for occasional changes of this dot into a square by a button press. The goal here was to make sure that participants maintained central fixation throughout the experiment and that they attended to the visual stimulation. The square appeared simultaneously with the experimental displays on fifteen percent of all trials (i.e., on average about every 7 seconds). Trials overlapping with the fixation change were discarded.

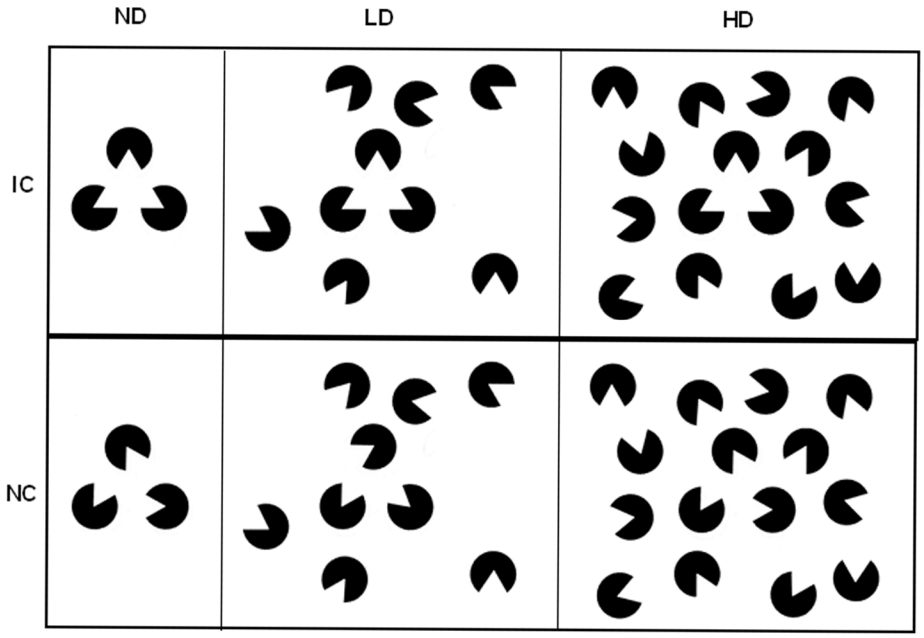

Figure 7. Exemplar Stimulus Arrays Across Clutter Levels**.**

IC-forming stimuli are displayed in the top row, control NC stimuli are displayed in the bottom row. Left-most column displays uncluttered IC stimuli, middle column displays low level of clutter (i.e., 6 extra distracter pacmen), right-most column displays high level of clutter (i.e., 12 extra distracter pacmen).

Electrophysiological Data Acquisition and ERP Derivation

Continuous EEG was acquired through a Biosemi ActiveTwo system from 72 scalp electrodes, digitized at 512 Hz, and referenced to the CMS-DRL ground (which functions as a

feedback loop driving the average potential of the subject, i.e. the Common Mode voltage, as close as possible to the AC reference voltage of the AD box, i.e. the amplifier zero). EEG processing and analyses were performed using the Cartool software by Denis Brunet (http://brainmapping.unige.ch/cartool.htm). Epochs of continuous EEG (-100 ms before stimulus onset to 400 ms after stimulus onset) were separately averaged from each subject in response to each stimulus type. An artifact rejection criterion of ±75 μV was used at all scalp sites to reject trials with excessive EMG, horizontal or vertical eye movements, and other noise transients. The average number of accepted sweeps per condition was 208±27 with a range of 146 to 243 sweeps. Data from electrodes containing major noise transients for each subject and ERP were interpolated according to the average digitized electrode positions for the particular electrode cap array (Perrin, et al., 1987). Prior to group-averaging, ERP data were recalculated to the fronto-polar reference (Fpz) and baseline corrected around stimulus onset from –50 to +20ms. Statistical and topographic mapping for all experiments in this study was performed on broadband data. A 45Hz low-pass filter was used in waveform figures purely for ease of visualization.

Detection of Temporal Effects

To calculate the timing of illusory contour sensitivity, we employed point-wise paired *t*-tests between ERP responses for each condition. The method allowed us to identify the onset of differential IC responses across the three clutter conditions. For each electrode, the first time point where the *t* test exceeded the 0.05 α criterion across a temporal cluster of no fewer than five consecutive data points (9.77 ms at a 512 Hz digitization rate) was labeled as the onset of the effects (see Wylie, Javitt, & Foxe, 2003 for rationale).

Statistical Analyses of the ERP Components

We used the N1 and the Ncl components as established metrics of illusory contour sensitivity to compare IC effects across different conditions of clutter. The temporal windows for analyses of the N1 and the Ncl ERP components were defined based on the results of the topographic pattern analysis, described below. Mean amplitude measures over time of the N1 and the Ncl components were submitted to a 2x3x2 Multivariate Analysis of Variance (MANOVA) with the factors of contour presence, clutter level and hemisphere using PASW Statistics 18. The following time-periods were used: 160-188 ms for the N1 and 250-283 ms for the Ncl. Electrodes for all tests were picked based on the peak N1 amplitude electrode in the group average data (P9 and P10), consistent with previous work (Murray et al., 2002). Since we made *a-priori* predictions regarding the direction of contour effects across different levels of clutter, protected follow-up comparisons were set up to compare the magnitudes of contour effects between conditions. We used three 2x2x2 MANOVAs with the factors of contour presence, clutter level and hemisphere. It should be noted that the early and late P1 components were not analyzed since stimulus arrays did not match in low-level visual characteristics across the three levels of clutter. Effects were deemed significant at 0.05 α level for all tests.

Topographic Analyses

To further characterize electric field potentials for the different types of stimuli, periods of stable topography were estimated using topographic pattern analysis (Michel, et al., 2001). A modified cross-validation criterion determined the number of maps that explained the whole group-averaged data set (Pascual-Marqui, Michel, & Lehmann, 1995). This method is reference independent and insensitive to pure amplitude modulation across conditions and over time. Different topographic maps reflect differences in the active generators of the brain. The maps

obtained as a result of the above procedure were used to define the stable topographic time periods for ERP statistical analyses (MANOVAs).

In order to statistically identify periods of topographic modulation, the topographic analysis of variance (TANOVA) procedure was used. This method computes global dissimilarity (Lehmann & Skrandies, 1980) between conditions for each time point of each subject's data. Global dissimilarity is an index of configuration differences between two electric fields, independent of their strength. This parameter equals the square root of the mean of the squared differences between the potentials measured at each electrode (vs. the average reference), each of which is first scaled to unitary strength by dividing by the instantaneous standard deviation. Dissimilarity can range from 0 to 2, where 0 indicates topographic homogeneity and 2 indicates topographic inversion. A Monte Carlo MANOVA is then applied (Manly, 1997) to test for statistical differences in the dissimilarity between conditions. This is a nonparametric bootstrapping procedure, wherein each subject's data from each time point is permutated such that they could "belong" to either stimulus condition. The dissimilarity is then calculated for each of 10000 such permutations for each time point and is used to generate a distribution of values against which the observed data are compared. From this, we determined the probability of obtaining a dissimilarity value from the permutations that exceeded the actual measured value. Since electric field changes are indicative of changes in the underlying generator configuration (Lehmann, 1987); this test provides a statistical means of determining if and when the brain network activated by the two conditions differs.

Results

In this investigation of IC processing under varying conditions of clutter, we used a well-established electrophysiological metric of illusory contour sensitivity – the IC effect. We examined how adding distractors to obscure the salience of the illusory contour influences this highly replicable ERP difference between inducer configurations forming an illusory contour and those not forming a contour. This effect reflects modulations in the strength of neural generators in the N1 IC and the Ncl timeframes respectively. ERP waveforms from a set of exemplar posterior scalp locations situated at the maxima of the N1 topography are displayed in Figure 8 (panels A-F). Consistent with our prior studies, visual inspection of these group-averaged ERPs revealed a clear difference between IC and NC conditions that peaked during the N1 component at ~170ms post-stimulus onset for the ND condition. The magnitude of this modulation gradually decreased across the clutter conditions; it was largest for the ND condition, smaller in the LD condition and appeared to be entirely absent in the HD condition.

Analyses of the N1 IC and the Ncl effects

Our first level of analysis was aimed at illuminating the differences in the temporal processing of the ICs across the distracter conditions. To this end, we performed a series of timepoint-by-timepoint paired *t*-tests between IC and NC conditions in response to each distracter level over the entire electrode array see Figure 8 (panels G-J and Materials and Methods for details). These statistical cluster plots indicate that ND and LD stimuli induced a robust N1 IC effect beginning at around 146 ms, whereas HD stimuli resulted in a much more delayed effect around 223 ms, already in the Ncl timeframe. Although a single posterior electrode (P8) in the LD condition met our statistical criterion somewhat earlier at 128 ms, the timing of the majority of occipital electrodes in the ND and LD conditions did not differ. The

general latency and morphology of these IC-effects is highly consistent with previous findings (e.g., Foxe, et al., 2005; Halgren, et al., 2003; Kruggel, et al., 2001; Murray, Foxe, et al., 2004; Murray, et al., 2006; Murray, et al., 2002; Pegna, et al., 2002; Shpaner, et al., 2009).

To quantitatively assess the influence of clutter on IC salience, we submitted the ERP data across all conditions to an omnibus MANOVA. The MANOVA revealed an effect of condition ($F_{(2,12)}$=12.054; p=0.001), reflecting different N1 amplitudes across conditions. This amplitude difference was likely due to the differences in the low-level visual characteristics between conditions. There was also an interaction between contour and condition ($F_{(2,12)}$=5.183; p=0.024), due to larger contour effects in the ND and LD conditions than the HD condition. Notably, the main effect of contour did not reach significance threshold ($F_{(1,13)}$=6.612; p=0.23). No other main effect and no interaction reached the 0.05 significance criterion.

To further characterize the interaction between contour and condition, we conducted protected pair-wise comparisons across different conditions. When we compared ND and LD contour effects, there was the main effect of contour ($F_{(1,13)}$=12.154; p=0.004), reflecting the IC effect in both conditions, i.e. higher N1 amplitude for the IC stimuli. The main effect of condition reached significance with higher amplitude of N1 for the ND condition ($F_{(1,13)}$=7.319; p=0.018). Importantly, there was no interaction between condition and contour ($F_{(1,13)}$=0.193; p=0.668). The N1 effect between ND and LD conditions was equivalent. Next, we compared the ND and the HD conditions. We found the main effect of condition ($F_{(1,13)}$=21.859; p<0.001), reflecting the different N1 amplitudes between these conditions; and an interaction between contour and condition ($F_{(1,13)}$=8.366; p=0.013), reflecting absence of the IC effect in the HD condition. The interaction between electrode and conditions also reached significance ($F_{(1,13)}$=7.127; p<0.019), due to the more negative N1 in the left hemisphere than the right

hemisphere in the ND condition. Finally, the comparison of LD and HD conditions revealed the main effect of condition ($F_{(1,13)}$=19.319; p<0.001) and an interaction of contour and condition ($F_{(1,13)}$=9.176; p=0.01). The interaction between electrode and conditions also reached significance ($F_{(1,13)}$=5.595; p<0.034), due to the more negative N1 in the left hemisphere than the right hemisphere in the LD condition. Both the ND and the LD waveforms exhibited a lateralization of the N1, while the HD waveforms did not. No other main effect or interaction reached the 0.05 significance criterion. These tests confirmed robust *N1 IC* effects in the ND and LD but not the HD conditions. The absence of the IC effect in the HD condition is highlighted by the topographic display of the subtraction between IC and NC waveforms (Figure 10). The ND and LD subtractions reveal clear amplitude modulations over a number of posterior electrodes, while the HD condition appears to be flat across the electrode array.

We proceeded to further characterize the IC effects over the Ncl time-window. Here, the omnibus MANOVA revealed the main effect of contour ($F_{(1,13)}$=14.833; p=0.002), reflecting more negative deflection for IC-forming stimuli across all conditions. The main effect of condition was also significant ($F_{(2,12)}$=19.529; p<0.001); waveforms were more negative overall for the ND than the LD than the HD conditions. Importantly, there was no interaction between contour and condition ($F_{(2,12)}$=.392; p=0.684). All three clutter conditions resulted in IC-related modulation over the Ncl time-window. The extent of the IC effects can be estimated from the topographic display of the subtraction between IC and NC waveforms (Figure 10). The ND and LD subtractions reveal widely distributed modulations over a number of posterior electrodes, while the HD subtraction is not as extensive.

Figure 8. ERP Waveforms Across Clutter Levels and Statistical Cluster Plots

Top-most row (panels A, B, G) displays no-distracter condition, middle row (panels C, D, H) displays low-distracter condition, bottom row (panels E, F, J) displays high-distracter condition (stimulus arrays are included for easy referencing). N1 IC effect is apparent in the ND and LD conditions, but not the HD condition. Ncl differences are present across all clutter levels. IC waveforms are in red, NC waveforms are in blue. The waveform plots display activity in the P9 (orange boxes) and P10 (green boxes) electrodes. The position of the electrodes is marked in the insert of panel A. The statistical cluster plots (panels G, H, J) depict the results of the pair-wise running t-tests (threshold criterion of $p<0.05$ for 9.77 consecutive ms). The onset of IC effects is similar for ND and LD conditions, but significantly delayed for HD condition. Abscissa is time in ms for both the waveforms and the statistical cluster plots; ordinate is amplitude in μV for the waveforms and electrode identity for the statistical cluster plots (the approximate electrode location is color-coded according to a stylized head in the insert of panel G).

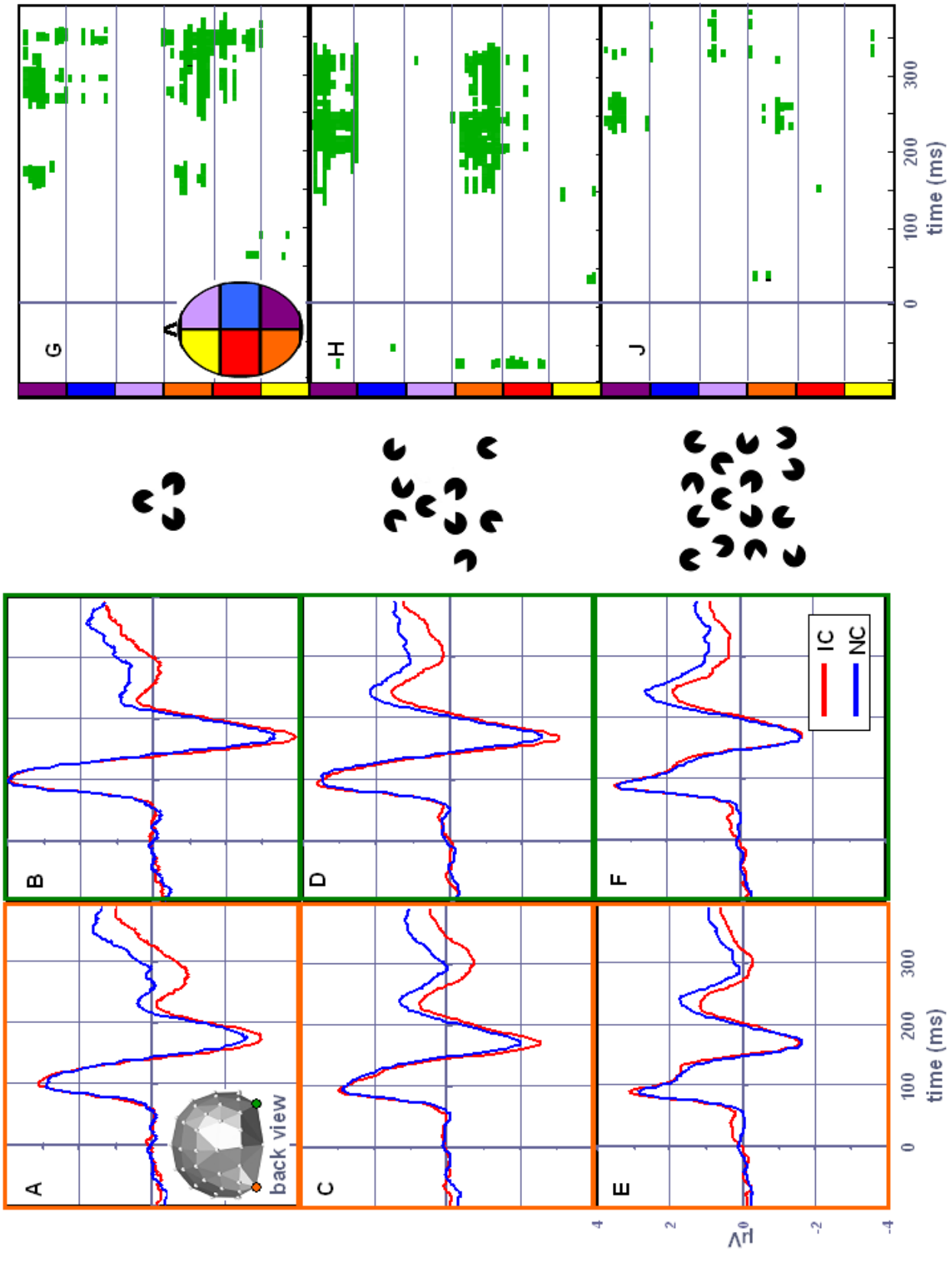
A
B
C
D
E
F
G
H
J
back view
IC
NC
μV
time (ms)
time (ms)

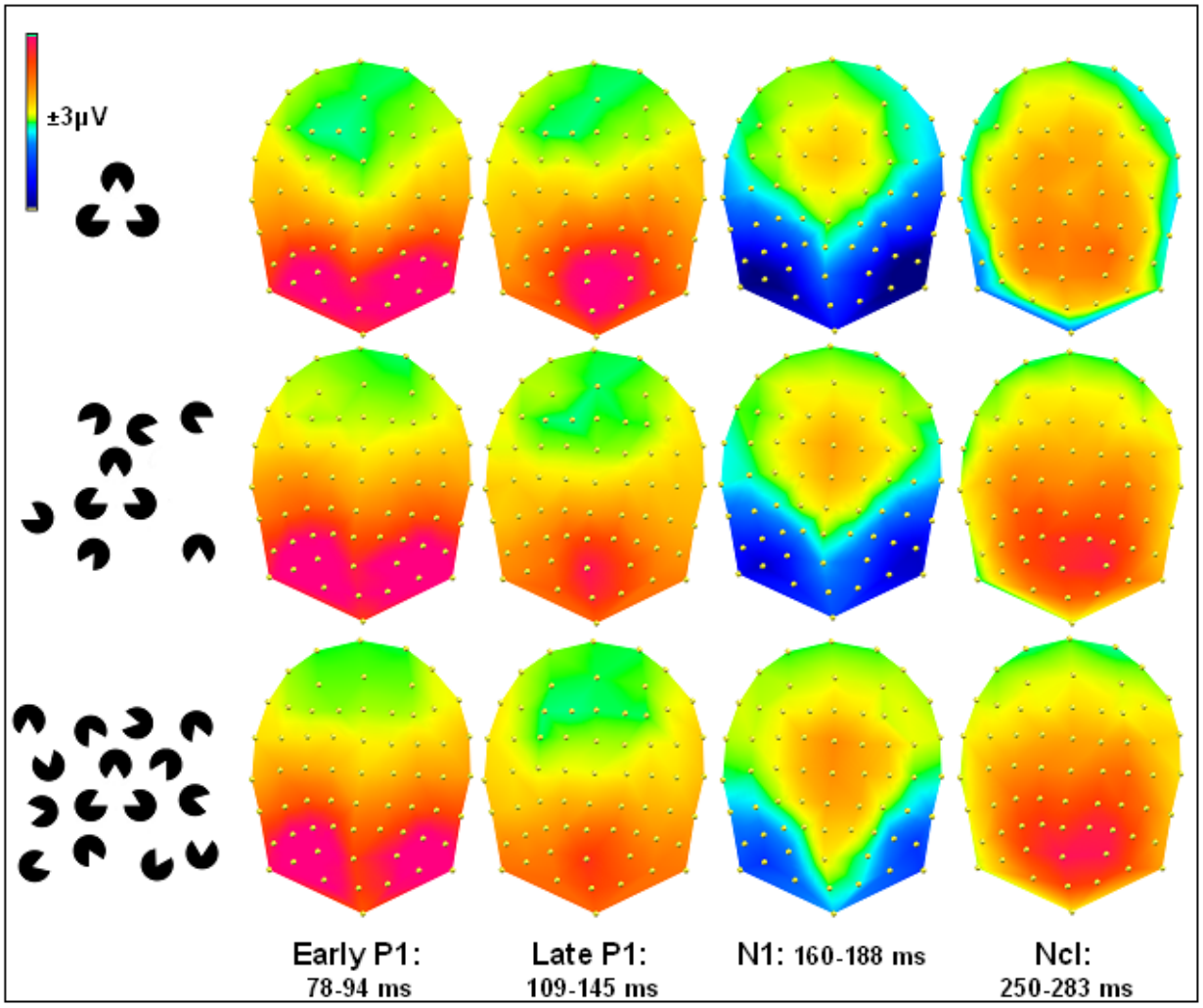

Figure 9. Scalp Topographies Across Clutter Levels

Topographies for different clutter conditions are displayed on a flattened electrode array. Time periods were defined based on the topographic pattern analysis procedure. Top-most row displays no-distracter condition, middle row displays low-distracter condition, bottom row displays high-distracter condition (stimulus arrays are included for easy referencing). Since topographies did not differ between IC and NC conditions in the P1, N1 and early Ncl time-periods, only a single topography is depicted.

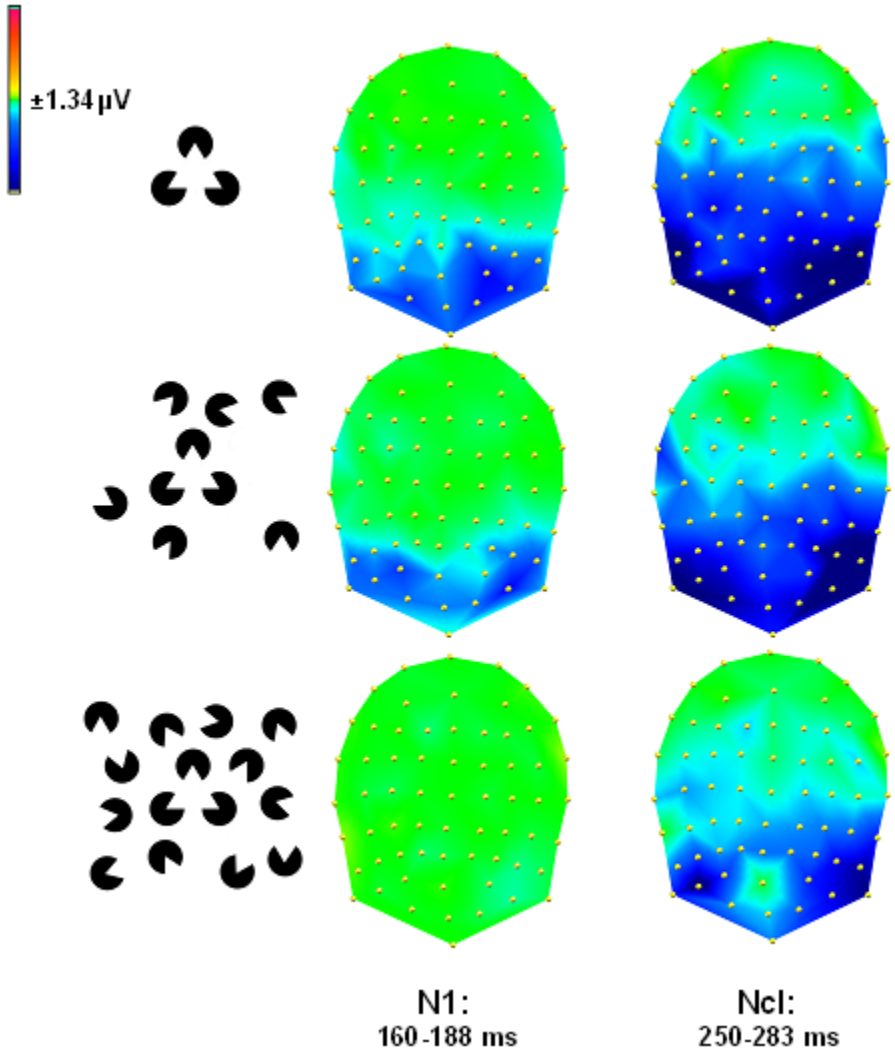

Figure 10. IC-NC Subtraction Topographies Across Clutter Levels.

Subtraction topography of contour-forming and control conditions in the N1 IC and the Ncl timeframes are displayed on a flattened electrode array. N1 IC effect is present in the ND and LD conditions but is absent in the HD condition. Ncl effect is present in all conditions, albeit weakened in the HD condition.

General Topographic Analyses

The IC effect topography in response to each stimulus type was also statistically compared using non-parametric analyses of Global Dissimilarity. Temporally sustained topographic IC differences between IC and NC stimuli were detected over 266-275 ms and 293-315 ms timeframes for the ND condition and over 275-334 ms timeframes in the LD condition. Interestingly, no topographic differences were observed in the HD condition. Due to their relatively late timing, these topographic differences are likely to reflect higher-order object-recognition processes. Visual observation of the topographies between distracter conditions also reveals topographic differences across all timeframes with the notable exception of the late P1 timeframe (109-145 ms). When we performed the same statistical analysis between distracter conditions in a pair-wise fashion (i.e., comparing ND vs. LD, LD vs. HD & ND vs. HD), we observed early (80, 95, and 82 ms onset, respectively) and sustained effects over the early P1 timeframe, the N1 timeframe and the Ncl timeframe. These effects were likely due to differences in retinotopic organization of our stimulus set and to the inherent differences between clutter conditions in terms of overall stimulus energy (i.e., number of elements).

Discussion

The results of this study indicate that increasing the difficulty of global scene analysis influences the neural timecourse of illusory contour perception. The earliest phase of IC processing (the IC effect) was significantly delayed in cluttered displays, to the point of virtual disappearance of the early automatic effect, (as indexed by the absence of the N1 IC effect) in the most cluttered condition. At the same time, the late Ncl effect remained intact under all clutter conditions. Although the perceptual strength of the illusory contour was not assessed directly across clutter levels, the contour readily pops out under high clutter conditions and

identifying contour-present arrays would be a trivial task for a normal human observer, resulting in an intact Ncl effect.

A number of visual processing models propose that global scene analysis precedes local image processing (Bar, 2004; Hamker, 2005; Stanley & Rubin, 2003; Walther & Koch, 2006). While there may be disagreement on the neural substrates of global scene analysis in the literature, many believe it takes place in the initial sweep of activity along the dorsal visual stream, which later influences object-related ventral stream activity via feedback and lateral interactions (Bar, 2003; Bullier, 2001; Chen, et al., 2007; Lamme & Roelfsema, 2000; Vidyasagar, 1999 for descriptions of similar "frame-and-fill" models). In an effort to obtain more direct evidence of dorsal stream influences on the cortex, Zanon and colleagues (2010) recorded TMS-induced potentials in humans. This is a fairly new methodology where scalp EEG is recorded while TMS is applied to the specific regions of the brain. Similarly to ERPs, TMS-locked average response is calculated and taken to reflect the neural activity induced by the application of TMS itself. As compared to a sham condition where a physical barrier was placed between the coil and the scalp, TMS over the left parietal regions evoked a differential response in left temporo-occipital cortex peaking around 170 ms after the stimulation. The temporal aspect of the N1 IC effect is consistent with possible integration of such dorsal and ventral inputs—a matter of pure speculation here. The possibility of dorsal-ventral interaction in perception is supported by the relative speeds of processing in the parallel streams, that is, the fast conduction velocities of the magnocellular channel (e.g., Kaplan, 2008) and the rapid activation of the dorsal stream areas (Bullier, 2001; Chen, et al., 2007; Foxe & Simpson, 2002; Schroeder, et al., 1998) and the relatively slow conduction velocities of the parvocellular channel (e.g., Kaplan, 2008) and the ventral stream (Chen, et al., 2007; Schroeder, Mehta, & Foxe, 2001; Schroeder, et al.,

1998). The feedforward laminar profiles (i.e., initial granular activations) in the dorsal stream areas and nonfeedforward laminar profiles (i.e., initial extragranular activations) in the ventral stream regions also confirm the idea that higher-order or parallel regions of the visual hierarchy may affect incoming feedforward information in the ventral stream (Chen, et al., 2007; Schroeder, et al., 1998). Initial global scene analysis in the dorsal stream becomes particularly important in naturalistic conditions where multiple and overlapping objects may be present.

The limitation of this study is the fact that we used an indirect measure of global scene analysis. Spatial processing can be most directly assessed with ERPs in the P1 latency (65-100ms) because dorsal stream generators have been shown to contribute substantially to the P1 component (Di Russo, et al., 2002; Foxe, et al., 2005; Foxe & Simpson, 2002), and the P1 is well-known to be responsive to spatial attentional manipulations (e.g., Hillyard & Mangun, 1987; Martinez, et al., 1999). In this study, we could not directly compare P1 responses between clutter conditions because our stimulus arrays had different numbers of inducers, resulting in topographically and morphologically different P1 responses (Figure 9). The differences in topographic distributions were confirmed by TANOVA analysis (also see Figure 9), which revealed significant divergence between clutter conditions starting as early as 80 ms post stimulus onset. Correlating dorsal stream processing (as indexed by P1) with electrophysiological markers of ventral stream processing is an important avenue for future research.

Certain clinical populations, such as patients with schizophrenia, have well-documented dorsal stream deficits (Butler & Javitt, 2005; Butler et al., 2007; Foxe, et al., 2001; Foxe, et al., 2005; Yeap et al., 2008; Yeap et al., 2006; Yeap, Kelly, Thakore, & Foxe, 2008). Such populations present an opportunity to study visual processing within the framework of a

"functional" lesion. Contrary to our understanding of the dorsal stream's role within the "frame-and-fill" model, studies of perceptual filling-in and illusory contours in schizophrenia show impaired dorsal stream responses and intact initial ventral stream responses (Doniger, et al., 2002; Foxe, et al., 2005; Sehatpour, et al., 2010). That is, in our previous studies, the early N1 IC effect remained intact in schizophrenia; raising the possibility that the dorsal stream is not critical for this relatively automatic process. Alternatively, it is possible that the dorsal stream functioning was not properly assessed because presentation of a single object or illusory contour did not require global scene analysis.

Studies in patients with anatomical lesions present another opportunity to test the contributions of the dorsal stream to object recognition in the ventral stream. Patients with lesions in the parietal areas have well-documented impairments in orienting to the contralateral space, particularly striking for the right-side lesions (Driver, Vuilleumier, & Husain, 2004). They consistently fail to detect objects in the contralateral hemi-space presented simultaneously with objects in the ipsilateral hemi-space—a syndrome named extinction. Additionally, they suffer from spatial neglect, the inability to orient toward the contralateral side of the space on a number of different tasks. The different roles of the processing streams are highlighted by the intact "depth from stereo" cues perception and impaired "object from stereo" cues perception in patients with occipito-temporal lesions (Vaina, 1989). That is, these patients only exhibited specific deficits in extrapolating object-related representations from stereo cues, driven by the intact dorsal stream (Farivar, 2009). Surprisingly, neglect patients appear to have intact illusory contour processing. That is, in patients whose damage is limited to the parietal areas with spared lateral occipital areas, there is recovery from extinction when objects on the right are part of an illusory contour spanning across the midline (Conci et al., 2009; Mattingley, Davis, & Driver,

1997). Moreover, when asked to bisect an illusory line, patients make the same number of rightward bisection errors as for a real line—an error, which disappears for control disjointed stimuli, not forming an illusory contour (Vuilleumier, Valenza, & Landis, 2001). If scene analysis along the dorsal stream is a prerequisite for contour interpolation, it is not clear why patients with parietal damage have no apparent problems interpolating a contour, which presumably requires scene analysis (but see discussion of the same inconsistency in schizophrenia above). Similarly to patients with anatomical lesions of the dorsal stream, schizophrenic patients with corresponding "functional" lesions show signs of a right shift in bisection judgments, possibly stemming from the underlying magnocellular dysfunction (McCourt, Shpaner, Javitt, & Foxe, 2008). The paradigm used in this study can be applied to schizophrenia or spatial neglect in order to better understand the influence of the dorsal stream impairment on ventral stream processing.

The role of the dorsal stream in object recognition remains a matter of debate. While traditional views described strict functional separation between parallel processing streams (Goodale & Milner, 1992; Mishkin, et al., 1983), more recent views underscore their interaction and functional unity (Cardoso-Leite & Gorea, 2010; Farivar, 2009; McIntosh & Schenk, 2009). The strict perception-action dichotomy of Goodale and Milner (1992), according to which the ventral stream achieves perception while the dorsal stream guides action, has been questioned in view of recent experimental observations of similar response properties in the parallel streams. For example, Konen and Kastner (2008) reported sensitivity of the dorsal stream areas to objects in a recent fMRI study. Specifically, they observed that intermediate areas along the dorsal stream (V3A, MT and V7) had object-selective, size-dependent and viewpoint-dependent responses (just like the intermediate V4 in the ventral stream), while posterior parietal cortex (a

higher-order dorsal area) was invariant to image transformations (just like the hierarchically equivalent inferotemporal cortex). They argued that dorsal stream representations of objects might be similar to ventral stream representations and independent of action planning because participants were not engaged in a task related to the objects they saw. At the same time, shape selectivity in the lateral intraparietal (LIP) cortex has been observed in animal models for 2D (Lehky & Sereno, 2007; Sereno & Maunsell, 1998) and 3D displays (Nakamura et al., 2001; Shikata, Tanaka, Nakamura, Taira, & Sakata, 1996). However, when Lehky and Sereno (2007) compared shape selectivity in LIP of the dorsal stream and anterior inferotemporal (AIT) area of the ventral stream, they found greater shape selectivity in the ventral stream, presumably underlying the capacity to make finer shape discriminations. Importantly, it has been suggested that ventral stream object recognition critically depends on the extraction of its 3D structure in the dorsal stream (Farivar, 2009). Thus, a picture is emerging of segregated, yet interacting parallel streams of information with possible overlapping functionalities. Clearly, future studies call for disentangling the dynamic nature of this interaction.

Summary

The findings presented here provide additional support for the idea that spatial characteristics of the scene have a direct effect on the formation of object-related representations. Specifically, early and automatic processing in the ventral stream, as shown here for illusory contours, critically depends on rapid scene analysis. Further examination of the temporal dynamics between the dorsal and the ventral streams will be most informative in fleshing out the apparent ambiguity and overlap in their response characteristics.

CHAPTER 3

Serial Facilitation or Input Pooling?

Disambiguating the Role of V1 in Contour Completion

Introduction

Contour integration, the ability to link collinear but disconnected visual information across space, is an essential element of object and scene perception. It is a mechanism by which the visual system groups relevant spatial elements at a relatively basic level. Despite significant progress in our understanding of the physiology of the visual cortex, the precise neural mechanisms of contour integration remain unclear. Two alternative neural mechanisms have been suggested. The first relies on lateral horizontal connections within the primary visual cortex, which connect cells with similar orientation tuning characteristics across the visual field. These so-called collinear cells, which are sensitive to neighboring regions of visual space, are posited to communicate via the long-range horizontal connections resulting in local integration of contour elements (possibly through oscillatory loops) (Bauer & Dicke, 1997; Bauer & Heinze, 2002; Gray, 1999; Grossberg & Williamson, 2001; Hess, Hayes, & Field, 2003; Kapadia, Ito, Gilbert, & Westheimer, 1995; Kovacs, 1996; Stettler, Das, Bennett, & Gilbert, 2002). The second possible mechanism relies on interactions across the regions of the visual hierarchy, i.e. on pooling of information in higher order visual areas as the first step in the process (Hubel & Wiesel, 1962; Spillmann & Werner, 1996). These two mechanisms make a set of clearly dissociable predictions. If the initial integration step occurs locally in V1, one would predict correspondingly temporally early differential neural response modulations originating from neuronal ensembles in the primary visual cortex (Gray, 1999; Hess, et al., 2003; Kapadia, et al., 1995; Kovacs, 1996; Stettler, et al., 2002) Alternatively, the initial

contour-specific response will be detected later in processing and in higher order visual areas (Murray, et al., 2002). Here, we employed high-density mapping and source-localization techniques to adjudicate between these competing accounts, which rely on inherently different spatio-temporal predictions.

Arguments in support of contour computation in the primary visual cortex come from anatomical and physiological studies in animal models suggesting that V1 is capable of integrating information over a larger extent of the visual field than initially considered. Although classical receptive fields extend only a fraction of a degree in the fovea (Hubel & Wiesel, 1962), they can be modulated by local horizontal connections responding to visual elements outside the classical receptive field (Allman, Miezin, & McGuinness, 1985; Angelucci et al., 2002; Blakemore & Tobin, 1972; Gilbert, Das, Ito, Kapadia, & Westheimer, 1996; Gilbert, Hirsch, & Wiesel, 1990; Levitt & Lund, 1997; Nelson & Frost, 1978; Rockland & Lund, 1983; Walker, Ohzawa, & Freeman, 1999). Neurons of a given orientation selectivity are preferentially connected to other neurons (across orientation columns) with a similar orientation preference and adjacent receptive fields (Hirsch & Gilbert, 1991; Schwarz & Bolz, 1991; Stettler, et al., 2002; Ts'o, Gilbert, & Wiesel, 1986; Weliky, Kandler, Fitzpatrick, & Katz, 1995). These connections can span up to 5 mm of cortical distance in primates (Angelucci, et al., 2002). Despite being extremely informative, these anatomical findings lack the direct physiological evidence necessary for a comprehensive understanding of the mechanisms of contour integration. What's more, neurons in V1 can also be modulated by top down connections (Lund, Angelucci, & Bressloff, 2003). The relative roles of feedback and horizontal connections have not been fully elucidated, leaving the role of V1 in contour completion and figure-ground segregation as yet unclear.

At the same time, behavioral tests of the physical constraints of contour integration suggest parameters that are in some cases consistent with the physical organization of hypercolumns within the primary visual cortex. One of the classical psychophysical paradigms explores the so-called “association fields” of the visual cortex, using “pathfinder displays.” Here, Gabor patches (designed to be well-matched to the tuning properties of cells in V1) are arranged to form continuous contours of about ten-element length while their relative orientation and distance is varied (e.g., Figure 11) (Field, Hayes, & Hess, 1993). The term “association field” describes the tendency of neighboring elements to be grouped together within certain constrains (i.e., ≤ 6 carrier wavelengths (λ) spatial separation and ≤30° orientation difference). Together with anatomical considerations (i.e., preferential connectivity between hypercolumns with similar tuning characteristics) (Das & Gilbert, 1995; Gilbert & Wiesel, 1989; Malach, Amir, Harel, & Grinvald, 1993; Ts'o, et al., 1986), the behavioral tests of “association field” have been taken to suggest that V1 plays a major role in contour processing (Field, et al., 1993; Kovacs, 1996). One of the theoretical rationales for V1 involvement is the notion that along with the inducers (i.e., aligned Gabors), any of the adjacent “noise” elements would also show up in the higher order cortical areas with large receptive fields (e.g., a 5° receptive field in V4). A cell with a large receptive field will “see” both inducers and distractors, making it difficult for such a cell to compute which elements should be joined to construct a contour.

A parallel line of research has concentrated on elucidating cortical mechanisms underlying illusory contour (IC) perception. This can be thought of as an example of contour integration. Although earlier intracranial studies in animal models and human neuroimaging studies localized IC processing to the hierarchically earliest visual cortical regions of V1 and

V2 (Bakin, et al., 2000; Ffytche & Zeki, 1996; Larsson, et al., 1999; Lee & Nguyen, 2001; Peterhans & von der Heydt, 1989; Ramsden, et al., 2001; Seghier, et al., 2000; von der Heydt & Peterhans, 1989), these studies did not assess the temporal aspects of the effects. More recent functional magnetic resonance imaging (fMRI) and high-density ERP studies have emphasized the contributions of major generators within higher-order regions of the Lateral Occipital Complex (LOC) (Foxe, et al., 2005; Halgren, et al., 2003; Kruggel, et al., 2001; Mendola, et al., 1999; Murray, Foxe, et al., 2004; Murray, et al., 2006; Murray, et al., 2002; Ritzl, et al., 2003b; Shpaner, et al., 2009). On the whole, these later studies support a model whereby IC processing occurs first in the LOC as part of the ventral stream response, with subsequent feedback into lower-tier areas of V1/V2. Illusory contour mechanisms have been compared to real contour mechanisms in at least one ERP study (Pegna, et al., 2002). Both illusory and real stimulus types were found to modulate the same neural network, suggesting that IC processing represents a special case of more general contour integration dynamics.

To arbitrate between the idea that contour integration occurs as a result of long-range horizontal connections in V1 and the idea that it relies initially on processing in higher-level visual cortex (e.g., the LOC), we investigated the timing and topography of the visual evoked response to stimuli used in “association field” studies. High-density ERP responses were compared to stimuli with and without contours, which were embedded in noise. The relatively slow speed of lateral horizontal connections (see Bullier, 2001 for review) provides for a slow mechanism of integration and presents a challenge if interpretation is solely based on temporal arguments. However, source localization techniques helped us disambiguate the underlying cortical generators. Specifically, our methods provided for enough spatial resolution to separate striate and extrastriate cortical activations (Vanni et al., 2004).

Materials and Methods

The key question for the current study is the delineation of the timecourse and localization of contour integration. To this end, special care was taken to achieve enough power to detect the earliest cortical differences. C1 is the earliest visual ERP component, believed to be a marker of V1 activity due to its highly retinotopic distribution, early timing (peaking between 65-90 ms) and repeated source localization to the primary visual cortex (Di Russo, et al., 2002; Gomez Gonzalez, et al., 1994; Jeffreys & Axford, 1972b). V1 has been shown to have highly variable anatomy across subjects, a feature likewise observed in subject-by-subject analysis of the C1 (Foxe & Simpson, 2002; Jeffreys & Axford, 1972b; Molholm et al., 2002; Rademacher, Caviness, Steinmetz, & Galaburda, 1993). At the same time, subjects with a robust C1 will reliably exhibit "typical" C1 topography (e.g. upper field stimuli will produce a contralateral negative potential, while lower field stimuli will produce a contralateral positive potential) (Kelly, Gomez-Ramirez, & Foxe, 2008). In this study, we used retinotopically constructed presentations and all subjects had a robust C1 component; all were, thus, included in analyses.

Subjects

Twenty neurologically normal paid volunteers participated. Four participants were dropped from the study because they did not cooperate with the task (based on the assessment of the EEG technician and confirmed by very low behavioral accuracy as indicated through calculation of *d*' values), an additional participant was dropped because he could not maintain fixation. The remaining fifteen participants (6 female) were between 22 and 40 years of age (mean age = 28±5). All participants had normal or corrected-to-normal vision, were right-handed as assessed with the Edinburgh Handedness Inventory (Oldfield, 1971). Participants provided written informed consent, and the Institutional Review Boards of the Nathan Kline Institute for

Psychiatric Research and the City College of New York approved all procedures. All procedures conformed to the principles of the Helsinki declaration. Participants received a modest monetary compensation ($10 per hour).

Design and Task

Gabor patches of 0.25 carrier wavelength, λ, (i.e., 4 cpd) were used to generate forty different contours embedded in randomly oriented Gabor elements to avoid adaptation (an algorithm from the original Field and Hess paper (Field, et al., 1993) was used in Matlab v. 15). Contours consisted of ten Gabor elements, oriented within ± 30 degrees relative to the neighboring elements, with no phase shift, presented at 100 percent contrast. Arrays of ten by ten elements were constructed. Inter-element separation was jittered around 4-6 λ (i.e., 1-1.5 degrees visual angle). Contours did not close to form full geometric shapes. Forty randomly oriented displays of Gabor patches were also constructed by randomly rotating the orientation of the contour elements. This resulted in identical displays for the contour-present and contour-absent conditions, except for the orientation of the ten aligned contour elements (Figure 11). Stimulus arrays subtended 10x10 degrees visual angle (with each Gabor occupying 1 degree visual angle), and were presented either to the upper left or the lower right quadrant of the screen (as mirror images). Off-center presentation was necessary to ascertain presence of C1. Only displays with contours relatively close to the central fixation cross were selected by visual inspection, as peripheral contours proved to be too difficult to detect, with participants performing at chance during pilot sessions. Stimuli flashed on the screen for 200 ms, after which participants had unlimited time to make a button push response to the presence or absence of the contour, the response was followed by a 100-500 ms variable inter-trial interval. Participants maintained fixation on the centrally presented cross. Each of the 80 possible displays (40

contours and 40 no-contours) was presented 12 times in random order for a total of 480 sweeps per condition. To assess behavioral performance, *d*' measures were calculated based on the formula appropriate for a forced choice paradigm: $d' = 2z\,[1/2(1+[2p(c)-1]^{1/2})s]$ (Macmillan NA, 2005, p. 216). The *d'* measures were submitted to a two-tailed paired Student's t-test with the factor of side of presentation.

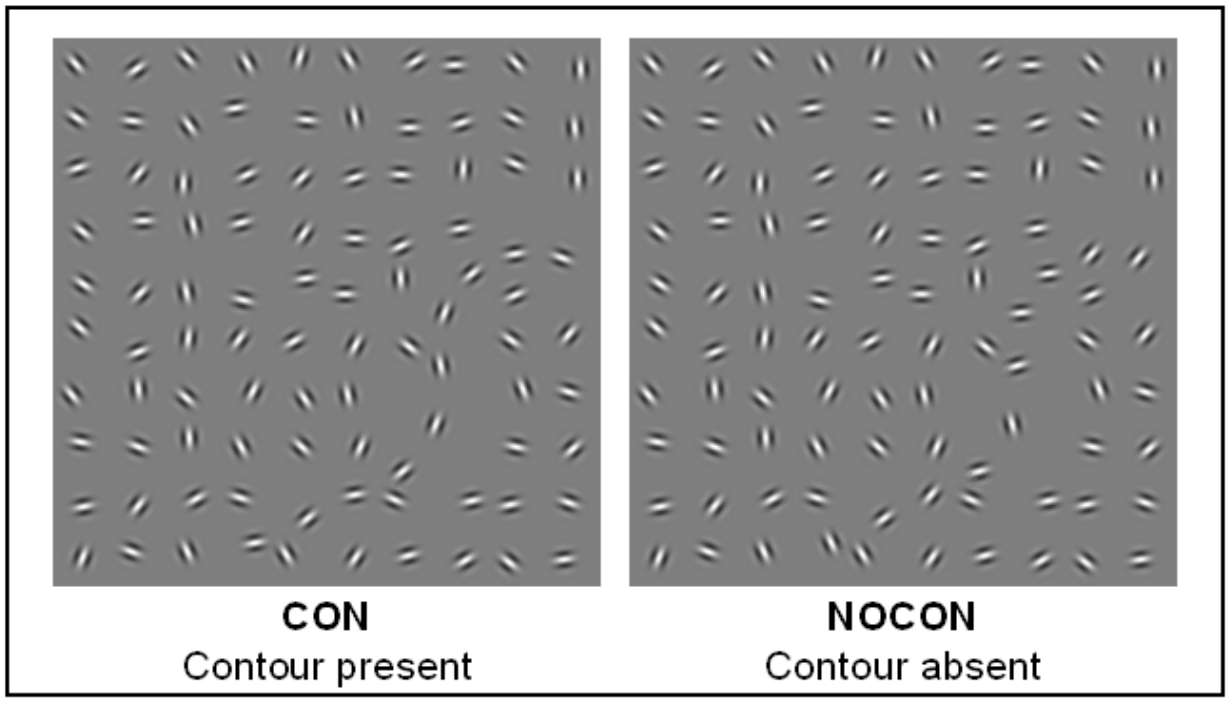

Figure 11. Exemplar Pathfinder Stimulus Arrays
A snaking contour pops out in the left hand panel, lower right corner. The control array is identical, except the contour-inducing elements are randomly rotated.

Electrophysiological Data Acquisition and ERP Derivation

Continuous EEG was acquired through a Biosemi ActiveTwo system from 168 scalp electrodes, digitized at 512 Hz, and referenced to the CMS-DRL ground (which functions as a feedback loop driving the average potential of the subject, i.e. the Common Mode voltage, as close as possible to the AC reference voltage of the AD box, i.e. the amplifier zero). EEG

processing and analyses were performed using the Cartool software by Denis Brunet (http://brainmapping.unige.ch/cartool.htm). Epochs of continuous EEG (-200 ms before stimulus onset to 500 ms after stimulus onset) were separately averaged from each subject in response to each condition and stimulus type. Only correct responses were accepted into the average. An artifact rejection criterion of ±75 μV was used at all scalp sites to reject trials with excessive EMG, horizontal or vertical eye movements, and other noise transients. The average number of accepted sweeps per condition was 301±82 with a range of 127 to 439 sweeps. Data from electrodes containing major noise transients for each subject and ERP were interpolated according to the average digitized electrode positions for the particular cap electrode array (Perrin, et al., 1987). Prior to group-averaging, ERP data were baseline corrected around stimulus onset from –50 to +20ms and recalculated to the common average reference. Statistical and topographic mapping for all experiments in this study were performed on broadband data. A 45Hz low-pass filter was used in waveform figures for ease of visualization.

Earliest ERP Component Analysis Strategy

We first undertook the analysis of the C1 component to determine whether earliest cortical contour integration effects can be established in V1. Due to the high degree of inter-subject variability in the topography and timing of the C1 component, C1 was defined on an individual basis as the earliest deflection peaking before 100 ms post-stimulus onset (Kelly, et al., 2008). Peak positive and negative C1 electrode sites were identified automatically in Cartool software. The peak electrodes were not perfectly conserved across subjects. Since these electrodes presumably represented activity from the same underlying generators in the primary visual cortex, a group average was created. Focusing on the peak electrodes also increased the power for detecting contour-specific effects by reducing inter-subject variability across electrode

sites. Mean amplitude over time (68-100 ms) was submitted to a 2x2x2 MANOVA with the factors of spatial location, electrode (across the different hemispheres) and contour presence.

Power Analysis

Power estimations were derived using the software package, 'Power and Precision ™' release 4.0. In this study, enough power has to be obtained for a meaningful C1 component modulation (ten percent), as they are the hardest to detect. We submitted the standard deviations of the peak amplitude values of the C1 component in the two electrode sites of interest (see preceding paragraph) together with obtained correlations for each set of electrode data to a two-tailed (α=0.05) power analysis.

Statistical Analyses of Later Components

The temporal windows for analyses of all ERP components was defined based on the results of the topographic pattern analysis, described below. Mean amplitude measures over time of the major components were submitted to a 2x2x2 MANOVA with the factors of spatial location, contour presence and hemisphere. The following time-periods were used: 165-193 ms for the N1 and 315-350 ms for the Ncl ("closure negativity"). Electrodes for all tests were picked based on the peak amplitude electrode in the group average data.

Detection of Temporal Effects

To calculate the timing of contour sensitivity, we employed point-wise paired *t*-tests between ERP responses for each condition. The method allowed us to identify the onset of differential responses between our conditions ("contour" vs. "no contour"). For each electrode, the first time point where the *t* test exceeded the 0.05 α criterion for at least 10 consecutive data points (19.5 ms at a 512 Hz digitization rate) was labeled as the onset of the effects (see Wylie, et al., 2003 for rationale).

Topographic Analyses

In order to statistically identify periods of topographic modulation, the topographic analysis of variance (TANOVA) procedure was used. It computes global dissimilarity (Lehmann & Skrandies, 1980) between conditions for each time point of each subject's data. Global dissimilarity is an index of configuration differences between two electric fields, independent of their strength. This parameter equals the square root of the mean of the squared differences between the potentials measured at each electrode (vs. the average reference), each of which is first scaled to unitary strength by dividing by the instantaneous standard deviation. Dissimilarity can range from 0 to 2, where 0 indicates topographic homogeneity and 2 indicates topographic inversion. A Monte Carlo MANOVA is then applied (Manly, 1997) to test for statistical differences in the dissimilarity between conditions. This is a nonparametric bootstrapping procedure, wherein each subject's data from each time point is permutated such that they could "belong" to either stimulus condition. The dissimilarity is then calculated for each of 8000 such permutations for each time point and is used to generate a distribution of values against which the observed data are compared. From this, we determined the probability of obtaining a dissimilarity value from the permutations that exceeded the actual measured value. Since electric field changes are indicative of changes in the underlying generator configuration (Lehmann, 1987); this test provides a statistical means of determining if and when the brain network activated by the two conditions differs.

To further characterize electric field potentials for the different types of stimuli, periods of stable topography were estimated using topographic pattern analysis (Michel, et al., 2001). A modified cross-validation criterion determined the number of maps that explained the whole group-averaged data set (Pascual-Marqui, et al., 1995). This method is reference independent

and insensitive to pure amplitude modulation across conditions and over time. Different topographic maps reflect differences in the active generators of the brain. The maps obtained as a result of the above procedure were used to define the stable topographic time periods for ERP statistical analyses and for estimating the sources of the ERP modulation for each stimulus type, using the LAURA distributed linear inverse solution (Grave de Peralta, et al., 2001; Grave de Peralta, et al., 2004). Since we did not detect any topographic differences in the contour and no-contour responses in the C1 and N1 timeframes, contour and no-contour conditions were combined for C1 and N1 localizations. LAURA employs a realistic head model with 4024 nodes, arranged in a 6X6X6 mm grid within the gray matter of the Montreal Neurological Institute's average brain. The procedure selects the best source configuration based on the biophysical behavior of electric vector fields according to electromagnetic laws. Individual source models for each subject were obtained and averaged to produce the grand average model. Differences in the inverse solution space were also obtained for the Ncl time-period by subtracting solution for the no-contour condition from the contour condition. Strength modulations of over 20 percent are reported.

Results

Behavioral Results

The contour detection task proved to be quite challenging for participants likely due to the lateralized presentations. *d*' for the left and right visual field presentations was 1.17±0.32 and 1.16±0.28 respectively. A relatively high number of participants could not perform the task with an acceptable degree of precision and were dropped from further analysis (as described in Methods). Most participants were biased to respond as if no contour was present. The t-test with

the factor of side of presentation was not significant (t=0.8); neither stimulus location resulted in an advantage in behavioral performance.

Earliest ERP Component Originating in the Primary Visual Cortex

This study was designed to uncover the earliest possible ERP modulations resulting from contour integration processes. The C1 component inverted polarity in a retinotopically predictable fashion for opposite sides of presentation as anticipated, and there was a clear

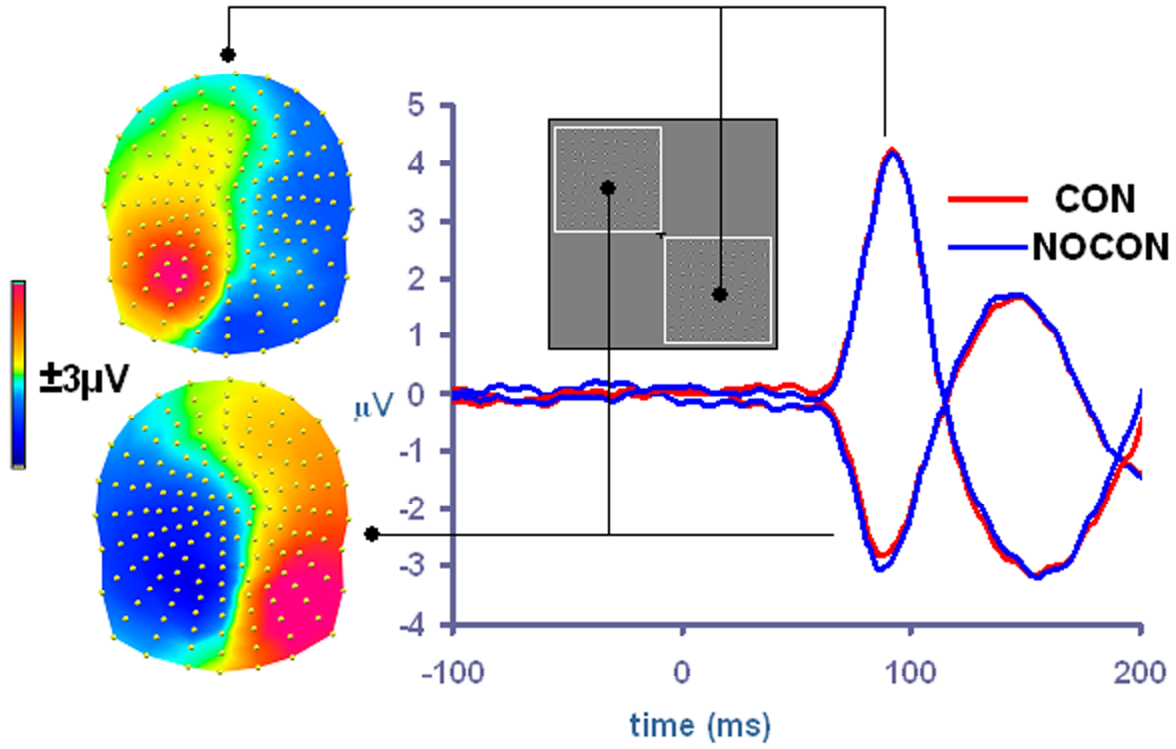

Figure 12. ERP Waveforms and Topography in the C1 Timeframe.

Individual peak C1 electrodes were used to make the group average. Red trace is the contour-present condition, blue trace is the contour-absent condition. The positive C1 peak is shown for lower-right presentations and the negative C1 peak is shown for upper-left presentations. The CON and NOCON traces overlap almost completely. To the left of the ERP graph, group-averaged topographies of the C1 peak (over 68-100 ms) are displayed on a flattened electrode array. Top topography corresponds to the lower-right location; bottom topography corresponds to the upper-left location. A polarity inversion can be observed between corresponding electrodes for the two stimulus locations, consistent with the retinotopic organization of V1.

inversion across the electrode sites distributed over the head (Figure 12). Consistent with the literature, left-lateralized presentations resulted in a C1 negativity over the medial occipital sites and a positivity over the right lateral occipital sites (Di Russo, et al., 2002; Kelly, et al., 2008). Right-lateralized presentations resulted in a positivity over the left medial occipital sites and a negativity over the right lateral occipital sites. Visual inspection of the waveforms revealed no differences between contour and no-contour conditions for either side of presentation. The MANOVA over the 68-100 ms, as well as the Running *t*-tests (Figure 14), confirmed this null finding ($F_{1,14}$=0.606, p=0.449). As expected, there was an interaction between hemisphere and side of presentation ($F_{1,14}$=141.865, p<0.001) consistent with the C1 inversion. The main effect of hemisphere also reached significance with more positive waveforms on the right overall ($F_{1,14}$=4.821, p=0.045). LAURA solutions were consistent with generators within the primary visual cortex. The upper-left stimuli led to generator sources in the lower bank of the calcarine fissure within the lingual gyrus (x=-17, y=-87, z=1), while the lower-right stimuli had generators in the middle occipital gyrus (x=29, y=-81, z=4), on the upper bank of the calcarine fissure.

C1 Power Analysis

In order to embrace the null hypothesis of the lack of contour-related differences in the C1 timeframe, we tested whether we have indeed achieved adequate power to detect meaningful differences in C1 amplitude. Power analysis on the peak amplitude values from our dataset is summarized in Table 1. The table provides power levels for the ten and fifteen percent modulations of the C1 component, in addition to the modulation detectible at the conventional power level of 80 percent. With the exception of the negative electrode site for the right-side presentations, where we were only powered to detect a 23 percent modulation of the C1

component, overall we were powered to detect very small C1 differences. For example, in the cleanest electrode (positivity for left-side presentations), we achieved conventional levels of power to detect a seven percent amplitude modulation (in this case the mean amplitude$\pm$SD was 6.97$\pm$1.9 μV). Power analysis supported the lack of observable differences between contour and no-contour conditions.

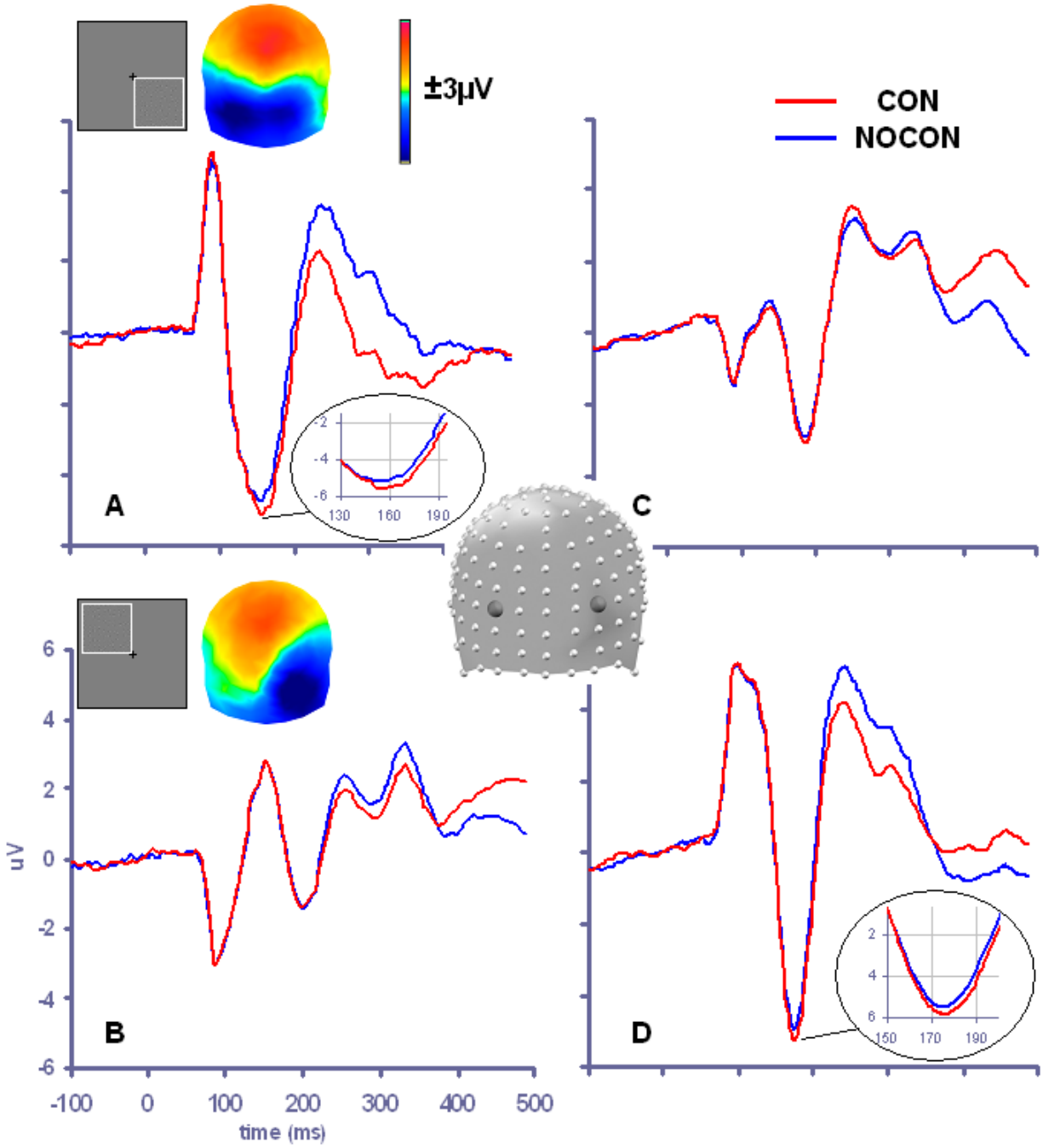

Figure 13. ERP Waveforms over the Entire Epoch and N1 Topography.
ERP waveforms from two occipital electrodes (highlighted on the head montage in the center) are displayed for each location. Panels A and C display waveforms for the lower-right location; panels B and D display upper-left locations. Red trace is the contour-present condition; blue trace is the contour-absent condition. The N1 peaks contralateral to the presentation side are blown up for ease of visualization in panels A and D. Panels A and B also display scalp topographies over the N1 timeframe (165-193 ms) for each location on a flattened electrode array. Clear lateralization of components and effects can be observed, with stronger effects on the contralateral side of presentation.

Later ERP Components

ERP responses to the contour and the no-contour conditions are displayed in Figure 13, together with topographic plots for the N1 time-period (165-193 ms). The running t-tests were used to determine the temporal onset of differences between conditions (Figure 14). Differences started around the peak of the N1 component as a more negative deflection for the contour condition for both sides of presentation (Figure 13) and highly consistent with previous ERP and MEG results (Foxe, et al., 2005; Halgren, et al., 2003; Kruggel, et al., 2001; Mendola, et al., 1999; Murray, Foxe, et al., 2004; Murray, et al., 2006; Murray, et al., 2002; Ritzl, et al., 2003b). The omnibus MANOVA revealed a main effect of contour ($F_{1,14}$=9.71, p=0.008) with greater negative amplitudes for the contour than the no-contour condition. There was a three-way interaction between contour, hemisphere and side of presentation ($F_{1,14}$=10.552, p=0.006). The contour-related effect was lateralized primarily to the contralateral scalp relative to the side of presentation, as evident from the topographical plots (see insets of Figure 13, panels A and B). The MANOVA also resulted in a main effect of hemisphere ($F_{1,14}$=15.814, p=0.001), with more negative N1 amplitudes over the right hemiscalp; and an interaction between hemisphere and side of presentation ($F_{1,14}$=14.787, p=0.002), with more negative N1 amplitude on the contralateral side of presentation. Shortly after the onset of statistical differences, a topographic divergence followed at 190 ms for the left presentation and 195 ms for the right, as assessed with the TANOVA (gray shaded areas on Figure 14). Inverse solutions in this timeframe were consistent with intracranial generators in the LOC and were stronger in the LOC contralateral to the side of presentation (Figure 15, panel A). The solution maxima were found in the inferior occipital gyrus (x=29, y=-81, z=-4) for the left side of presentation and in the middle temporal gyrus (x=–47, y=-58, z=0) for the right side of presentation.

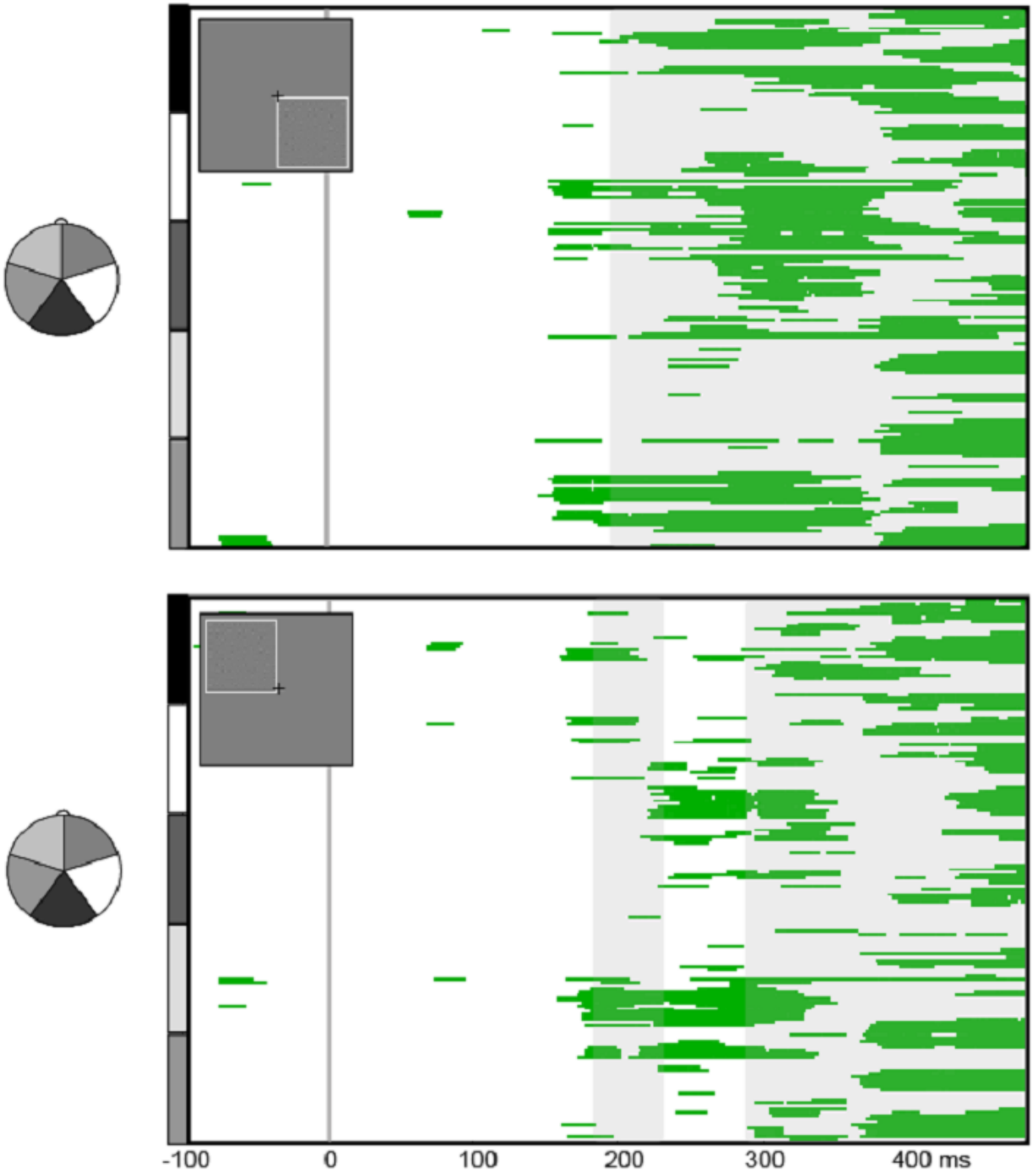

Figure 14. Statistical Cluster Plots of Contour Effects

The statistical cluster plots depict the results of the pair-wise running *t*-tests (threshold criterion of $p<0.05$ for 19.5 ms consecutive ms). The onset of contour effects is similar for both stimulus locations, in the N1 timeframe and persisting into the Ncl timeframe. Electrodes are arranged vertically according to the head montage on the left. Upper panel is the lower-right stimulus location; lower panel is the upper-left stimulus location. Gray shading reflects periods of topographic divergence as estimated with the TANOVA procedure.

The waveforms diverged further around the Ncl component (closure negativity), in close agreement with the prior illusory contour and object recognition literatures (Foxe, et al., 2005; Kruggel, et al., 2001; Murray, Foxe, et al., 2004; Murray, et al., 2006; Murray, et al., 2002; Shpaner, et al., 2009). Responses in the contour-present condition were more negative-going than for no-contour, an effect often referred to as the Ncl (Doniger, et al., 2000; Doniger, et al., 2001; Foxe, et al., 2005; Sehatpour, et al., 2010; Sehatpour, et al., 2006; Sehatpour, et al., 2008). This main effect of contour was statistically significant ($F_{1,14}$=9.652, p=0.008). There was an interaction between hemisphere and contour ($F_{1,14}$=5.522, p=0.034), with larger contour effects on the left. There was also an interaction between side and hemisphere ($F_{1,14}$=19.792, p=0.001): in the left hemisphere, responses to the contralateral presentations were more negative than to the ipsilateral presentations while the opposite trend held in the right hemisphere. Finally, there was a three-way interaction ($F_{1,14}$=13.153, p=0.003): in the right hemisphere, classical contour effects for the left side presentation were present (i.e., contour waveforms were more negative than no-contour waveforms), while the contour effect for the right side presentation had the opposite trend (i.e., no-contour waveforms were more negative than contour waveforms); in the left hemisphere, contour effect was larger for the right-side than the left-side presentations. Source localization in this timeframe revealed bilateral sources in the temporal and occipital lobes, within Brodmann areas 37, 22, 21 and 19 (see Table 1 and Figure 15, panel B). The major sources of topographic divergence (obtained by subtracting no-contour from contour conditions) led to source generators in the left frontal and the left post-central gyri for the right presentations. Left-side presentations had bilateral source distribution in the middle temporal and postcentral gyri on the left and the precuneus and middle frontal gyrus on the right (Table 2).

Figure 15. Source Estimations of Contour-Related Effects.

Group-averaged LAURA distributed linear source estimations were calculated for the ERP waveforms over the N1 (165-193 ms) time period (panel A) and the Ncl (315-350 ms) time period (panel B). Since no topographic divergence was observed in the N1 time-period, only a single source estimation is presented for each stimulus location. Stronger contributions from inferior occipital gyrus (left side presentation) and middle temporal gyrus (right side presentation) in the N1 time period for the CON condition are shown. The center panel displays the ventral view (R= right side, L=left side). Topographies were different for contour-present and contour-absent conditions over the Ncl time-period, hence, they are broken down by condition. More distributed sources of activations were observed over the occipital and temporal regions (see Table 2 for specific details).

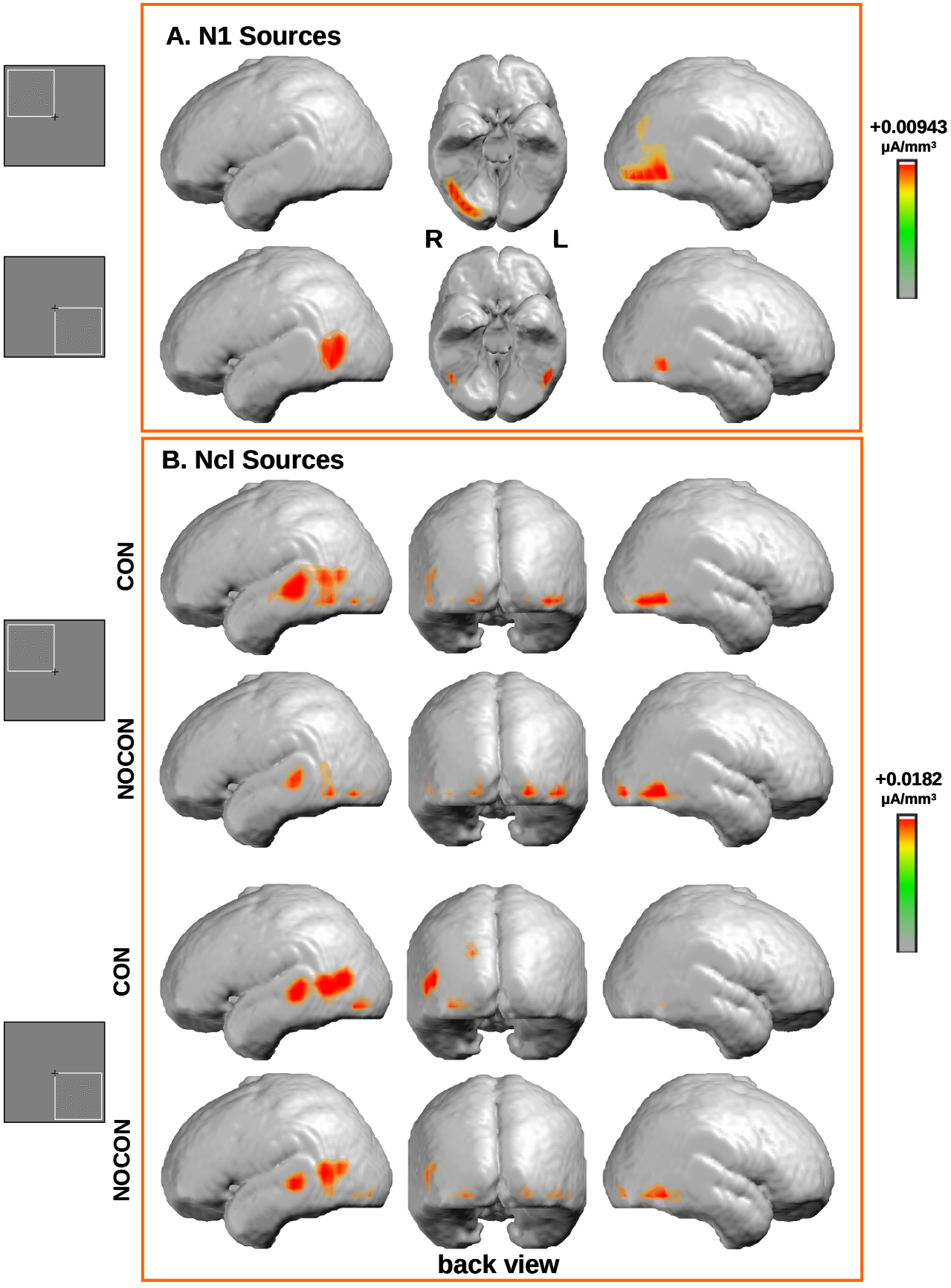
A. N1 Sources
R
L
+0.00943
μA/mm³
B. Ncl Sources
CON
NOCON
CON
NOCON
+0.0182
μA/mm³
back view

Discussion

This study of contour integration revealed earliest ERP differences in the N1 time period beginning around 170 ms. Importantly, the differences were localized to the higher tier ventral stream visual areas, primarily the LOC, and not to the primary visual cortex. No topographic differences were identified over this time period, pointing to a modulation in the strength of identical intracranial generators. The initial divergence was followed by a further topographic difference, onsetting around 190 ms. These results support the model whereby initial contour integration occurs via pooling of neuronal responses in the LOC. In contrast, despite specific efforts to invoke larger early activations of V1/V2 through the use of retinotopic mapping strategies, we found no evidence of modulations in the C1 timeframe. Our findings suggest that any effects observed in lower tier visual areas in the literature are likely due to feedback.

In order to embrace the lack of effects in early visual areas, we needed to ascertain that our metrics have sensitivity to detect such effects. Prior studies reported modulations of the C1 component ranging from 20 to 50 percent in response to different levels of luminance contrast (e.g., Butler et al, 2007) as well as in the context of attentional amplification (Kelly et al., 2008) and multisensory integration (Molholm et al., 2002). Analogous amplitude modulations can be found in animal literature, where early attentional (McAdams & Reid, 2005) and contrast-related (Pooresmaeili, Poort, Thiele, & Roelfsema, 2010) effects have been reported in the spiking rates of V1 cells. Power analysis of our data indicated that we were powered to detect very small modulations of the C1 component in the range of 7 to 23 percent (see Table 1). The high level of power achieved in our dataset gives us confidence that activity stemming

from the primary visual cortex was indeed adequately sampled. In what follows we discuss these results in the context of the available literature.

To date, there exist less than a handful of human ERP studies that can speak to association field theory (Khoe, Freeman, Woldorff, & Mangun, 2004; Mathes & Fahle, 2007; Mathes, Trenner, & Fahle, 2006). To recap, the association field theory argues that contour integration is based upon interactions between neighboring receptive fields in V1 that lie upon a smooth curve. Mathes and colleagues (2007; 2006) used contours embedded in noise to study the physiology of contour integration. They consistently found a relatively late (>200 ms) ERP negativity for contours as compared to noise. Earlier effects, in the timeframe of the visual N1 (~170 ms peak) were somewhat inconsistent. Although the authors attributed these inconsistencies to different task demands, it is more likely that they lacked the statistical power to observe early effects due to the low sweep counts and subject numbers used in these studies. Data in these studies were not tested for any earlier ERP differences than the N1. Our data are consistent with these results since we also observed ERP differences in the N1 and Ncl timeframes; moreover, earlier differences were not detected even with a design specifically targeting early components. Khoe and colleagues (2004), on the other hand, detected early differences in ERP measures, however, arguably, their stimuli tapped a different neural mechanism (discussed below).

Bauer and Heize (2002) recorded single cell spiking activity in supragranular layers of the primary visual cortex of monkeys in response to pathfinder displays. They compared cellular response to the display where the classic Response Field (cRF) was part of a path to the sum of responses where the cRF was not part of a path and where the path was present but the Gabor in the cRF was actually missing (i.e., there was a gap in the path). A non-linearity

between the comparison conditions (the response to the contour was not a linear sum of its parts) was taken to signal integration. They found initial inhibition of the transient response to the continuous path followed by facilitation around 150 to 200 ms post-stimulus onset. These authors choose to interpret these results in terms of local facilitation via long-range horizontal connections; however, given the very late timing and the present results, feedback facilitation would also be consistent.

Studies Challenging the Involvement of Local Horizontal Connections in Contour Completion

There are a number of recent studies qualifying the involvement of long-range horizontal connections in contour completion. Using a binocular rivalry paradigm, Alais et al. (2006) measured inter- and intra-hemispheric association strength between two Gabor patches. Subjects viewed two Gabor patches and two random noise patches in corresponding locations dichoptically. They were asked to respond to the presence of the Gabor patches with two buttons, each corresponding to a certain Gabor patch. Gabor patch coherence was assessed as a function of the probability of seeing two Gabor patches (alternatively, subjects might see a Gabor patch and a noise stimulus or two noise stimuli, but responses were only made to the presence of the Gabor patches). The relative timecourses of the two response streams tracking the simultaneous perception of the Gabors were correlated as a measure of coherence. V1 does not have local horizontal connection spanning across the hemispheres and ipsilateral perception in V1 is limited by a small area of nasotemporal overlap (Fendrich & Gazzaniga, 1989; Sugishita, Hamilton, Sakuma, & Hemmi, 1994; Sugishita, Hemmi, Sakuma, Beppu, & Shiokawa, 1993; Wessinger, Fendrich, Ptito, Villemure, & Gazzaniga, 1996). If local horizontal connections were at play, one would expect much lower coherence across the

hemispheres than within the hemispheres. The relatively high degree of coherence between stimuli presented to different cerebral hemispheres (albeit of lower strength and smaller spatial extent than the intra-hemispheric effects) was taken as evidence for the involvement of feedback from higher-level areas in contour perception.

Samonds et al. (2006) tested how well synchronous activity in layers 2/3 of cat V1 supports predictions of the association field theory. They compared firing rates and synchronous activity in response to gratings and ring stimuli. They reasoned that if lateral horizontal connections are facilitative, gratings would induce higher firing rates than rings due to their higher degree of alignment (supporting the orientation rule of the association field theory). However, when synchronous activity was contrasted with firing rates, it was found to be a better predictor of the orientation rule; and, conversely, the firing rates were nearly the same between stimulus conditions. The authors also speculated that the observed synchrony was not due to direct excitatory connections, since there were no consistent lag times between pairs of cells tested. They concluded that such synchronous activity must be integrated in higher order visual areas.

A number of developmental considerations also point against exclusive involvement of lateral horizontal connections in contour integration. While basic spatial acuity matures relatively early in infancy, contour detection abilities are much more protracted in humans and monkeys alike (Kiorpes & Bassin, 2003; Kovacs, 2000; Kovacs, Kozma, Feher, & Benedek, 1999). At the same time, the anatomy of the lateral horizontal connections has a relatively early maturational timecourse (Burkhalter, Bernardo, & Charles, 1993; Callaway, 1998; Coogan & Van Essen, 1996), while the network of intercortical projections has a much slower maturation profile (Barone, Dehay, Berland, Bullier, & Kennedy, 1995; Batardiere et al., 2002; Burkhalter,

et al., 1993; Coogan & Van Essen, 1996). It appears that the ability to detect contours is more temporally consistent with the development of recurrent intercortical projections rather than lateral horizontal connections (Kiorpes & Bassin, 2003).

Putative Function of the Long-range Horizontal Connections

What then is the functional significance of the long-range horizontal connections? Another behavioral paradigm often used to study contour integration is the so-called lateral masking paradigm (Polat & Sagi, 1993), where threshold detection of the central low-contrast Gabor patch is facilitated by flanking high-contrast Gabor patches of similar orientation and close proximity (maximal within 2-3λ separation). The assumption is that lower thresholds in these studies signify higher degrees of lateral interactions. Using the lateral interaction paradigm, Khoe and colleagues (2004) investigated neurophysiological markers of collinear facilitation. Early C1 effects were observed when collinear flankers were compared to orthogonal flankers. The topography of the effects was consistent with V1 sources, suggesting a putative role for long-range horizontal connections in this task. Based on our results, it appears that low-contrast threshold stimuli could be processed in a different manner than high-contrast suprathreshold contours (Hess, Dakin, & Field, 1998; Hess, et al., 2003). In fact, Polat and colleagues (1998) found suppression, not facilitation, of neural response in the striate cortex when high contrast stimuli were presented with two flanking stimuli in anesthetized cats. In Khoe et al. (2004), while the flankers had a relatively high contrast of 0.5 (Michelson contrast), recruiting primarily the parvocellular system, the pedestal contrasts were fixed at 0.1, putatively relying mostly on the magnocellular system. The interaction between the two systems could be quite different under such conditions than under conditions of high contrast throughout.

Angelucci and colleagues (2002) showed that horizontal connections in the primate V1 are isotropic and attributed contour completion to anisotropic feedback connections. These authors implicated local horizontal connections in **short-range** collinear facilitation; i.e. enhancement of the classical receptive field response to a low-contrast stimulus by co-oriented and coaxial high-contrast stimuli, a phenomenon possibly underlying upstream perceptual grouping of contour elements (Khoe, et al., 2004; Khoe, Freeman, Woldorff, & Mangun, 2006; Polat & Sagi, 1993, 1994). Taken together with the results of this study, these reports suggest that contour integration mechanisms may depend on low-level visual features as well as on the spatial extent of contours.

Summary

In this study of pathfinder displays in humans, we assessed the timecourse of early cortical mechanisms of contour integration in order to arbitrate between two possible mechanisms of contour integration, one relying on local horizontal connections in V1 and another relying on pooling of neuronal responses in higher-order cortical areas. Our data show that contour integration initially relies more heavily on pooling of information in higher order visual cortices (i.e., the LOC), at least under high contrast conditions, while long-range horizontal connections may play a role in contour integration under low-contrast conditions.

condition	% modulation	power
left negative	15	0.92
left negative	10	0.61
left negative	13	0.8
left positive	15	1
left positive	10	0.94
left positive	7	0.8
right positive	15	1
right positive	10	0.89
right positive	9	0.8
right negative	15	0.27
right negative	10	0.23
right negative	23	0.8

Table 1. C1 Power Analysis Results

Power calculations based on the peak C1 amplitudes are displayed. Percent amplitude modulation and the achieved power are separated by stimulus location and electrode site. “Left” and “right” indicate stimulus location. “Positive” and “negative” indicate direction of the C1 peak at the two corresponding electrode sites. With the exception of the “right negative” electrode site, adequate power was achieved to detect very small modulations of the C1 component.

condition	*x*	*y*	*z*	Anatomical structure	BA
con left	41	-70	-4	Right Inferior Occipital Gyrus	BA 19
con left	-59	-28	3	Left Superior Temporal Gyrus	BA 22
nocon left	47	-58	-5	Right Inferior Temporal Gyrus	BA 19
con right	-53	-51	9	Left Superior Temporal Gyrus	BA 22
con right	-47	-63	10	Left Middle Temporal Gyrus	BA 37
nocon right	47	-58	0	Right Inferior Temporal Gyrus	BA 19
nocon right	-53	-51	9	Left Superior Temporal Gyrus	BA 22
nocon right	-59	-29	-1	Left Middle Temporal Gyrus	BA 21
right-diff	-47	18	28	Left Middle Frontal Gyrus	BA 9
right-diff	-65	-21	30	Left Postcentral Gyrus	BA 2
left-diff	-47	-69	10	Left Middle Temporal Gyrus	BA 39
left-diff	-41	-37	59	Left Postcentral Gyrus	BA 2
left-diff	17	-73	38	Right Precuneus	BA 7
left-diff	47	8	45	Right Middle Frontal Gyrus	BA 6

Table 2. Ncl Source Estimations.

Talairach coordinates for the focal points of the inverse solutions for the Ncl timeframe (‘diff’ indicates at least 20% strength modulation between contour and no-contour conditions).

GENERAL DISCUSSION

This thesis examined the cortical dynamics of visual processing within the framework of the "frame-and-fill" models (Bar, 2003; Bullier, 2001; Chen, et al., 2007; Vidyasagar, 1999). Such models are based on the recent advancements in understanding the complexities of cortical processing. While earlier research efforts concentrated on defining the distinctive properties of the parallel streams of information in the cortex, we are now in a position to study their commonalities and interactions. Specifically, the general sequence of cortical events related to object recognition in naturalistic scenes can be roughly outlined as follows: 1) visual information is first received from parallel retinal processing streams by the primary visual cortex, where it is recombined and passed further on to higher order visual areas; 2) due to the so-called "magnocellular advantage" underlying the fast processing speed of the dorsal visual stream, parietal areas of the cortex produce a rough representation of the scene (global scene analysis) and subsequently guide fine-tuning of this rough representation in the ventral stream; 3) this is achieved by recurrent interactions between multiple areas of the brain including higher order ventral visual areas, the prefrontal cortex, the primary visual cortex and the hippocampus, whereby visual information is matched to a stored mental representation emerging into conscious perception (also see Figure 1). Such a model describes the temporal dynamics of visual perception, thus, testing the model critically depends on using temporally-sensitive methodology. In humans, this can be achieved with event-related potentials (ERPs).

The first study of this thesis (Chapter 1) addressed whether earliest contour interpolation effects observed in illusory contour studies in the ventral stream regions signal contour interpolation or global scene segmentation. Illusory contour and object recognition ERP studies reveal consistent object-related modulations of the visual N1 component. Global scene analysis

must precede this object-related processing if it is to guide it. The contention that global scene segmentation takes place in the ventral stream would be inconsistent with the temporal scale of the "framing" of the scene as well as with the putative role of the dorsal stream. When we tested stimuli designed to tap salient regions without inducing the perception of an illusory contour, we found stronger early sensitivity of ventral stream areas to illusory contours. Specifically, the N1 IC effect was higher in amplitude to illusory contours as compared to salient regions. These results reinforced our original model whereby initial illusory contour processing takes place in the LOC (Murray, et al., 2002) and are entirely consistent with the general "frame-and-fill" hypothesis.

In an attempt to validate the role of global scene analysis in illusory contour processing, we assessed how increasing the difficulty of "framing" the scene influences illusory contour interpolation (Chapter 2). We hypothesized that the increase in processing demands on the "framing" step will lead to a temporal delay in the N1 IC effect, provided "framing" is a prerequisite for fast contour interpolation. In order to make "framing" more difficult, we introduced pacmen distractors to clutter our illusory contour array. The N1 IC effect remained intact at the intermediate level of clutter but was delayed by about 80 ms for the highest level of clutter. It appeared that cluttering the scene lead to the breakdown of automatic IC processing and a switch to a more effortful mode of contour interpolation, as indexed by the Ncl component. Such temporal delay is already in the range of synchronization of the distributed object-recognition network (Sehatpour, et al., 2010).

The final study of this thesis (Chapter 3) examined perception of Gabor contours embedded in Gabor noise ("pathfinder displays"). Here, we set out to assess the role of the primary visual cortex in contour integration. It has been suggested that such contours may be

completed by pair-wise facilitative interactions between collinear cells via long-range horizontal connections in V1 (Bauer & Dicke, 1997; Bauer & Heinze, 2002; Gray, 1999; Grossberg & Williamson, 2001; Hess, et al., 2003; Kapadia, et al., 1995; Kovacs, 1996; Stettler, et al., 2002). Alternatively, activity from the collinear cells may be integrated in higher-order visual areas by pooling of inputs from lower visual areas (Hubel & Wiesel, 1962; Spillmann & Werner, 1996). In order to arbitrate between these competing hypotheses, we looked at the timecourse of contour-related cortical activations paying special attention to the activity stemming from the primary visual cortex, as indexed by the C1 visual ERP component. We found no contour-related activations in the C1 timeframe; indeed, the earliest effects were in the N1 timeframe over ventral visual areas. The direction and timing of the effects was highly consistent with IC literature. Such distribution of effects is indicative of pooling of information in higher order cortical areas as the initial step in contour integration.

When considering the results of the third study (Chapter 3) in light of the results of the second study (Chapter 2), we need to reconcile the relatively early effects of contour integration in "pathfinder displays" with the disappearance of the early N1 effect in the cluttered illusory contour display. This inconsistency most likely reflects differences in the mechanisms of contour integration for the two stimulus types as well as different types of trials included in analyses. Only correctly detected contours were included in the analyses in the study of "pathfinder displays." That is, only those trials, which resulted in a conscious detection of a contour, elicited the early N1 modulation. Due to very low sweep counts, we could not compare the misses with the false alarms in our paradigm. When we looked at the Ncl component, however, it appeared to be response-dependent with more negative waveform for false alarms than the misses (due to low sweep counts the effects were not statistically robust and data are now shown here). On the

other hand, attention was not directed at the illusory contour in our second experiment, allowing us to measure contour effects independent of task demands. Murray and colleagues (2006) reported robust N1 IC effect in both correctly and incorrectly identified trials in the context of a shape discrimination task. This suggests that the N1 IC modulation is independent and separable from task and attentional demands; that is, even if attention were directed at the illusory contour by a task in the second study, we would still expect clutter to delay contour-related modulation (an issue to be tested empirically, of course). In contrast, the N1 modulation in "pathfinder displays" may be amenable to attentional demands. Here, we would expect this effect to track the relative ease of integration of contour elements. Some support for this assertion comes from a study by Mathes and colleagues (2006) who compared ERPs to closed and open "pathfinder displays" with the intent to vary the relative ease of path detection (easier to closed paths). They indeed reported a gradual decrease in the N1 amplitude as a result of decreased salience of contours in one of their paradigms. However, since the behavioral performance was at ceiling levels in all contour-present conditions and the ERP effect was highly inconsistent, unambiguous conclusions regarding the dependence of the N1 effect on task demands cannot be drawn based on that study.

The findings of this thesis provide additional support for the "frame-and-fill" model of visual processing. We show that contour integration within the ventral stream is affected by the spatial delineation of the scene, in that taxing the initial global scene analysis delays automatic processing of illusory contours. We also provide further evidence that early ventral stream processing is specific to contour-related manipulations and not to manipulation of the global scene parameters. Finally, we show that completion of contours does not rely on the local horizontal connections in the primary visual cortex in the initial stages of contour integration.

Some Future Directions

The “frame-and-fill” model described here is based on a sequence of specific dynamic interactions between areas of the cortex, each with a defined function role in object recognition. Although many lines of experimental evidence support the validity of this model, the processing steps of the model have not been tested directly. Definitive tests of this model have to be conducted in the context of object perception in humans or behaving animals. Moreover, stages of the model have to be tested separately.

The model makes specific predictions with respect to the causal links between different processing stages, therefore, their role can be investigated by disrupting neural activity in relevant anatomical structures at a specific temporal window. For example, while the contributions of feedback from MT in motion perception have been validated with TMS studies (Koivisto, et al., 2010; Pascual-Leone & Walsh, 2001; Silvanto, et al., 2005), corresponding experiments exploring the role of feedback in object recognition are lacking. Two different steps of the model can be assessed: 1) the interaction between the parietal areas and the higher order temporal areas, particularly under conditions of clutter, and 2) the interactions between the temporal areas and the primary visual cortex. Specifically, the model predicts early differential behavioral performance (before 150 ms, first step of the model) and later differential behavioral performance (after 150 ms, second step of the model). Correspondingly, in animal models, inactivation of a particular brain region can be achieved by cooling.

Future ERP research efforts in refining the role of the dorsal stream areas in object perception will be directed at testing the model in a population with functional lesions of the dorsal stream (as discussed in Chapter 3). Additionally, it would be interesting to combine TMS and ERP methodologies to establish causality of interactions within putative processing steps of

the model. Combined TMS and EEG recording is a relatively novel methodology, not without interpretational challenges (Miniussi & Thut, 2010), however, it offers an opportunity to investigate functional significance of the ERP components (e.g., Thut et al., 2003). For example, our metrics of IC processing can be submitted to this protocol to characterize the role of the dorsal stream in delineating the scene for object recognition.

The strengths of the "frame-and-fill" model can be explored by computational modeling. Relatively few computational models attempted to model cortical dynamics within the framework of parallel information processing streams and taking into consideration recurrent projections (but see Chikkerur, Serre, Tan, & Poggio, 2010; Walther & Koch, 2006). Chikkerur and colleagues (2010) incorporated certain feedback projections into a previously proposed model of purely feedforward processing (Serre, Oliva, et al., 2007). This resulted in a significant improvement in performance of the model, although the nature of interactions between parallel streams is inconsistent with the "frame-and-fill" outline of events, as the feedforward activity is largely restricted to the ventral stream (reaching parietal cortices through V4). As such, the "magnocellular advantage" is not incorporated into the model. Lack of *a-priori* temporal constraints with respect to the type of neuronal connections utilized in modeling appears to be a general pattern. This may result in models, which are arguably incompatible with the timeframes of cortical activations. For example, VanRullen and colleagues (VanRullen, et al., 2001; VanRullen & Thorpe, 2002) relied on lateral horizontal projections in V1 to enhance interactions between neighboring cells for contour detection. And even though their spike-timing algorithm (see General Introduction) has clear computational advantages, it is likely to be significantly slowed down once the conduction velocity of horizontal connections is incorporated into the model. A direct application of the framework advanced here would include the parallel

processing of different attributes of the scene (for example, low spatial frequencies in the dorsal stream, Fenske, Aminoff, Gronau, & Bar, 2006) and their corresponding processing speeds of the parallel streams. Once a computational model is constructed, its advantages compared to other available models, can be tested on object recognition in naturalistic scenes. Unifying the separate models of scene (Oliva & Torralba, 2006, 2007) and object (Chikkerur, et al., 2010; Serre, Oliva, et al., 2007; VanRullen, et al., 2001; VanRullen & Thorpe, 2002; Walther & Koch, 2006) recognition into a common framework presents an interesting challenge for computational modeling.

BIBLIOGRAPHY

Ahissar, M., & Hochstein, S. (2000). The spread of attention and learning in feature search: effects of target distribution and task difficulty. *Vision Res, 40*(10-12), 1349-1364. doi: S0042-6989(00)00002-X [pii]

Ahissar, M., Nahum, M., Nelken, I., & Hochstein, S. (2009). Reverse hierarchies and sensory learning. *Philos Trans R Soc Lond B Biol Sci, 364*(1515), 285-299. doi: 4744481G47K64150 [pii]
10.1098/rstb.2008.0253

Alais, D., Lorenceau, J., Arrighi, R., & Cass, J. (2006). Contour interactions between pairs of Gabors engaged in binocular rivalry reveal a map of the association field. *Vision Res., 46*(8-9), 1473-1487.

Allman, J., Miezin, F., & McGuinness, E. (1985). Direction- and velocity-specific responses from beyond the classical receptive field in the middle temporal visual area (MT). *Perception, 14*(2), 105-126.

Anderson, B. L. (2007). The demise of the identity hypothesis and the insufficiency and nonnecessity of contour relatability in predicting object interpolation: comment on Kellman, Garrigan, and Shipley (2005). *Psychol Rev, 114*(2), 470-487. doi: 2007-05396-011 [pii]
10.1037/0033-295X.114.2.470

Angelucci, A., Levitt, J. B., Walton, E. J., Hupe, J. M., Bullier, J., & Lund, J. S. (2002). Circuits for local and global signal integration in primary visual cortex. *J.Neurosci., 22*(19), 8633-8646.

Bakin, J. S., Nakayama, K., & Gilbert, C. D. (2000). Visual responses in monkey areas V1 and V2 to three-dimensional surface configurations. *J.Neurosci., 20*(21), 8188-8198.

Bar, M. (2003). A cortical mechanism for triggering top-down facilitation in visual object recognition. *J.Cogn Neurosci., 15*(4), 600-609.

Bar, M. (2004). Visual objects in context. *Nat.Rev.Neurosci., 5*(8), 617-629.

Bar, M. (2009). The proactive brain: memory for predictions. *Philos Trans R Soc Lond B Biol Sci, 364*(1521), 1235-1243. doi: 364/1521/1235 [pii]
10.1098/rstb.2008.0310

Barone, P., Dehay, C., Berland, M., Bullier, J., & Kennedy, H. (1995). Developmental remodeling of primate visual cortical pathways. *Cereb Cortex, 5*(1), 22-38.

Batardiere, A., Barone, P., Knoblauch, K., Giroud, P., Berland, M., Dumas, A. M., et al. (2002). Early specification of the hierarchical organization of visual cortical areas in the macaque monkey. *Cereb Cortex, 12*(5), 453-465.

Bauer, R., & Dicke, P. (1997). Fast cortical selection: a principle of neuronal self-organization for perception? *Biol Cybern, 77*(3), 207-215.

Bauer, R., & Heinze, S. (2002). Contour integration in striate cortex. Classic cell responses or cooperative selection? *Exp Brain Res, 147*(2), 145-152. doi: 10.1007/s00221-002-1178-6

Bentin, S., Allison, T., Puce, A., Perez, A., & McCarthy, G. (1996). Electrophysiological studies of face perception in humans. *Journal of Cognitive Neuroscience, 8,* 551-565.

Blakemore, C., & Tobin, E. A. (1972). Lateral inhibition between orientation detectors in the cat's visual cortex. *Exp.Brain Res., 15*(4), 439-440.

Bressler, S. L., Coppola, R., & Nakamura, R. (1993). Episodic multiregional cortical coherence at multiple frequencies during visual task performance. *Nature, 366*(6451), 153-156.

Bullier, J. (2001). Integrated model of visual processing. *Brain Res Brain Res Rev, 36*(2-3), 96-107. doi: S0165017301000856 [pii]

Burkhalter, A., Bernardo, K. L., & Charles, V. (1993). Development of local circuits in human visual cortex. *J Neurosci, 13*(5), 1916-1931.

Butler, P. D., & Javitt, D. C. (2005). Early-stage visual processing deficits in schizophrenia. *Curr Opin Psychiatry, 18*(2), 151-157. doi: 00001504-200503000-00008 [pii]

Butler, P. D., Martinez, A., Foxe, J. J., Kim, D., Zemon, V., Silipo, G., et al. (2007). Subcortical visual dysfunction in schizophrenia drives secondary cortical impairments. *Brain, 130*(Pt 2), 417-430. doi: awl233 [pii]
10.1093/brain/awl233

Callaway, E. M. (1998). Prenatal development of layer-specific local circuits in primary visual cortex of the macaque monkey. *J Neurosci, 18*(4), 1505-1527.

Cardoso-Leite, P., & Gorea, A. (2010). On the perceptual/motor dissociation: a review of concepts, theory, experimental paradigms and data interpretations. *Seeing Perceiving, 23*(2), 89-151. doi: 10.1163/187847510X503588

Chen, C. M., Lakatos, P., Shah, A. S., Mehta, A. D., Givre, S. J., Javitt, D. C., et al. (2007). Functional anatomy and interaction of fast and slow visual pathways in macaque monkeys. [bhl067 pii ;10.1093/cercor/bhl067 doi]. *Cereb.Cortex, 17*(7), 1561-1569.

Chikkerur, S., Serre, T., Tan, C., & Poggio, T. (2010). What and where: a Bayesian inference theory of attention. *Vision Res, 50*(22), 2233-2247. doi: S0042-6989(10)00234-8 [pii]
10.1016/j.visres.2010.05.013

Clark, v. P., Fan S., Hillyard, S.A. (1994). *Identification of Early Visual Evoked Potential Generators by Retinotopic and Topographic Analyses.* (Vol. 2).

Conci, M., Bobel, E., Matthias, E., Keller, I., Muller, H. J., & Finke, K. (2009). Preattentive surface and contour grouping in Kanizsa figures: evidence from parietal extinction. *Neuropsychologia, 47*(3), 726-732. doi: S0028-3932(08)00476-4 [pii]
10.1016/j.neuropsychologia.2008.11.029

Coogan, T. A., & Van Essen, D. C. (1996). Development of connections within and between areas V1 and V2 of macaque monkeys. *J.Comp Neurol., 372*(3), 327-342.

Das, A., & Gilbert, C. D. (1995). Long-range horizontal connections and their role in cortical reorganization revealed by optical recording of cat primary visual cortex. *Nature, 375*(6534), 780-784.

Di Russo, F., Martinez, A., Sereno, M. I., Pitzalis, S., & Hillyard, S. A. (2002). Cortical sources of the early components of the visual evoked potential. *Hum.Brain Mapp., 15*(2), 95-111.

Doniger, G. M., Foxe, J. J., Murray, M. M., Higgins, B. A., & Javitt, D. C. (2002). Impaired visual object recognition and dorsal/ventral stream interaction in schizophrenia. *Arch.Gen.Psychiatry, 59*(11), 1011-1020.

Doniger, G. M., Foxe, J. J., Murray, M. M., Higgins, B. A., Snodgrass, J. G., Schroeder, C. E., et al. (2000). Activation timecourse of ventral visual stream object-recognition areas: high density electrical mapping of perceptual closure processes. *J.Cogn Neurosci., 12*(4), 615-621.

Doniger, G. M., Foxe, J. J., Schroeder, C. E., Murray, M. M., Higgins, B. A., & Javitt, D. C. (2001). Visual perceptual learning in human object recognition areas: a repetition priming study using high-density electrical mapping. *Neuroimage., 13*(2), 305-313.

Driver, J., Vuilleumier, P., & Husain, M. (2004). Spatial Neglect and Extinction. In M. Gazzaniga (Ed.), *The Cognitive Neurosciences* (pp. 589-619). Cambridge: MIT Press.

Eckhorn, R., Gail, A., Bruns, A., Gabriel, A., Al-Shaikhli, B., & Saam, M. (2004). Neural mechanisms of visual associative processing. *Acta Neurobiol Exp (Wars), 64*(2), 239-252.

Engel, A. K., Roelfsema, P. R., Fries, P., Brecht, M., & Singer, W. (1997). Role of the temporal domain for response selection and perceptual binding. *Cereb.Cortex, 7*(6), 571-582.

Ewbank, M. P., Schluppeck, D., & Andrews, T. J. (2005). fMR-adaptation reveals a distributed representation of inanimate objects and places in human visual cortex. *Neuroimage, 28*(1), 268-279. doi: S1053-8119(05)00408-8 [pii]
10.1016/j.neuroimage.2005.06.036

Farivar, R. (2009). Dorsal-ventral integration in object recognition. *Brain Res Rev, 61*(2), 144-153. doi: S0165-0173(09)00071-X [pii]
10.1016/j.brainresrev.2009.05.006

Felleman, D. J., & Van Essen, D. C. (1991). Distributed hierarchical processing in the primate cerebral cortex. *Cereb.Cortex, 1*(1), 1-47.

Fender, D. H. (1987). Methods of analysis of brain electrical and magnetic signals. In A. S. Gevins & A. Remond (Eds.), *Handbook of electroencephalography and clinical neurophysiology* (Vol. 1, pp. 355-399). Amsterdam: Elsevier. (Reprinted from: NOT IN FILE).

Fendrich, R., & Gazzaniga, M. S. (1989). Evidence of foveal splitting in a commissurotomy patient. *Neuropsychologia, 27*(3), 273-281.

Fenske, M. J., Aminoff, E., Gronau, N., & Bar, M. (2006). Top-down facilitation of visual object recognition: object-based and context-based contributions. *Prog Brain Res, 155*, 3-21. doi: S0079-6123(06)55001-0 [pii]
10.1016/S0079-6123(06)55001-0

Ffytche, D. H., & Zeki, S. (1996). Brain activity related to the perception of illusory contours. *Neuroimage., 3*(2), 104-108.

Fiebelkorn, I. C., Foxe, J. J., Schwartz, T. H., & Molholm, S. (2010). Staying within the lines: the formation of visuospatial boundaries influences multisensory feature integration. *Eur J Neurosci, 31*(10), 1737-1743. doi: EJN7196 [pii]
10.1111/j.1460-9568.2010.07196.x

Field, D. J., Hayes, A., & Hess, R. F. (1993). Contour integration by the human visual system: evidence for a local "association field". *Vision Res., 33*(2), 173-193.

Foxe, J. J., Doniger, G. M., & Javitt, D. C. (2001). Early visual processing deficits in schizophrenia: impaired P1 generation revealed by high-density electrical mapping. *Neuroreport, 12*(17), 3815-3820.

Foxe, J. J., Murray, M. M., & Javitt, D. C. (2005). Filling-in in Schizophrenia: a High-density Electrical Mapping and Source-analysis Investigation of Illusory Contour Processing. *Cereb.Cortex.*

Foxe, J. J., & Simpson, G. V. (2002). Flow of activation from V1 to frontal cortex in humans. A framework for defining "early" visual processing. *Exp.Brain Res., 142*(1), 139-150.

Fries, P., Nikolic, D., & Singer, W. (2007). The gamma cycle. *Trends Neurosci., 30*(7), 309-316.

Fujita, I., Tanaka, K., Ito, M., & Cheng, K. (1992). Columns for visual features of objects in monkey inferotemporal cortex. *Nature, 360*(6402), 343-346. doi: 10.1038/360343a0

Gilbert, C. D., Das, A., Ito, M., Kapadia, M., & Westheimer, G. (1996). Spatial integration and cortical dynamics. *Proc.Natl.Acad.Sci.U.S.A, 93*(2), 615-622.

Gilbert, C. D., Hirsch, J. A., & Wiesel, T. N. (1990). Lateral interactions in visual cortex. *Cold Spring Harb.Symp.Quant.Biol., 55*, 663-677.

Gilbert, C. D., & Wiesel, T. N. (1989). Columnar specificity of intrinsic horizontal and corticocortical connections in cat visual cortex. *J.Neurosci., 9*(7), 2432-2442.

Gomez Gonzalez, C. M., Clark, V. P., Fan, S., Luck, S. J., & Hillyard, S. A. (1994). Sources of attention-sensitive visual event-related potentials. *Brain Topogr., 7*(1), 41-51.

Goodale, M. A., & Milner, A. D. (1992). Separate visual pathways for perception and action. *Trends Neurosci, 15*(1), 20-25. doi: 0166-2236(92)90344-8 [pii]

Grave de Peralta, M. R., Gonzalez, A. S., Lantz, G., Michel, C. M., & Landis, T. (2001). Noninvasive localization of electromagnetic epileptic activity. I. Method descriptions and simulations. *Brain Topogr., 14*(2), 131-137.

Grave de Peralta, M. R., Murray, M. M., Michel, C. M., Martuzzi, R., & Gonzalez Andino, S. L. (2004). Electrical neuroimaging based on biophysical constraints. *Neuroimage, 21*(2), 527-539.

Gray, C. M. (1999). The temporal correlation hypothesis of visual feature integration: still alive and well. *Neuron, 24*(1), 31-47, 111-125. doi: S0896-6273(00)80820-X [pii]

Grill-Spector, K. (2003). The neural basis of object perception. *Curr.Opin.Neurobiol., 13*(2), 159-166.

Grill-Spector, K., & Malach, R. (2004). The human visual cortex. *Annu.Rev.Neurosci., 27*, 649-677.

Grossberg, S., & Williamson, J. R. (2001). A neural model of how horizontal and interlaminar connections of visual cortex develop into adult circuits that carry out perceptual grouping and learning. *Cereb Cortex, 11*(1), 37-58.

Guthrie, D., & Buchwald, J. S. (1991). Significance testing of difference potentials. *Psychophysiology, 28*(2), 240-244.

Halgren, E., Mendola, J., Chong, C. D., & Dale, A. M. (2003). Cortical activation to illusory shapes as measured with magnetoencephalography. *Neuroimage., 18*(4), 1001-1009.

Hamker, F. H. (2005). The reentry hypothesis: the putative interaction of the frontal eye field, ventrolateral prefrontal cortex, and areas V4, IT for attention and eye movement. *Cereb Cortex, 15*(4), 431-447. doi: 15/4/431 [pii]
10.1093/cercor/bhh146

Haxby, J. V., Gobbini, M. I., Furey, M. L., Ishai, A., Schouten, J. L., & Pietrini, P. (2001). Distributed and overlapping representations of faces and objects in ventral temporal cortex. *Science, 293*(5539), 2425-2430. doi: 10.1126/science.1063736
293/5539/2425 [pii]

Hegde, J. (2008). Time course of visual perception: coarse-to-fine processing and beyond. *Prog Neurobiol, 84*(4), 405-439. doi: S0301-0082(07)00165-7 [pii]
10.1016/j.pneurobio.2007.09.001

Hess, R. F., Dakin, S. C., & Field, D. J. (1998). The role of "contrast enhancement" in the detection and appearance of visual contours. *Vision Res., 38*(6), 783-787.

Hess, R. F., Hayes, A., & Field, D. J. (2003). Contour integration and cortical processing. *J.Physiol Paris, 97*(2-3), 105-119.

Hillyard, S. A., & Mangun, G. R. (1987). Sensory gating as a physiological mechanism for visual selective attention. *Electroencephalogr.Clin.Neurophysiol.Suppl, 40*, 61-67.

Hirabayashi, T., & Miyashita, Y. (2005). Dynamically modulated spike correlation in monkey inferior temporal cortex depending on the feature configuration within a whole object. *J Neurosci, 25*(44), 10299-10307. doi: 25/44/10299 [pii]
10.1523/JNEUROSCI.3036-05.2005

Hirsch, J. A., & Gilbert, C. D. (1991). Synaptic physiology of horizontal connections in the cat's visual cortex. *J.Neurosci., 11*(6), 1800-1809.

Hochstein, S., & Ahissar, M. (2002). View from the top: hierarchies and reverse hierarchies in the visual system. *Neuron, 36*(5), 791-804. doi: S0896627302010917 [pii]

Hubel, D. H., & Wiesel, T. N. (1962). Receptive fields, binocular interaction and functional architecture in the cat's visual cortex. *J Physiol, 160*, 106-154.

Hung, C. P., Kreiman, G., Poggio, T., & DiCarlo, J. J. (2005). Fast readout of object identity from macaque inferior temporal cortex. *Science, 310*(5749), 863-866. doi: 310/5749/863 [pii]
10.1126/science.1117593

Hupe, J. M., James, A. C., Girard, P., Lomber, S. G., Payne, B. R., & Bullier, J. (2001). Feedback connections act on the early part of the responses in monkey visual cortex. *J Neurophysiol, 85*(1), 134-145.

Itier, R. J., Latinus, M., & Taylor, M. J. (2006). Face, eye and object early processing: what is the face specificity? *Neuroimage, 29*(2), 667-676.

Jeffreys, D. A., & Axford, J. G. (1972a). Source locations of pattern-specific components of human visual evoked potentials. I. Component of striate cortical origin. *Exp Brain Res, 16*(1), 1-21.

Jeffreys, D. A., & Axford, J. G. (1972b). Source locations of pattern-specific components of human visual evoked potentials. II. Component of extrastriate cortical origin. *Exp.Brain Res., 16*(1), 22-40.

Kanizsa, G. (1976). Subjective contours. *Sci Am, 234*(4), 48-52.

Kapadia, M. K., Ito, M., Gilbert, C. D., & Westheimer, G. (1995). Improvement in visual sensitivity by changes in local context: parallel studies in human observers and in V1 of alert monkeys. *Neuron, 15*(4), 843-856.

Kaplan, E. (2008). The P, M and K Streams fo the Primate Visual System: What Do They Do for Vision? In R. Masland, Albright, T.D. (Ed.), *Vision I* (Vol. 1, pp. 369-382). San Diego: Academic Press.

Kellman, P. J., Garrigan, P., & Shipley, T. F. (2005). Object interpolation in three dimensions. *Psychol.Rev., 112*(3), 586-609.

Kellman, P. J., Garrigan, P., Shipley, T. F., & Keane, B. P. (2007). Interpolation processes in object perception: reply to Anderson (2007). *Psychol Rev, 114*(2), 488-508. doi: 2007-05396-012 [pii]
10.1037/0033-295X.114.2.488

Kelly, S. P., Gomez-Ramirez, M., & Foxe, J. J. (2008). Spatial Attention Modulates Initial Afferent Activity in Human Primary Visual Cortex. *Cereb.Cortex.*

Khoe, W., Freeman, E., Woldorff, M. G., & Mangun, G. R. (2004). Electrophysiological correlates of lateral interactions in human visual cortex. *Vision Res., 44*(14), 1659-1673.

Khoe, W., Freeman, E., Woldorff, M. G., & Mangun, G. R. (2006). Interactions between attention and perceptual grouping in human visual cortex. *Brain Res., 1078*(1), 101-111.

Kiorpes, L., & Bassin, S. A. (2003). Development of contour integration in macaque monkeys. *Vis Neurosci, 20*(5), 567-575.

Koivisto, M., Railo, H., & Salminen-Vaparanta, N. (2010). Transcranial magnetic stimulation of early visual cortex interferes with subjective visual awareness and objective forced-choice performance. *Conscious Cogn*. doi: S1053-8100(10)00167-4 [pii]
10.1016/j.concog.2010.09.001

Konen, C. S., & Kastner, S. (2008). Two hierarchically organized neural systems for object information in human visual cortex. *Nat Neurosci, 11*(2), 224-231. doi: nn2036 [pii]
10.1038/nn2036

Kovacs, I. (1996). Gestalten of today: early processing of visual contours and surfaces. *Behav Brain Res, 82*(1), 1-11. doi: S0166432897811035 [pii]

Kovacs, I. (2000). Human development of perceptual organization. *Vision Res, 40*(10-12), 1301-1310. doi: S0042-6989(00)00055-9 [pii]

Kovacs, I., Kozma, P., Feher, A., & Benedek, G. (1999). Late maturation of visual spatial integration in humans. *Proc Natl Acad Sci U S A, 96*(21), 12204-12209.

Kruggel, F., Herrmann, C. S., Wiggins, C. J., & von Cramon, D. Y. (2001). Hemodynamic and electroencephalographic responses to illusory figures: recording of the evoked potentials during functional MRI. *Neuroimage., 14*(6), 1327-1336.

Lamme, V. A. (2003). Why visual attention and awareness are different. *Trends Cogn Sci., 7*(1), 12-18.

Lamme, V. A. (2004). Separate neural definitions of visual consciousness and visual attention; a case for phenomenal awareness. *Neural Netw., 17*(5-6), 861-872.

Lamme, V. A., & Roelfsema, P. R. (2000). The distinct modes of vision offered by feedforward and recurrent processing. *Trends Neurosci., 23*(11), 571-579.

Lamme, V. A., & Spekreijse, H. (2000). Modulations of primary visual cortex activity representing attentive and conscious scene perception. *Front Biosci., 5*, D232-D243.

Lamme, V. A., Super, H., Landman, R., Roelfsema, P. R., & Spekreijse, H. (2000). The role of primary visual cortex (V1) in visual awareness. *Vision Res., 40*(10-12), 1507-1521.

Larsson, J., Amunts, K., Gulyas, B., Malikovic, A., Zilles, K., & Roland, P. E. (1999). Neuronal correlates of real and illusory contour perception: functional anatomy with PET. *Eur.J.Neurosci., 11*(11), 4024-4036.

Lee, T. S., & Nguyen, M. (2001). Dynamics of subjective contour formation in the early visual cortex. *Proc.Natl.Acad.Sci.U.S.A, 98*(4), 1907-1911.

Lehky, S. R., & Sereno, A. B. (2007). Comparison of shape encoding in primate dorsal and ventral visual pathways. *J Neurophysiol, 97*(1), 307-319. doi: 00168.2006 [pii]
10.1152/jn.00168.2006

Lehmann, D. (1987). Principles of spatial analysis. In A. S. Gevins & A. Remond (Eds.), *Methods of Analysis of Brain Electrical and Magnetic Signals. Handbook of Electro-Encephalography and Clinical Neurophysiology* (pp. 309-354). Amsterdam: Elsevier. (Reprinted from: NOT IN FILE).

Lehmann, D., & Skrandies, W. (1980). Reference-free identification of components of checkerboard-evoked multichannel potential fields. *Electroencephalogr.Clin.Neurophysiol., 48*(6), 609-621.

Levitt, J. B., & Lund, J. S. (1997). Contrast dependence of contextual effects in primate visual cortex. *Nature, 387*(6628), 73-76.

Livingstone, M., & Hubel, D. (1988). Segregation of form, color, movement, and depth: anatomy, physiology, and perception. *Science, 240*(4853), 740-749.

Luck, S. J. (2005). *An Introduction to the Event-Related Potential Technique* (1st ed.). Cambridge, MA: The MIT Press.

Lund, J. S., Angelucci, A., & Bressloff, P. C. (2003). Anatomical substrates for functional columns in macaque monkey primary visual cortex. *Cereb.Cortex, 13*(1), 15-24.

Macmillan NA, C. C. (2005). *Detection Theory: A User's Guide.* (2 ed.). Mahwah, N.J. : Lawrence Erlbaum Associates.

Maertens, M., & Pollmann, S. (2005). fMRI reveals a common neural substrate of illusory and real contours in V1 after perceptual learning. *J.Cogn Neurosci., 17*(10), 1553-1564.

Malach, R., Amir, Y., Harel, M., & Grinvald, A. (1993). Relationship between intrinsic connections and functional architecture revealed by optical imaging and in vivo targeted biocytin injections in primate striate cortex. *Proc.Natl.Acad.Sci.U.S.A, 90*(22), 10469-10473.

Manly, B. F. J. (1997). *Randomization, Bootstrap and Monte Carlo Methods in Biology* (Vol. 2): Chpman and Hall, London.

Martinez, A., Anllo-Vento, L., Sereno, M. I., Frank, L. R., Buxton, R. B., Dubowitz, D. J., et al. (1999). Involvement of striate and extrastriate visual cortical areas in spatial attention. *Nat.Neurosci., 2*(4), 364-369.

Martinez, A., Teder-Salejarvi, W., & Hillyard, S. A. (2007). Spatial attention facilitates selection of illusory objects: Evidence from event-related brain potentials. *Brain Res., 1139*, 143-152.

Martinez, A., Teder-Salejarvi, W., Vazquez, M., Molholm, S., Foxe, J. J., Javitt, D. C., et al. (2006). Objects are highlighted by spatial attention. *J.Cogn Neurosci., 18*(2), 298-310.

Mathes, B., & Fahle, M. (2007). The electrophysiological correlate of contour integration is similar for color and luminance mechanisms. *Psychophysiology, 44*(2), 305-322.

Mathes, B., Trenner, D., & Fahle, M. (2006). The electrophysiological correlate of contour integration is modulated by task demands. *Brain Res., 1114*(1), 98-112.

Mattingley, J. B., Davis, G., & Driver, J. (1997). Preattentive filling-in of visual surfaces in parietal extinction. *Science, 275*(5300), 671-674.

Maturana, H. R., & Varela, F. (1992). *The tree of knowledge*. Boston, MA: Shambhala.

McAdams, C. J., & Reid, R. C. (2005). Attention modulates the responses of simple cells in monkey primary visual cortex. *J Neurosci, 25*(47), 11023-11033. doi: 25/47/11023 [pii] 10.1523/JNEUROSCI.2904-05.2005

McCourt, M. E., Shpaner, M., Javitt, D. C., & Foxe, J. J. (2008). Hemispheric asymmetry and callosal integration of visuospatial attention in schizophrenia: a tachistoscopic line bisection study. *Schizophr Res, 102*(1-3), 189-196. doi: S0920-9964(08)00163-1 [pii] 10.1016/j.schres.2008.03.021

McIntosh, R. D., & Schenk, T. (2009). Two visual streams for perception and action: current trends. *Neuropsychologia, 47*(6), 1391-1396. doi: S0028-3932(09)00080-3 [pii]
10.1016/j.neuropsychologia.2009.02.009

Mendola, J. D., Dale, A. M., Fischl, B., Liu, A. K., & Tootell, R. B. (1999). The representation of illusory and real contours in human cortical visual areas revealed by functional magnetic resonance imaging. *J.Neurosci., 19*(19), 8560-8572.

Michel, C. M., Murray, M. M., Lantz, G., Gonzalez, S., Spinelli, L., & Grave de, P. R. (2004). EEG source imaging. *Clin.Neurophysiol., 115*(10), 2195-2222.

Michel, C. M., Seeck, M., & Murray, M. M. (2004). The speed of visual cognition. *Suppl Clin.Neurophysiol., 57*, 617-627.

Michel, C. M., Thut, G., Morand, S., Khateb, A., Pegna, A. J., Grave de, P. R., et al. (2001). Electric source imaging of human brain functions. *Brain Res.Brain Res.Rev., 36*(2-3), 108-118.

Milner, A. D., & Goodale, M. A. (2008). Two visual systems re-viewed. *Neuropsychologia, 46*(3), 774-785. doi: S0028-3932(07)00354-5 [pii]
10.1016/j.neuropsychologia.2007.10.005

Miniussi, C., & Thut, G. (2010). Combining TMS and EEG offers new prospects in cognitive neuroscience. *Brain Topogr, 22*(4), 249-256. doi: 10.1007/s10548-009-0083-8

Mishkin, M., Lewis, M. E., & Ungerleider, L. G. (1982). Equivalence of parieto-preoccipital subareas for visuospatial ability in monkeys. *Behav.Brain Res., 6*(1), 41-55.

Mishkin, M., Ungerleider, L. G., & Macko, K. A. (1983). Object vision and spatial vision: two cortical pathways. *Trends in Neurosciences, 6*, 414-417. doi: Doi: 10.1016/0166-2236(83)90190-x

Molholm, S., Ritter, W., Murray, M. M., Javitt, D. C., Schroeder, C. E., & Foxe, J. J. (2002). Multisensory auditory-visual interactions during early sensory processing in humans: a high-density electrical mapping study. *Brain Res.Cogn Brain Res., 14*(1), 115-128.

Murray, M. M., Brunet, D., & Michel, C. M. (2008). Topographic ERP analyses: a step-by-step tutorial review. [10.1007/s10548-008-0054-5 doi]. *Brain Topogr., 20*(4), 249-264.

Murray, M. M., Foxe, D. M., Javitt, D. C., & Foxe, J. J. (2004). Setting boundaries: brain dynamics of modal and amodal illusory shape completion in humans. *J.Neurosci., 24*(31), 6898-6903.

Murray, M. M., Imber, M. L., Javitt, D. C., & Foxe, J. J. (2006). Boundary completion is automatic and dissociable from shape discrimination. *J.Neurosci., 26*(46), 12043-12054.

Murray, M. M., Molholm, S., Michel, C. M., Heslenfeld, D. J., Ritter, W., Javitt, D. C., et al. (2004). Grabbing Your Ear: Rapid Auditory-Somatosensory Multisensory Interactions in Low-level Sensory Cortices Are Not Constrained by Stimulus Alignment. *Cereb.Cortex*.

Murray, M. M., Wylie, G. R., Higgins, B. A., Javitt, D. C., Schroeder, C. E., & Foxe, J. J. (2002). The spatiotemporal dynamics of illusory contour processing: combined high-density electrical mapping, source analysis, and functional magnetic resonance imaging. *J.Neurosci., 22*(12), 5055-5073.

Murthy, V. N., & Fetz, E. E. (1996). Synchronization of neurons during local field potential oscillations in sensorimotor cortex of awake monkeys. *J Neurophysiol, 76*(6), 3968-3982.

Nakamura, H., Kuroda, T., Wakita, M., Kusunoki, M., Kato, A., Mikami, A., et al. (2001). From three-dimensional space vision to prehensile hand movements: the lateral intraparietal area links the area V3A and the anterior intraparietal area in macaques. *J Neurosci, 21*(20), 8174-8187. doi: 21/20/8174 [pii]

Nassi, J. J., & Callaway, E. M. (2009). Parallel processing strategies of the primate visual system. *Nat Rev Neurosci, 10*(5), 360-372. doi: nrn2619 [pii]
10.1038/nrn2619

Nelson, J. I., & Frost, B. J. (1978). Orientation-selective inhibition from beyond the classic visual receptive field. *Brain Res., 139*(2), 359-365.

Nieder, A. (2002). Seeing more than meets the eye: processing of illusory contours in animals. *J.Comp Physiol A Neuroethol.Sens.Neural Behav.Physiol, 188*(4), 249-260.

Oldfield, R. C. (1971). The assessment and analysis of handedness: the Edinburgh inventory. *Neuropsychologia, 9*(1), 97-113.

Oliva, A., & Torralba, A. (2006). Building the gist of a scene: the role of global image features in recognition. *Prog Brain Res, 155*, 23-36. doi: S0079-6123(06)55002-2 [pii]

10.1016/S0079-6123(06)55002-2

Oliva, A., & Torralba, A. (2007). The role of context in object recognition. *Trends Cogn Sci, 11*(12), 520-527. doi: S1364-6613(07)00255-0 [pii]
10.1016/j.tics.2007.09.009

Pascual-Leone, A., & Walsh, V. (2001). Fast backprojections from the motion to the primary visual area necessary for visual awareness. *Science, 292*(5516), 510-512.

Pascual-Leone, A., Walsh, V., & Rothwell, J. (2000). Transcranial magnetic stimulation in cognitive neuroscience--virtual lesion, chronometry, and functional connectivity. *Curr.Opin.Neurobiol., 10*(2), 232-237.

Pascual-Marqui, R. D., Michel, C. M., & Lehmann, D. (1995). Segmentation of brain electrical activity into microstates: model estimation and validation. *IEEE Trans.Biomed.Eng, 42*(7), 658-665.

Pasupathy, A., & Connor, C. E. (2002). Population coding of shape in area V4. *Nat Neurosci, 5*(12), 1332-1338. doi: 10.1038/nn972
nn972 [pii]

Pegna, A. J., Khateb, A., Murray, M. M., Landis, T., & Michel, C. M. (2002). Neural processing of illusory and real contours revealed by high-density ERP mapping. *Neuroreport, 13*(7), 965-968.

Perrin, F., Pernier, J., Bertrand, O., Giard, M. H., & Echallier, J. F. (1987). Mapping of scalp potentials by surface spline interpolation. *Electroencephalogr.Clin.Neurophysiol., 66*(1), 75-81.

Peterhans, E., & von der Heydt, R. (1989). Mechanisms of contour perception in monkey visual cortex. II. Contours bridging gaps. *J.Neurosci., 9*(5), 1749-1763.

Polat, U., Mizobe, K., Pettet, M. W., Kasamatsu, T., & Norcia, A. M. (1998). Collinear stimuli regulate visual responses depending on cell's contrast threshold. *Nature, 391*(6667), 580-584.

Polat, U., & Sagi, D. (1993). Lateral interactions between spatial channels: suppression and facilitation revealed by lateral masking experiments. *Vision Res., 33*(7), 993-999.

Polat, U., & Sagi, D. (1994). The architecture of perceptual spatial interactions. *Vision Res., 34*(1), 73-78.

Pooresmaeili, A., Poort, J., Thiele, A., & Roelfsema, P. R. (2010). Separable codes for attention and luminance contrast in the primary visual cortex. *J Neurosci, 30*(38), 12701-12711. doi: 30/38/12701 [pii]
10.1523/JNEUROSCI.1388-10.2010

Quiroga, R. Q., Reddy, L., Kreiman, G., Koch, C., & Fried, I. (2005). Invariant visual representation by single neurons in the human brain. *Nature, 435*(7045), 1102-1107. doi: nature03687 [pii]
10.1038/nature03687

Rademacher, J., Caviness, V. S., Jr., Steinmetz, H., & Galaburda, A. M. (1993). Topographical variation of the human primary cortices: implications for neuroimaging, brain mapping, and neurobiology. *Cereb.Cortex, 3*(4), 313-329.

Ramsden, B. M., Hung, C. P., & Roe, A. W. (2001). Real and illusory contour processing in area V1 of the primate: a cortical balancing act. *Cereb.Cortex, 11*(7), 648-665.

Reddy, L., & Kanwisher, N. (2006). Coding of visual objects in the ventral stream. *Curr Opin Neurobiol, 16*(4), 408-414. doi: S0959-4388(06)00080-8 [pii]
10.1016/j.conb.2006.06.004

Regan, D. (1989). *Human Brain Electrophysiology: Evoked Potentials and Evoked Magnetic Fields in Science and Medicine.* New York: Elsevier.

Riesenhuber, M., & Poggio, T. (1999). Hierarchical models of object recognition in cortex. *Nat Neurosci, 2*(11), 1019-1025. doi: 10.1038/14819

Ringach, D. L., & Shapley, R. (1996). Spatial and temporal properties of illusory contours and amodal boundary completion. *Vision Res., 36*(19), 3037-3050.

Ritzl, A., Marshall, J. C., Weiss, P. H., Zafiris, O., Shah, N. J., Zilles, K., et al. (2003a). Functional anatomy and differential time courses of neural processing for explicit, inferred, and illusory contours. An event-related fMRI study. *Neuroimage., 19*(4), 1567-1577.

Ritzl, A., Marshall, J. C., Weiss, P. H., Zafiris, O., Shah, N. J., Zilles, K., et al. (2003b). Functional anatomy and differential time courses of neural processing for explicit, inferred, and illusory contours. An event-related fMRI study. *Neuroimage, 19*(4), 1567-1577.

Rockland, K. S., & Lund, J. S. (1983). Intrinsic laminar lattice connections in primate visual cortex. *J.Comp Neurol., 216*(3), 303-318.

Roelfsema, P. R. (2006). Cortical algorithms for perceptual grouping. *Annu Rev Neurosci, 29*, 203-227. doi: 10.1146/annurev.neuro.29.051605.112939

Roelfsema, P. R., Engel, A. K., Konig, P., & Singer, W. (1997). Visuomotor integration is associated with zero time-lag synchronization among cortical areas. *Nature, 385*(6612), 157-161. doi: 10.1038/385157a0

Rossion, B., & Jacques, C. (2008). Does physical interstimulus variance account for early electrophysiological face sensitive responses in the human brain? Ten lessons on the N170. *Neuroimage, 39*(4), 1959-1979. doi: S1053-8119(07)00936-6 [pii]
10.1016/j.neuroimage.2007.10.011

Rousselet, G. A., Husk, J. S., Bennett, P. J., & Sekuler, A. B. (2005). Spatial scaling factors explain eccentricity effects on face ERPs. *J Vis, 5*(10), 755-763. doi: 10.1167/5.10.1 /5/10/1/ [pii]

Rousselet, G. A., Husk, J. S., Bennett, P. J., & Sekuler, A. B. (2007). Single-trial EEG dynamics of object and face visual processing. *Neuroimage, 36*(3), 843-862. doi: S1053-8119(07)00111-5 [pii]
10.1016/j.neuroimage.2007.02.052

Saalmann, Y. B., & Kastner, S. (2009). Gain control in the visual thalamus during perception and cognition. *Curr Opin Neurobiol, 19*(4), 408-414. doi: S0959-4388(09)00049-X [pii]
10.1016/j.conb.2009.05.007

Samonds, J. M., Zhou, Z., Bernard, M. R., & Bonds, A. B. (2006). Synchronous activity in cat visual cortex encodes collinear and cocircular contours. *J.Neurophysiol., 95*(4), 2602-2616.

Sary, G., Chadaide, Z., Tompa, T., Koteles, K., Kovacs, G., & Benedek, G. (2007). Illusory shape representation in the monkey inferior temporal cortex. *Eur J Neurosci, 25*(8), 2558-2564. doi: EJN5494 [pii]

10.1111/j.1460-9568.2007.05494.x

Sary, G., Koteles, K., Kaposvari, P., Lenti, L., Csifcsak, G., Franko, E., et al. (2008). The representation of Kanizsa illusory contours in the monkey inferior temporal cortex. *Eur J Neurosci, 28*(10), 2137-2146. doi: EJN6499 [pii]
10.1111/j.1460-9568.2008.06499.x

Schmolesky, M. T., Wang, Y., Hanes, D. P., Thompson, K. G., Leutgeb, S., Schall, J. D., et al. (1998). Signal timing across the macaque visual system. *J Neurophysiol, 79*(6), 3272-3278.

Schroeder, C. E., Mehta, A. D., & Foxe, J. J. (2001). Determinants and mechanisms of attentional modulation of neural processing. *Front Biosci., 6*, D672-D684.

Schroeder, C. E., Mehta, A. D., & Givre, S. J. (1998). A spatiotemporal profile of visual system activation revealed by current source density analysis in the awake macaque. *Cereb.Cortex, 8*(7), 575-592.

Schwarz, C., & Bolz, J. (1991). Functional specificity of a long-range horizontal connection in cat visual cortex: a cross-correlation study. *J.Neurosci., 11*(10), 2995-3007.

Seghier, M., Dojat, M., on-Martin, C., Rubin, C., Warnking, J., Segebarth, C., et al. (2000). Moving illusory contours activate primary visual cortex: an fMRI study. *Cereb.Cortex, 10*(7), 663-670.

Sehatpour, P., Dias, E. C., Butler, P. D., Revheim, N., Guilfoyle, D. N., Foxe, J. J., et al. (2010). Impaired visual object processing across an occipital-frontal-hippocampal brain network in schizophrenia: an integrated neuroimaging study. *Arch Gen Psychiatry, 67*(8), 772-782. doi: 67/8/772 [pii]
10.1001/archgenpsychiatry.2010.85

Sehatpour, P., Molholm, S., Javitt, D. C., & Foxe, J. J. (2006). Spatiotemporal dynamics of human object recognition processing: an integrated high-density electrical mapping and functional imaging study of "closure" processes. *Neuroimage, 29*(2), 605-618.

Sehatpour, P., Molholm, S., Schwartz, T. H., Mahoney, J. R., Mehta, A. D., Javitt, D. C., et al. (2008). A human intracranial study of long-range oscillatory coherence across a frontal-occipital-hippocampal brain network during visual object processing. *Proc.Natl.Acad.Sci.U.S.A, 105*(11), 4399-4404.

Senkowski, D., Gomez-Ramirez, M., Lakatos, P., Wylie, G. R., Molholm, S., Schroeder, C. E., et al. (2007). Multisensory processing and oscillatory activity: analyzing non-linear electrophysiological measures in humans and simians. [10.1007/s00221-006-0664-7 doi]. *Exp.Brain Res., 177*(2), 184-195.

Senkowski, D., Rottger, S., Grimm, S., Foxe, J. J., & Herrmann, C. S. (2005). Kanizsa subjective figures capture visual spatial attention: evidence from electrophysiological and behavioral data. *Neuropsychologia, 43*(6), 872-886.

Sereno, A. B., & Maunsell, J. H. (1998). Shape selectivity in primate lateral intraparietal cortex. *Nature, 395*(6701), 500-503. doi: 10.1038/26752

Serre, T., Kreiman, G., Kouh, M., Cadieu, C., Knoblich, U., & Poggio, T. (2007). A quantitative theory of immediate visual recognition. *Prog Brain Res, 165*, 33-56. doi: S0079-6123(06)65004-8 [pii]
10.1016/S0079-6123(06)65004-8

Serre, T., Oliva, A., & Poggio, T. (2007). A feedforward architecture accounts for rapid categorization. *Proc Natl Acad Sci U S A, 104*(15), 6424-6429. doi: 0700622104 [pii]
10.1073/pnas.0700622104

Sharon, E., Brandt, A., Basri, R. . (2000). *Fast Multiscale Image Segmentation.* Paper presented at the Proc IEEE Conf. on Computer Vision and Pattern Recognition, South Carolina.

Sherman, S. M. (2005). Thalamic relays and cortical functioning. *Prog Brain Res, 149*, 107-126. doi: S0079-6123(05)49009-3 [pii]
10.1016/S0079-6123(05)49009-3

Shi, J., Malik, J. (2000). Normalized Cuts and Image Segmentation. *IEEE Trans. Patt. Anal. Mach Intel., 22*, 17.

Shikata, E., Tanaka, Y., Nakamura, H., Taira, M., & Sakata, H. (1996). Selectivity of the parietal visual neurones in 3D orientation of surface of stereoscopic stimuli. *Neuroreport, 7*(14), 2389-2394.

Shpaner, M., Murray, M. M., & Foxe, J. J. (2009). Early processing in the human lateral occipital complex is highly responsive to illusory contours but not to salient regions. *Eur J Neurosci, 30*(10), 2018-2028. doi: EJN6981 [pii]
10.1111/j.1460-9568.2009.06981.x

Silvanto, J., Lavie, N., & Walsh, V. (2005). Double dissociation of V1 and V5/MT activity in visual awareness. *Cereb Cortex, 15*(11), 1736-1741. doi: bhi050 [pii]
10.1093/cercor/bhi050

Sincich, L. C., & Horton, J. C. (2005). The circuitry of V1 and V2: integration of color, form, and motion. *Annu Rev Neurosci, 28*, 303-326. doi: 10.1146/annurev.neuro.28.061604.135731

Singer, W., & Gray, C. M. (1995). Visual feature integration and the temporal correlation hypothesis. *Annu.Rev.Neurosci., 18*, 555-586.

Spillmann, L., & Werner, J. S. (1996). Long-range interactions in visual perception. *Trends Neurosci, 19*(10), 428-434. doi: S0166223696100382 [pii]

Spinelli, L., Andino, S. G., Lantz, G., Seeck, M., & Michel, C. M. (2000). Electromagnetic inverse solutions in anatomically constrained spherical head models. *Brain Topogr., 13*(2), 115-125.

Stanley, D. A., & Rubin, N. (2003). fMRI activation in response to illusory contours and salient regions in the human lateral occipital complex. *Neuron, 37*(2), 323-331.

Stettler, D. D., Das, A., Bennett, J., & Gilbert, C. D. (2002). Lateral connectivity and contextual interactions in macaque primary visual cortex. *Neuron, 36*(4), 739-750.

Sugase, Y., Yamane, S., Ueno, S., & Kawano, K. (1999). Global and fine information coded by single neurons in the temporal visual cortex. *Nature, 400*(6747), 869-873. doi: 10.1038/23703

Sugishita, M., Hamilton, C. R., Sakuma, I., & Hemmi, I. (1994). Hemispheric representation of the central retina of commissurotomized subjects. *Neuropsychologia, 32*(4), 399-415.

Sugishita, M., Hemmi, I., Sakuma, I., Beppu, H., & Shiokawa, Y. (1993). The problem of macular sparing after unilateral occipital lesions. *J.Neurol., 241*(1), 1-9.

Super, H., Spekreijse, H., & Lamme, V. A. (2001). Two distinct modes of sensory processing observed in monkey primary visual cortex (V1). *Nat.Neurosci., 4*(3), 304-310.

Talairach, J., & Tournoux, P. (1988). Co-Planar Stereotaxic Atlas of the Human Brain Thieme, New York. (Reprinted from: NOT IN FILE).

Tallon-Baudry, C. (2009). The roles of gamma-band oscillatory synchrony in human visual cognition. *Front Biosci, 14*, 321-332. doi: 3246 [pii]

Tallon-Baudry, C., & Bertrand, O. (1999). Oscillatory gamma activity in humans and its role in object representation. *Trends Cogn Sci, 3*(4), 151-162. doi: S1364-6613(99)01299-1 [pii]

Tallon-Baudry, C., Bertrand, O., Delpuech, C., & Pernier, J. (1996). Stimulus specificity of phase-locked and non-phase-locked 40 Hz visual responses in human. *J.Neurosci., 16*(13), 4240-4249.

Tanaka, K. (1996). Inferotemporal cortex and object vision. *Annu Rev Neurosci, 19*, 109-139. doi: 10.1146/annurev.ne.19.030196.000545

Thorpe, S., Fize, D., & Marlot, C. (1996). Speed of processing in the human visual system. *Nature, 381*(6582), 520-522. doi: 10.1038/381520a0

Thut, G., Northoff, G., Ives, J. R., Kamitani, Y., Pfennig, A., Kampmann, F., et al. (2003). Effects of single-pulse transcranial magnetic stimulation (TMS) on functional brain activity: a combined event-related TMS and evoked potential study. *Clin Neurophysiol, 114*(11), 2071-2080. doi: S1388245703002050 [pii]

Ts'o, D. Y., Gilbert, C. D., & Wiesel, T. N. (1986). Relationships between horizontal interactions and functional architecture in cat striate cortex as revealed by cross-correlation analysis. *J.Neurosci., 6*(4), 1160-1170.

Tulving, E., & Schacter, D. L. (1990). Priming and human memory systems. *Science, 247*(4940), 301-306.

Uhlhaas, P. J., Pipa, G., Lima, B., Melloni, L., Neuenschwander, S., Nikolic, D., et al. (2009). Neural synchrony in cortical networks: history, concept and current status. *Front Integr Neurosci, 3*, 17. doi: 10.3389/neuro.07.017.2009

Vaina, L. M. (1989). Selective impairment of visual motion interpretation following lesions of the right occipito-parietal area in humans. *Biol Cybern, 61*(5), 347-359.

Vanni, S., Warnking, J., Dojat, M., Delon-Martin, C., Bullier, J., & Segebarth, C. (2004). Sequence of pattern onset responses in the human visual areas: an fMRI constrained VEP source analysis. *Neuroimage, 21*(3), 801-817. doi: 10.1016/j.neuroimage.2003.10.047 S1053811903007055 [pii]

VanRullen, R., Delorme, A., & Thorpe, S. J. (2001). Feed-forward Contour Integration in Primary Visual Cortex Based on Asynchronous Spike Propagation. *Neurocomputing, 38-40*(1-4), 1003-1009.

VanRullen, R., Guyonneau, R., & Thorpe, S. J. (2005). Spike times make sense. *Trends Neurosci, 28*(1), 1-4. doi: S0166-2236(04)00354-6 [pii] 10.1016/j.tins.2004.10.010

VanRullen, R., & Thorpe, S. J. (2002). Surfing a spike wave down the ventral stream. *Vision Res, 42*(23), 2593-2615. doi: S0042698902002985 [pii]

Vidyasagar, T. R. (1999). A neuronal model of attentional spotlight: parietal guiding the temporal. *Brain Res.Brain Res.Rev., 30*(1), 66-76.

von der Heydt, R., & Peterhans, E. (1989). Mechanisms of contour perception in monkey visual cortex. I. Lines of pattern discontinuity. *J.Neurosci., 9*(5), 1731-1748.

Vuilleumier, P., Valenza, N., & Landis, T. (2001). Explicit and implicit perception of illusory contours in unilateral spatial neglect: behavioural and anatomical correlates of preattentive grouping mechanisms. *Neuropsychologia, 39*(6), 597-610.

Walker, G. A., Ohzawa, I., & Freeman, R. D. (1999). Asymmetric suppression outside the classical receptive field of the visual cortex. *J.Neurosci., 19*(23), 10536-10553.

Walther, D., & Koch, C. (2006). Modeling attention to salient proto-objects. *Neural Netw, 19*(9), 1395-1407. doi: S0893-6080(06)00215-2 [pii] 10.1016/j.neunet.2006.10.001

Weliky, M., Kandler, K., Fitzpatrick, D., & Katz, L. C. (1995). Patterns of excitation and inhibition evoked by horizontal connections in visual cortex share a common relationship to orientation columns. *Neuron, 15*(3), 541-552.

Wessinger, C. M., Fendrich, R., Ptito, A., Villemure, J. G., & Gazzaniga, M. S. (1996). Residual vision with awareness in the field contralateral to a partial or complete functional hemispherectomy. *Neuropsychologia, 34*(11), 1129-1137.

Wylie, G. R., Javitt, D. C., & Foxe, J. J. (2003). Task switching: a high-density electrical mapping study. *Neuroimage., 20*(4), 2322-2342.

Yeap, S., Kelly, S. P., Sehatpour, P., Magno, E., Garavan, H., Thakore, J. H., et al. (2008). Visual sensory processing deficits in Schizophrenia and their relationship to disease state. *Eur.Arch.Psychiatry Clin.Neurosci.*

Yeap, S., Kelly, S. P., Sehatpour, P., Magno, E., Javitt, D. C., Garavan, H., et al. (2006). Early visual sensory deficits as endophenotypes for schizophrenia: high-density electrical mapping in clinically unaffected first-degree relatives. *Arch Gen Psychiatry, 63*(11), 1180-1188.

Yeap, S., Kelly, S. P., Thakore, J. H., & Foxe, J. J. (2008). Visual sensory processing deficits in first-episode patients with Schizophrenia. *Schizophr.Res.*

Yoshino, A., Kawamoto, M., Yoshida, T., Kobayashi, N., Shigemura, J., Takahashi, Y., et al. (2006). Activation time course of responses to illusory contours and salient region: a high-density electrical mapping comparison. *Brain Res., 1071*(1), 137-144.

Yuval-Greenberg, S., Tomer, O., Keren, A. S., Nelken, I., & Deouell, L. Y. (2008). Transient induced gamma-band response in EEG as a manifestation of miniature saccades. *Neuron, 58*(3), 429-441. doi: S0896-6273(08)00301-2 [pii]
10.1016/j.neuron.2008.03.027

Zanon, M., Busan, P., Monti, F., Pizzolato, G., & Battaglini, P. P. (2010). Cortical connections between dorsal and ventral visual streams in humans: Evidence by TMS/EEG co-registration. *Brain Topogr, 22*(4), 307-317. doi: 10.1007/s10548-009-0103-8